ULUS, YENER, PHD. The Impact of Saltwater Intrusion on Mercury Cycling in Coastal Plain Wetlands. (2021)
Directed by Dr. Martin Tsz-Ki Tsui. 90 pp.

Coastal wetlands are considered hotspots and the primary source of mercury (Hg) to adjacent waters. Because of the global sea level rise and hurricanes low-lying coastal areas are experiencing saltwater intrusion causing alteration in Hg biogeochemistry. However, limited studies have focused on saltwater effects on Hg in coastal wetlands. To explore potential salinity impact on Hg levels and bioaccumulation in food web, we collected water, sediment, and invertebrate samples for multiple times over two years along with *in situ* water quality measurements in the natural forest-marsh salinity gradient. Sampling sites consist of a freshwater wetland (FW; salinity < 0.5 ppt), partially degraded wetland (PDW; salinity < 5 ppt), and saltmarsh (SM; salinity < 18 ppt) and are located near Winyah Bay (South Carolina) and Albemarle - Pamlico Sound (North Carolina). We found that while elevated salinities ultimately reduced overall mercury levels by reducing dissolved organic carbon levels, dissolved oxygen and sulfate/chloride ratio are important determinants for methylmercury (MeHg) production in water column after the hurricanes in coastal wetlands of North Carolina. Similarly, mean sediment mercury levels were decreasing in the order of FW, PDW, and SM with increasing salinities in South Carolina. However, mean biota mercury levels did not show difference in FW and PDW but significantly lower in SM. Overall, we found a strong empirical evidence that salinity controls MeHg levels in sediment and its bioaccumulation in food web in coastal wetlands. My results suggest that increasing salinity levels can significantly reduce mercury levels in sediment and attenuate its accumulation in biota in coastal plain wetlands.

# THE IMPACT OF SALTWATER INTRUSION ON MERCURY CYCLING IN COASTAL PLAIN WETLANDS

by

Yener Ulus

A Dissertation

Submitted to

the Faculty of The Graduate School at

The University of North Carolina at Greensboro

in Partial Fulfillment

of the Requirements for the Degree

Doctor of Philosophy

Greensboro

2021

Approved by

Dr. Martin T.K. Tsui
Committee Chair

# DEDICATION

This dissertation is dedicated to my role model, my uncle Cemil Ulus, and his wife, Barbara Gottschalk, who supported me since elementary school, and to my friends, Hilal & Levent Sahin, for believing in me and supporting me through this endeavor. Finally, I dedicate this work to Prashant Waiker, who treated me like a real brother and helped in all possible ways during my Ph.D. studies.

APPROVAL PAGE

This dissertation written by Yener Ulus has been approved by the following committee of the Faculty of The Graduate School at The University of North Carolina at Greensboro.

| | |
|---|---|
| Committee Chair | Dr. Martin T.K. Tsui, Chair |
| Committee Members | Dr. Sally E. Koerner |
| | Dr. Ayalew L. Osena |
| | Dr. Dan Royall |

3/3/2021
Date of Acceptance by Committee

3/3/2021
Date of Final Oral Examination

ACKNOWLEDGEMENTS

I am fortunate and grateful to work with my adviser, Dr. Martin Tsui. He is a brilliant, thoughtful, and humble mentor who patiently guided me through my Ph.D. research. I also thank my committee members Dr. Sally E. Koerner, Dr. Ayalew L. Osena, and Dr. Phillip D. Royall for constructive comments, suggestions, and feedback. Thank you to Dr. Alex Chow and Dr. Marcelo Ardón and their team for sharing their expertise and for providing me field sites and water quality analysis. I also thank my family and friends. My father, Mehmet Ulus, always believed in education, and my mother, Fatma Ulus, gave me motivation. Thank you to my lab partners Peijia Ku, Kristina Morales, and Hanhan Li as well as friends Reuben Garshong and Carlos Vega-Melendez for helping and supporting me when I needed it. I also must mention undergraduate students Aslihan Sakar, Paul Nyarko, Thomas Cohen, Nadia Aitmbarek, Mikah Bass, Merve Ozdemir, and Egemen Ulus (my brother) for assisting in the field to collect and process samples. Also, I would like to thank my friend Romesh Ruwan Thanuja and Elif Dil for helping me with the statistical analysis. Finally, I am grateful for the UNC-Greensboro Biology Department's funding, NC WRRI & Sea Grant, and W. John O'Brien Award for funding my work.

TABLE OF CONTENTS

LIST OF TABLES

LIST OF FIGURES

# CHAPTER I: INTRODUCTION

## Background and Literature Review

### *Sea level rise (SLR)*

Sea level has been risen and fallen throughout geologic history. Even though changes in the ocean's basin size and shape play an essential role in the determination of sea level, the main cause of sea level rise is a consequence of climate change (Titus, 1988). Sea Level Rise (SLR) has rapidly increased since the early 20th-century. Intergovernmental Panel on Climate Change (IPCC) estimates that the global mean sea level will reach 22 to 50 cm above 1990 levels by 2090. Two main factors drive global SLR (i.e., absolute sea-level change): thermal expansion of warming ocean water and the enhanced melting of land-based ice (Bindoff et al., 2007). Coastal areas in the mid-Atlantic and southeastern United States are considered the hotspots for accelerated SLR (Kopp, 2013). Regional sea-level rise (i.e., relative sea-level change) could be more extensive compared to global mean SLR due to atmospheric and oceanic circulations (i.e., varying ocean currents and wind) and thermostatic and halosteric effects (i.e., variations in ocean temperature and salinity) (Stammer et al., 2013). For example, on the Carolina (North and South) coast, sea level has increased by 26.6 cm since 1950 (NOAA, 2018). Estimations (low and high $CO_2$ emissions) from different models suggest that coastal North Carolina (NC) will be experiencing a relative SLR in the range of 24-132 cm by the end of this century (Kopp et al., 2015).

### *Hurricanes and floods*

Due to the warming of the ocean surface, the frequency and intensity of Atlantic hurricanes are predicted to increase in the next few decades (Bender et al., 2010). Previous work has shed light on the consequence of ocean warming on hurricanes' frequency and intensity in the Atlantic tropical cyclogenesis regions from 1886 to 2017 (Hosseini et al., 2018). Based on the findings, the frequency of category five hurricanes strongly correlates with the Atlantic sea-surface temperature, and the intensity of the storms (i.e., category five or higher) is affected by the elevated temperature of the

Atlantic Ocean. Extreme weather conditions such as storm surges and extreme tides will have a greater impact than base sea-level rise (Kemp & Horton, 2013). Consequently, extreme flooding and temporary inundation of low-lying areas will be expected to be more frequent (Valle-Levinson et al., 2017).

*Coastal wetlands*

Coastal wetlands provide numerous ecosystem services (e.g., storm protection, habitat for diverse groups, water purification, and food source) and are the most productive ecosystems (per unit area) on the earth's surface (Li et al., 2018). They arise alongside the United States' (US) coastline, with the largest area through the Gulf of Mexico and southeastern Atlantic coasts. Southeastern parts of the US seem to be the most sensitive areas for storms, inundation, flooding, and SLR, as they contain over 50% of the nation's barrier islands and 85% of the coastal wetlands (Gornitzf et al., 1994). A

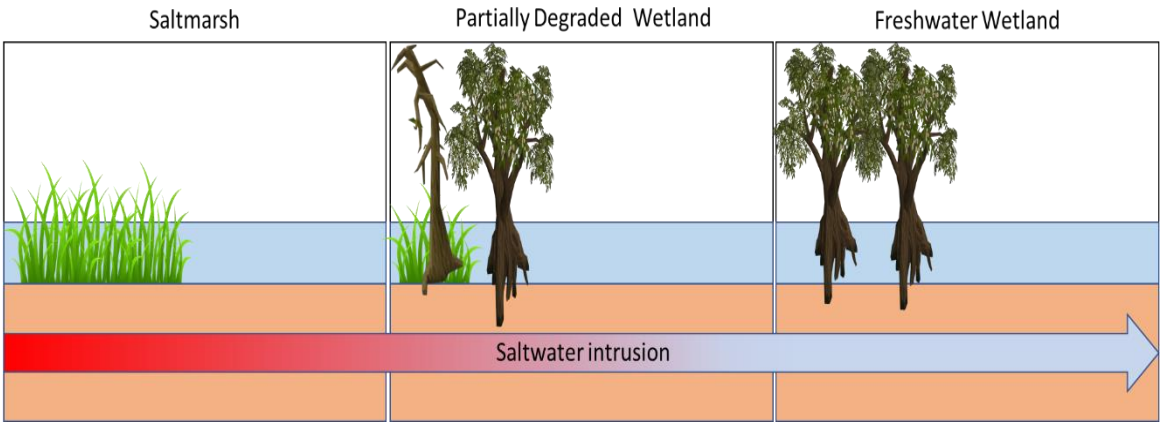


Figure 1. 1: Conceptual model of saltwater intrusion impact on coastal plain wetlands.

combination of storm surges, droughts of inland habitats, and SLR create a trend where seawater encroaches and results in elevated salinities in these low-lying regions (Barendregt & Swarth, 2013). Submergence and salinization are two of several significant impacts of SLR on coastal ecosystems. As the submergence can create a deficiency of drainage, the extent of waterlogging of soils can increase in low-lying areas. Thus, primary productivity can decline and eventually lead to diebacks (e.g., partially degraded wetland (PDW)) in coastal zones (Day et al., 2008). Over the last 30 years, the losses of coastal wetlands and their degradation have accelerated, mainly

due to SLR, land reclamation, urbanization, aquaculture, and human-made channels (Li et al., 2018). With global climate change leading to SLR, many coastal freshwater wetlands (FW), defined by salinity levels < 0.5 ppt, (Odum et al. 1984) are getting infiltrated with saltwater to become PDW, mean salinity of the surface water can reach up to 2 ppt, (Krauss et al., 2009) and eventually converted into saltmarsh (SM) (Figure 1.1). For instance, previous work demonstrated that in bottomland forest, exposure to salinity of higher than 3 ppt of saltwater promotes leaf burning (i.e., browning of plant tissues) and reduction up to 84% carbon assimilation in seedlings of different species, which eventually result in potential long term habitat changes in these forests (Pezeshki et al., 1990).

*The effect of SLR on biogeochemical cycles in coastal wetlands*

In addition to habitat changes and degradation, SLR can also bring significant changes to coastal wetlands' elemental cycles. While wetland soil contains approximately 45 - 70% of terrestrial organic carbon (C), C accumulation rates are a small portion of total C inputs to a wetland due to mineralization and hydrologic removal of C (Neubauer et al., 2013). Heterotrophic bacteria with terminal electron acceptors (e.g., sulfate and iron (III)) mediate organic carbon mineralization (Luo et al., 2019). Elevated salinity alters microbial C cycling, where methanogenesis is suppressed by high sulfate ($SO_4^{2-}$) availability in freshwater wetlands (Herbert et al., 2015). Chambers et al. (2011) indicated that oligohaline seawater (3.5 g kg/l) escalates overall C mineralization by producing carbon dioxide ($CO_2$) and methane ($CH_4$) as a consequence of short-term increases in $SO_4^{2-}$ reduction rate without suppressing methanogenesis (Chambes et al., 2011). Furthermore, SLR can threaten the cycling of nutrients, such as nitrogen. The existence of sea salt physiologically impacts nitrification and denitrification bacteria by lowering their activities (Rysgaard et al., 1999). In the presence of sea salt, specifically when salinity increased from 0 to 10 ppt, nitrification, denitrification, and potential nitrification rates in sediments were significantly reduced (Rysgaard et al., 1999). Moreover, Joye & Hollibaugh (1995) demonstrated that nitrification is inhibited by the elevation of sulfide ($HS^-$) due to the increased extent of $SO_4^{2-}$ reduction (Joye & Hollibaugh, 1995). A recent study has investigated drought-induced saltwater incursion

on nitrogen export in a wetland at the coastal plain of North Carolina (Ardón et al., 2013) (at one of the study sites in aim 2). It provided the first evidence of increased reactive nitrogen (N) release because of drought-induced saltwater incursion due to cation exchange and decreased nitrification. The study further suggests that saltwater incursion into coastal FW could cause increased loading of N to susceptible coastal waters (Ardón et al., 2013).

Seawater contains a high amount of halogens, such as chloride ($Cl^-$) and bromide ($Br^-$) (Kendrick, 2018). Haloforms, very short-lived substances, are the sources of stratospheric chlorine and bromine, which decrease the ozone ($O_3$) layer in the lower stratosphere (Hossaini et al., 2015). Natural sources account for approximately 90% of chloroform ($CHCl_3$) (Laturnus et al., 2002) and 70% of bromoform globally (Carpenter & Liss, 2000). Wang et al. (2016) investigated haloform formation from *in situ* field chambers alongside a salinity gradient (FW, PDW, and SM) to understand the SLR effect on haloform emissions at Winyah Bay, South Carolina (study area for aim 1 and 3). Their results suggest that $CHCl_3$ production was limited by the deficiency of halides, while PDW and SM are the hotspots for haloform production due to the presence of dissolved organic matter (DOM) and halogens supplied by saltwater (derived from seawater intrusion) in these saltwater-impacted wetlands.

It is necessary to understand DOM's biogeochemical properties because the fate of many chemical pollutants (e.g., metals) is coupled to DOM in aquatic systems (Jiang et al., 2017). For example, the speciation and transport of mercury (Hg), a global pollutant and highly toxic metal are strongly controlled by DOM through binding with thiol groups; thus, DOM can mediate the speciation, solubility, and toxicity of Hg in the environment (Ravichandran, 2004).

*Mercury cycling*

Mercury (Hg) is released to the environment from natural sources, such as volcanic, geothermal activities (Boening, 2000), and anthropogenic sources, including coal combustion, biomass burning, and gold mining (Whitacre, 2014). Due to its physicochemical properties, gaseous form of Hg (abbreviated as Hg0) can travel across

the globe, Hg is thus considered a global pollutant (Selin, 2009; Schwesig & Matzner, 2011). Therefore, over 140 countries have agreed to enact a legally binding treaty on reducing Hg emissions. Mercury is a neurotoxin and can cause significant human health risks (Hsu-Kim et al., 2013). Humans are exposed to its organic form, called methylmercury (MeHg), mainly through fish consumption (Amos et al., 2014). Estimations show that more than 410,000 children are exposed to MeHg in the womb, which is related to MeHg induced neurological problems in the United States every year (Driscoll et al., 2007).

There are three primary forms of Hg: elemental Hg (Hg0), inorganic Hg (HgII), and organic Hg (MeHg). Mercury can be in the gaseous form (Hg0) at low temperature due to its low boiling point (356.7 ℃). Gaseous Hg0 can be oxidized in the atmosphere to Hg(II) and then deposited in soil, rivers, lakes, and oceans by wet deposition (Whitacre, 2014) (Figure 1.2). Generally, Hg0 can be taken up by plants through stomatal uptake and can be oxidized to HgII in plant tissues, which is called dry deposition. Once it enters the terrestrial and aquatic ecosystems, a small portion of HgII can be converted to MeHg (Fitzgerald et al., 2007).

The fate of Hg in the environment is influenced by the atmospheric Hg deposition, including dry deposition and wet deposition. Areas containing trees (e.g., coastal freshwater wetlands) and shrubs will have elevated atmospheric Hg deposition in contrast to unvegetated areas (Zillioux et al., 1993) due to the stomatal uptake of atmospheric Hg0 by the leaves (Ericksen et al., 2003).

In aquatic ecosystems, methylation of inorganic Hg in waters and sediments is crucial in Hg cycling as MeHg is the bioavailable form of Hg. The environmental MeHg concentration represents net production due to the simultaneous Hg methylation and demethylation processes (Ullrich et al., 2001). The demethylation processes are predominantly mediated by sunlight and microbes, while Hg methylation is mainly mediated through anaerobic microbial processes (Hsu-Kim et al., 2013). Several anaerobic microorganisms, such as Iron-reducing bacteria (IRB) and Sulfate-reducing

bacteria (SRB), have been revealed to produce MeHg in pure culture studies (Fitzgerald et al., 2007).

Sulfate-reducing bacteria (SRB) use $SO_4^{2-}$ to metabolize organic matter where conditions are anaerobic (Paranjape & Hall, 2017). Sulfur (S) is reduced to sulfide ($S^{2-}$), which forms an essential mechanism for metal precipitation in anaerobic environments. In SRB, respiration processes involve $SO_4^{2-}$, terminal electron acceptor, which produces $S^{2-}$ (King et al., 2002). $S^{2-}$ typically restricts Hg methylation by complexing with available HgII into mercury sulfide (HgS). Generally, MeHg levels in sediment vary between 1 to 1.5% of the total Hg concentration. Nevertheless, the amount of MeHg accumulated in fish and other aquatic biota can be much higher due to biomagnification of MeHg along the food chain (Ullrich et al., 2001).

*Applications of stable isotopes in mercury cycling studies*

Stable carbon isotopes ($^{13}C/^{12}C$ expressed as $\delta^{13}C$), stable nitrogen isotopes ($^{15}N/^{14}N$ expressed as $\delta^{15}N$), and stable sulfur isotopes ($^{34}S/^{32}S$ expressed $\delta^{34}S$) are widely used for tracing energy sources and/or estimating trophic positions in natural food webs. Also, they are commonly used to investigate the source, bioaccumulation, and trophic transfer of chemical contaminants such as Hg in terrestrial and aquatic ecosystems (Al-Reasi et al., 2007; Bank et al., 2007; Fry & Chumchal, 2012; Tsui et al., 2019; Willacker et al., 2017).

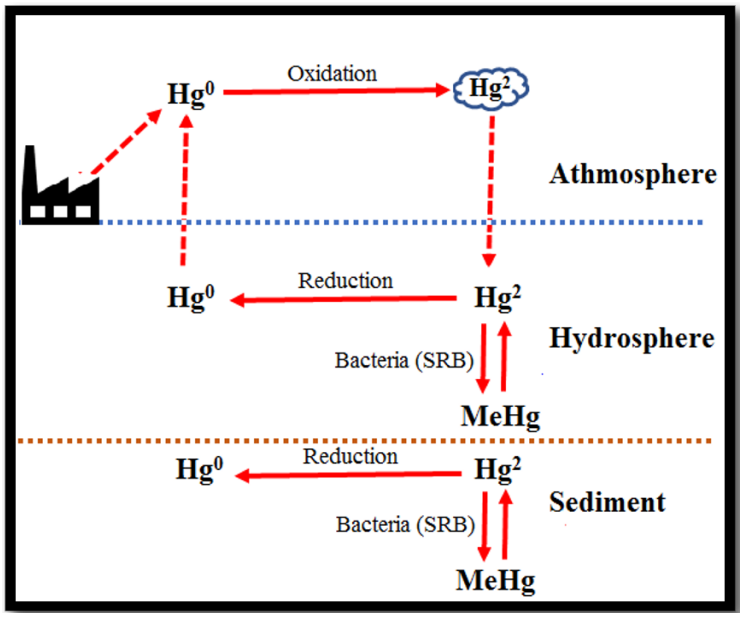


Figure 1.2: Mercurcy cycling in atmosphere, hydrosphere and sediment.

The food source is an essential factor that influences MeHg bioaccumulation in the food web. $\delta^{13}C$ values generally are used to infer the origins of the food web's carbon sources as $\delta^{13}C$ differ only around 0.4 ‰ (per trophic level) when they pass through the food web (Post, 2002). On the contrary, $\delta^{15}N$ values increase by ~3.4 ‰ (per trophic level); therefore, they have been used to evaluate the organism's trophic position, which is generally well correlated with Hg bioaccumulation (Chételat et al., 2020; Post, 2002). Generally, the organic matter between freshwater and marine ecosystem has distinct $\delta^{34}S$ values; thus, $\delta^{34}S$ is used as a complementary tool to explore energy flow along salinity gradient (e.g., estuaries), in a combination with $\delta^{13}C$ and $\delta^{15}N$.

*Mercury in coastal wetlands*

Wetlands are ideal ecosystems to promote MeHg production due to high deposition levels of nutrients and organic matter under a reducing environment (Black et al., 2012). Even though wide-ranging wetlands, which are ideal for promoting MeHg production exist in the southeastern United States' coastal plain, only a few Hg distribution and speciation studies have been carried out in coastal wetland ecosystems (O'Driscoll et al., 2011; Hall et al., 2008). Several components, such as microbial growth, metabolic

function, and Hg(II) availability, regulate the quantity of MeHg produced in an environment. While the rate of substrate supply, including labile DOC and $SO_4^{2-}$, pH, and temperature are substantial influences for bacterial growth, production of microbial MeHg relies on Hg(II) that can cross the cell membrane of methylating bacteria (Hall et al., 2008). MeHg readily bioaccumulates both in terrestrial (Tsui et al., 2019) and the aquatic food webs (Fitzgerald et al., 2007). In aquatic ecosystems, aqueous MeHg is taken up and concentrated by phytoplankton (Chen et al., 2008), which biomagnifies along with the food web as predators (e.g., fish) eat other prey organisms (Black et al., 2012). Fish in the southeastern part of NC contains the highest documented MeHg concentrations in the US (Figure 1.3; adapted from Sackett et al., 2009).

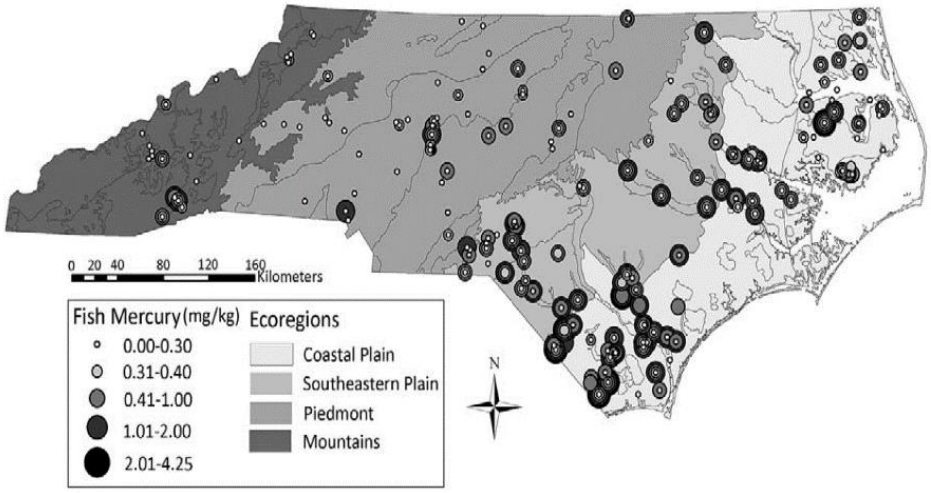


Figure 1. 3: Geographically distribution of mean total mercury levels in fish tissue for 12 species (adapted from Sackett et al., 2009).

Because of that, largemouth bass (*Micropterus salmoides*), a popular freshwater game fish, is under statewide consumption advisory. Ambient levels of sulfate have essential control on the MeHg production under reducing conditions. An earlier conceptual model (Figure 1.4) developed by Gilmour & Henry (1991) predicted that low $SO_4^{2-}$ level ($<10^1$ µM) would limit HgII methylation (i.e., sulfate-limited; Jeremiason et al., 2006) while high $SO_4^{2-}$ level ($>10^4$ µM) as found in estuarine waters and seawater may also inhibit HgII methylation due to the buildup of excessive reduced $S^{2-}$, as $S^{2-}$ can extensively sequester HgII and inhibit further bacterial HgII methylation (Benoit et al., 1999).

Interestingly, the peak of HgII methylation is predicted to be at intermediate $SO_4^{2-}$ level ($10^2$-$10^3$ µM) as this would provide sufficient $SO_4^{2-}$ for extensive HgII methylation while not leading to an excessive buildup of $S^{2-}$.

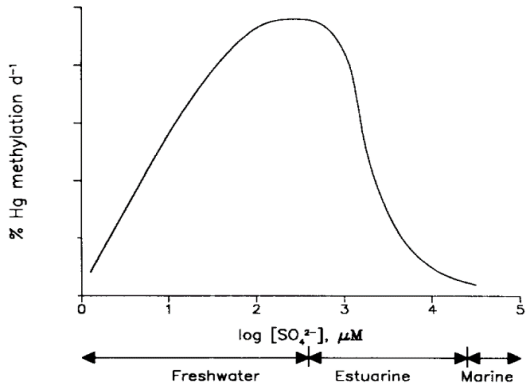


Figure 1. 4: Theoretical relationship water sulfate concentrations and mercury methylation rate in sediments (modified from Gilmour & Henry (1991)).

**Therefore, I hypothesize that saltwater will enhance microbial production of MeHg in coastal freshwater wetlands mainly because saltwater can provide abundant, yet not excessive $SO_4^{2-}$ to stimulate sulfate reduction in sulfate-limited freshwater ecosystems in the coastal plain of Carolinas.**

Below are my three specific research questions to test my working hypothesis.
*Question 1 (Chapter II):* How does saltwater intrusion (gradual) influence MeHg concentrations along the salinity gradient in coastal freshwater wetlands?
*Question 2 (Chapter III):* How does hurricane-induced (episodic) storm surge affect aqueous MeHg levels and its transfer to adjacent waters in coastal wetlands?
*Question 3 (Chapter IV):* How does food web MeHg accumulation vary among coastal wetlands along a salinity gradient?

# CHAPTER II: EFFECT OF SALTWATER INTRUSION ON METHYLMERCURY PRODUCTION IN COASTAL PLAIN WETLANDS


## Abstract

Coastal wetlands are considered hotspots and the primary source of methylmercury (MeHg) to adjacent waters. Due to global sea level rise, low-lying coastal areas are experiencing saltwater intrusion, potentially leading to an alteration in Hg biogeochemistry. To explore salinity impact on MeHg levels, I collected water and sediment samples five times for over two years (i.e., spring, summer, and fall) along with *in situ* water quality measurements in a natural forest-marsh salinity gradient. Sampling sites consisted of a freshwater wetland (FW; salinity < 0.5 ppt), partially degraded wetland (PDW; salinity < 5 ppt), and saltmarsh (SM; salinity < 10 ppt) and were located near Winyah Bay, Georgetown, South Carolina. Overall mean filtered surface water methylmercury (MeHg) levels were similar among FW and PDW, but both were significantly ($p = 0.003$) higher than that of SM. Interestingly, there was a positive relationship ($r^2 = 0.69$) between surface water MeHg and salinity levels only in PDW. Mean sediment (dry wt.) MeHg levels decreased significantly in the order of FW, PDW, and SM (with increasing salinities). Although sediment MeHg levels in PDW were significantly lower than FW and water MeHg levels were similar in both wetlands, mean biota MeHg (dry wt.) levels did not show a significant difference between FW and PDW, but the values were significantly lower in SM. The findings suggest that while increasing salinities ( > 5 ppt ) would attenuate MeHg production in the surface sediment and potentially reduce MeHg bioaccumulation.

## Introduction

Sea level rise (SLR) along with storm surges, droughts, and hurricanes enhance seawater intrusion and landward movement of saltwater, which threaten low-lying coastal wetlands globally (Barendregt & Swarth, 2013; Herbert et al., 2015). Consequently, many coastal freshwater wetlands (FW) are experiencing salinization, transitioning to partially degraded wetland (PDW; oligohaline wetland), and eventually converted to saltmarsh (SM) (Hackney et al., 2007; Krauss et al., 2009). These changing environments may alter the biogeochemistry of many important elements such as carbon (C), nitrogen (N), and mercury (Hg).

Hg is a neurotoxin that can pose a risk to human health mainly through the consumption of mercury-tainted fish (Amos et al., 2014; Li et al., 2015). Middle Atlantic Coastal Plain ecoregion of the United States includes many fish species under consumption advisories for Hg (SCDHEC, 2018), and have the highest concentrations of tissue Hg in fish among the Piedmont and Southern Coastal Plain ecoregions (Glover et al., 2010). Coastal wetlands are ideal ecosystems for producing MeHg, a toxic form of Hg, due to large deposits of nutrient and organic matter under reducing environment (Hall et al., 2008). MeHg is produced when anaerobic microbes such as sulfate-reducing bacteria (SRB) transform inorganic Hg (HgII) to MeHg under reducing conditions (Fitzgerald et al., 2007). SRB uses sulfate ($SO_4^{2-}$) to metabolize organic matter under anaerobic conditions (Paranjape & Hall, 2017). Even though previous laboratory work and mesocosm field monitoring demonstrated MeHg production has a positive correlation with sulfate levels in surface water, where $SO_4^{2-}$ levels span from 0.5 to 20 mg/L, excessive sulfide ($S^{2-}$) levels (i.e., $S^{2-}$ >1 mg/L) could prevent the production of MeHg in surface water at Everglades National Park in Florida U.S.A. (Gilmour et al., 2007; Orem et al., 2011). Thus, it is crucial to investigate saltwater intrusion in coastal FW since a small increase in salinity (e.g., from ~ 0.3 - 2.5 ppt) can significantly elevate $SO_4^{2-}$ (e.g., ~ 1.5 - 120 mg/L) levels and potentially further stimulates/inhibit sulfate-reduction and microbial Hg methylation.

There are several recent investigations on saltwater intrusion in coastal wetlands of the Carolinas. For example, Ardón et al. (2013) showed that saltwater incursion could cause increased N loading to coastal waters. In South Carolina, where the present study was performed, Wang et al. (2016) examined haloform releases from *in situ* field chambers and suggested that in FW, chloroform ($CHCl_3$) production was limited by the availability of halides (Wang et al., 2016). PDW and SM are considered hotspots for haloform production due to the high abundance of dissolved organic matter (DOM) and halides in these saltwater-impacted wetlands.

The effects of salinity on Hg cycling, mainly in sediment, have been examined both in the field (Boyd et al., 2017; Chakraborty et al., 2019; Hollweg et al., 2009; Noh et al., 2013; Wu et al., 2011) and in laboratory settings (Blum & Bartha, 1980; Compeau & Bartha, 1987; de Oliveira et al., 2015; Dongmei et al., 2020). Some studies (Hollweg et al., 2009; Wu et al., 2011) showed a positive relationship between salinity and sediment MeHg levels, while others (Blum & Bartha, 1980; Compeau & Bartha, 1987; Boyd et al., 2017) reported a negative relationship. However, many of these study ecosystems (e.g., estuaries and hypersaline lakes) contain high salinity levels (i.e., 2 - 300 ppt), not representing the small and long-term salinity changes due to SLR in many coastal freshwater wetlands. Hall et al. (2008) investigated Hg cycling with a range of salinities (i.e., ~ 0.04 - 17 ppt) in the coastal wetlands in the southern U.S.; however, their sampling generally occurred only once for many sites in coastal Louisiana. Since temporal variations in temperature, organic carbon, and nutrients strongly influence MeHg production in wetlands (Marvin-DiPasquale et al., 2003), it is crucial to investigate Hg cycling in different seasons. I studied (i) the influence of salinity on temporal Hg speciation and (ii) interaction of Hg with other common biogeochemical variables (e.g., DOC, OM, $SO_4^{2-}$, and $Cl^-$) in hydrologically connected coastal wetlands, FW, PDW, and SM in different seasons at Georgetown, South Carolina.

## Methods

*Study sites*

The sampling sites are located along a forest-marsh transect with a salinity gradient and are located in Georgetown, South Carolina (Figure 2.1). Sites include FW (healthy freshwater forested wetland), PDW (i.e., oligohaline wetland), and SM (i.e., mesohaline saltmarsh) (Wang et al., 2016).

FW consists of a highly productive forested wetland with an average litterfall input of 548 g $m^{-2}$ $yr^{-1}$, significantly higher than the surrounding depressional freshwater wetlands (Busbee et. al., 2003). This wetland is dominated by bald cypress *(Taxodium distictum)*, water tupelo *(Nyssa aquatica),* and swamp tupelo *(Nyssa sylvatica var.*


Figure 2. 1: Map of sample collection sites. Freshwater wetland (FW), partially degraded wetland (PDW) and saltmarsh (SM), Georgetown, SC, USA.

*biflora)* (Busbee et al., 2003), and has a salinity generally well below 0.5 ppt (Chow et al., 2013). PDW is a degraded freshwater forested wetland due to moderate saltwater intrusion connected to a nearby mesohaline saltmarsh (SM) by surface and groundwater flow (Krauss et al., 2009). The salinity of this wetland varies between 0.5 and 5 ppt, and the number of plant species diminishes compared to FW, with only bald cypress and swamp tupelo remaining (Wang et al., 2016). The mesohaline saltmarsh (SM) is dominated by cordgrass (*Spartina alterniflora)* and receives direct saltwater input from the estuary (Winyah Bay) with salinity less than 18 ppt (Morris et al., 2002).

*Sampling and sample processing*

All field sampling was conducted in 2018 (March, August, and November) and 2019 (March and September). I collected surface water (n = 33) and groundwater samples (n = 24) by wading into the wetlands. Groundwater samples were collected using a hand-operated pump from the PVC pipe inserted at 0.5 m below the surface. Water samples were placed into acid-cleaned 500 ml Teflon bottles. Upon arriving at the lab, samples were filtered with a pre-baked 0.7-µm filter paper (Whatman GF/F) for THg, MeHg, DOC, $SO_4^{2-}$, and $Cl^-$ analyses. During each sampling, *in situ* water quality parameters such as dissolved oxygen (DO), conductivity (as a proxy for salinity), and temperature were recorded with a handheld YSI probe (PRO 2030).

In total, 73 sediment samples (5 replicates each site per sampling except SM in September 2019 due to no water) were collected from the surface (0 – 5 cm) with a clean stainless-steel shovel and immediately placed into a Ziplock bag in a cooler for THg, MeHg, $\delta^{13}C$, $\delta^{15}N$, and organic matter (by loss-on-ignition) analyses. Before the analysis, sediment samples were lyophilized (VirTis benchtop K) and later sieved with a 2-mm polypropylene mesh and mixed for homogenization.

*Water sample processing and Hg analyses*

All THg and MeHg analyses were performed at the UNCG analytical laboratory using Brooks Rand Model III cold vapor atomic fluorescence spectrometer (CVAFS). THg analysis in water samples included a digestion step in which the samples were kept at 60 ℃ overnight after adding an acidic mixture of permanganate and persulfate

(analytical grade; Fisher Scientific) that was followed by THg analysis (Woerndle et al., 2018). To preserve water samples for MeHg analysis, 0.4 % HCl (for freshwater) or 0.2 % $H_2SO_4$ (if water samples with $Cl^-$ > 500 mg/L) was added (Parker & Bloom, 2005) and kept at 4 ℃ before MeHg analysis.

Analysis of THg in water samples was initiated by neutralizing digested water samples (~100 mL) with hydroxylamine ($NH_2OH$; Alfa Aesar), then placing them into a Hg-free glass bubbler. Subsequently, 200 µL of 20% tin(II) chloride ($SnCl_2$; Alfa Aesar) was added to the bubbler to completely reduce Hg(II) to gaseous elemental Hg(0). Finally, Hg(0) was purged together by a stream of Hg-free nitrogen ($N_2$) gas for 15 min to concentrate Hg(0) onto a gold trap. Hg(0) was then heat-desorbed and measured using the Brooks Rand Model III cold vapor atomic fluorescence spectrometer (CVAFS) (USEPA, 2002). Analysis of MeHg in water samples began with distilling water samples (each ~50 mL) to eliminate the matrix interference. Water samples were then buffered with sodium acetate ($CH_3COONa$) and ethylated with an ice-cold 1% sodium tetraethylborate (NaB(Et)4) for 25 minutes (with 5 min shaking intervals) in a glass bubbler. Preconcentration of organic Hg species from the bubbler into the Tenax TA traps (Supelco) was performed via purging with Hg-free $N_2$ for 12 minutes. Then, the Tenax traps were dried with Hg-free $N_2$ gas for 7 minutes, and MeHg was finally quantified using the Brooks Rand Model III CVAFS with an isothermal GC separation and pyrolysis (Horvat et al., 1993).

*Sediment sample processing and Hg analyses*

The method for sediment THg analysis (based on dry wt.) THg analysis involved the aqua regia digestion step (i.e., cold digestion), in which samples were weighed into 40 mL borosilicate glass vials and added with 8 mL of $HNO_3$ and HCl mixture (3:1 ratio, respectively; both trace metal grade; Fisher Scientific) for 24 hours in the room temperature (Olund et al., 2004). Later, 22 mL of 5% bromine chloride (BrCl) was added into the glass vials containing pre-digested sediment samples and placed in a water bath (i.e., hot digestion) at 80 ℃ overnight for the subsequent THg analysis.

Total-Hg analyses were initiated by adding digested sediment samples (0.2 to 1 mL) into a glass bubbler containing ~100 mL nanopure water (18.2 MΩ/cm) along with 200 µL $NH_2OH$. Each digestion batch included samples, blanks, and standard reference material (SRM; IAEA-158 Marine Sediment). Hg-loaded traps were then heat-desorbed at 400 - 500 ℃, which was eventually quantified with a Brooks Rand Model III CVAFS. The mean recovery for IAEA-158 Marine Sediment (n=12) was 127.06 ± 9.26 ng/g, within the certified values (132 ± 14 ng/g).

For sediment MeHg extraction, a chemical mixture (~0.1 g sediment, 30 mL nanopure water, 0.2 mL of 20%, KCl, 0.4 mL of 9 M $H_2SO_4$, and 1 M $CuSO_4$) was placed into a Teflon vial in a 140 ℃ aluminum hot block, which was eventually distilled (~60% to ~80%) into another Teflon vial and submerged in an ice bath of 5 ml of nanopure water. Distillates were then added to the bubblers and proceeded as described in the method for MeHg analysis in water samples (Hammerschmidt & Fitzgerald, 2004).

*Sample processing and analyses of water and sediment parameters*

Water $SO_4^{2-}$, $Cl^-$, and DOC were analyzed on a Metrohm 930 Flex Ion Chromatograph using chemical suppression and conductivity detection (EPA 300.1), and a Teledyne Tekmar Torch TOC combustion analyzer with a total nitrogen module in the Department of Forestry and Environmental Resources at North Carolina State University. The sediment organic matter (OM) was estimated using the loss on ignition (LOI) method with a muffle furnace. In this method, a clean porcelain crucible was weighed before and after adding ~5.0 g (weighed) of dry sediment sample followed by placing into the furnace for 4 hours at 500 °C. Lastly, a cooling step followed with re-weighing to determine the OM content (Ku et al., 2018).

*Statistical analyses*

All data were statistically analyzed by using SigmaPlot 12.5 (Systat) software and the significance were tested $\alpha = 0.05$.

## Results and Discussion

*Physiochemical properties of surface water and groundwater*

For all sites, the results of surface water and groundwater quality, including DO, water temperature, salinity, DOC, $SO_4^{2-}$, and $Cl^-$, are shown in Appendix B (Table S1). These wetlands generally showed an increasing amount of DO in surface water with increasing salinity toward Winyah Bay, and levels were 1.65 ± 0.32 mg/L, 3.10 ± 1.52 mg/L, and 5.92 ± 3.33 mg/L in FW, PDW, and SM, respectively.

Generally, water temperatures were similar among the sites each season but in summer and late summer, August 2018 (FW; 25.6 ℃, PDW; 25 ℃, SM; no water) and September 2019 (FW;19.5 ℃, PDW;22.5 ℃, SM; 25.9 ℃), were the highest among the different sampling seasons.

Overall, the mean surface water salinity levels in FW, PDW and SM were 0.11 ± 0.03 ppt , 1.86 ± 2.04 ppt , and 6.18 ± 2.84 ppt, respectively. Whereas the mean groundwater salinity levels in FW, PDW, and SM were 0.14 ± 0.04 ppt, 1.75 ± 1.10 ppt, and 7.99 ± 0.48 ppt, respectively. Water column salinity is well mixed as there is only a small variation between surface water and groundwater salinities in each wetland.

*Aqueous mercury concentrations and temporal variation in surface water*

Water mercury values (size, mean, and std. dev.) are shown in Appendix B (Table S2). All seasons combined (total n = 31) average filtered THg (FTHg) concentrations in the FW (5.09 ± 3.80 ng/L; n = 11) and PDW (5.70 ± 3.95 ng/L; n = 11) were similar but both FW and PDW had significantly higher filtered THg ($p = 0.007$) than SM (1.86 ± 0.71 ng/L; n = 8).

Although habitat types were diverse (i.e., SM and FW), generally, the mean THg concentrations in surface water were similar between the sites in different seasons (Figure 2.1.A). However, I observed a peak in filtered THg values at all sites in August 2018. Values were significantly higher ($P < 0.001$) in the FW (10.83 ± 0.73 ng/L), PDW (11.45 ± 0.98 ng/L), and SM (9.70 ± 3.85 ng/L) compared to other seasons (it should be noted that in August 2018, there was no water sample collected in the SM site;

therefore, surface water was only collected by opening a minor canal in the sediment surface, which might not represent surface water but porewater).

Since it is well known that DOC and Hg have a positive relationship in aquatic environments (Ravichandran, 2004; Barringer et al., 2010; Tsui & Finlay, 2011), the elevated Hg levels in August 2018 is likely due to presence of elevated DOC (i.e., 66 mg C/L, 85 mg C/L, and 45 mg C/L, respectively) levels in August of 2018 (Appendix B; Table S1). In current work, filtered THg values are noticeably higher than previous work conducted in both freshwater (1.64 ± 0.11 ng/L) and brackish (1.62 ± 0.28 ng/L) wetland at southern Louisiana and the Gulf of Mexico (Hall et al., 2008). Nevertheless, our results are consistent with a study conducted in a Coastal  Plain Watershed in New Jersey (Barringer et. al., 2010).

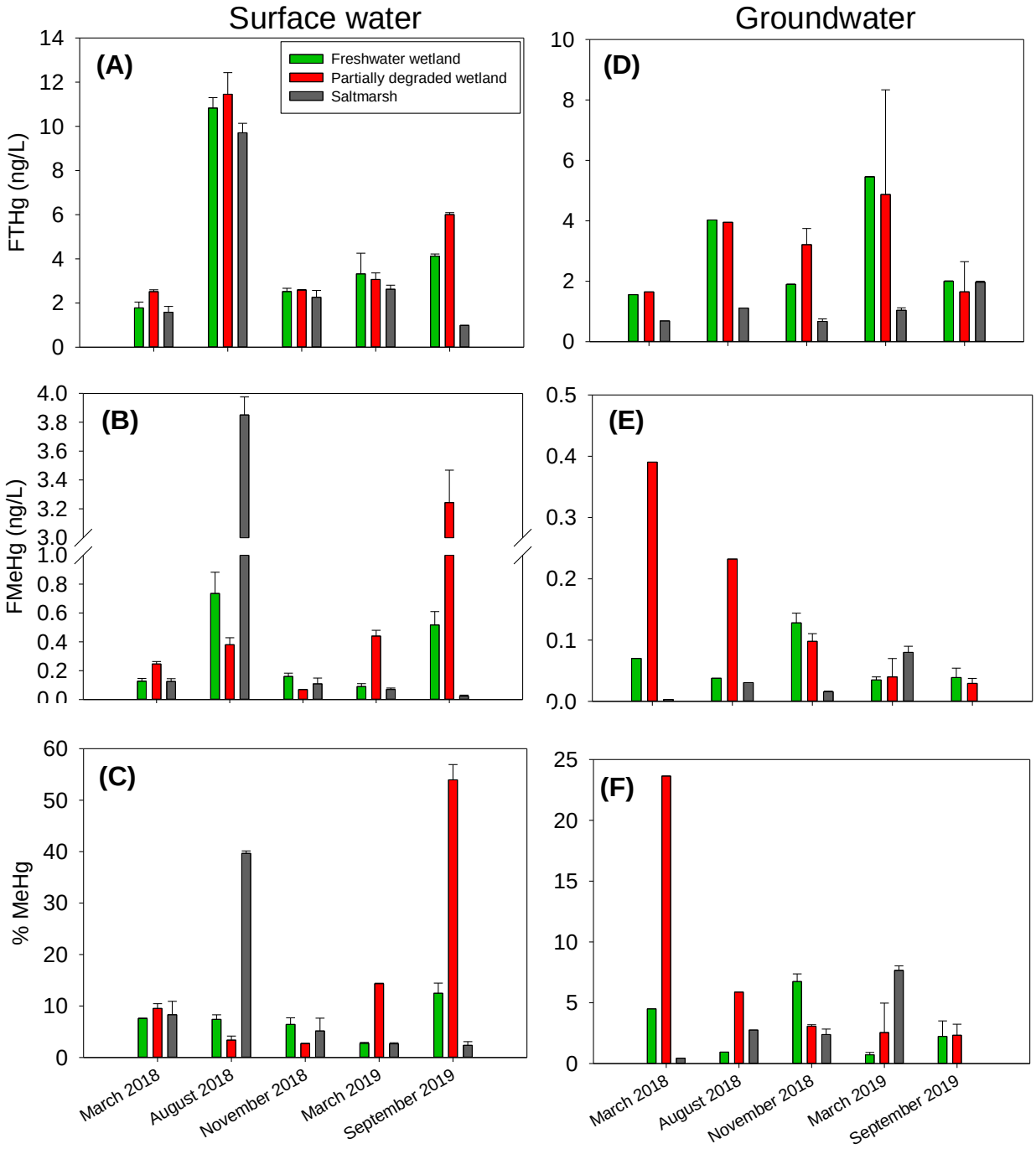


Figure 2. 2: Mean mercury levels in different seasons: (A) filtered total-mercury (FTHg; n = 2 for each seasons and site), (B) filtered methylmercury (FMeHg), (C) percent mercury (%MeHg) of surface water and (D) FTHg, (E) FMeHg, (F) %MeHg of groundwater samples in freshwater wetland, partially degraded wetland, and saltmarsh.

.

Overall (n = 33) mean filtered MeHg (FMeHg) levels were similar for FW and PDW, but SM concentrations were significantly lower (Figure 2.2.B). FMeHg concentrations varied significantly between the sites (each season) and individual sites in different seasons. In the FW site (n = 13), I observed significantly higher ($p < 0.001$) FMeHg levels in summer and late summer (August 2018 and September 2019) in comparison to other seasons. During the August 2018 and September 2019, DOC levels were also elevated (i.e., 66 mg/L and 51.95 mg/L, respectively). Since microorganisms utilize organic matter as an energy source in sulfate-limited environments, high DOC levels in the sulfate-limited freshwater wetland may elevate microbial activity and lead to increased microbial Hg methylation in the water column (see review by Ravichandran, 2004).

For all sites and seasons, the peak average FMeHg (3.24 ng/L) and % FMeHg (~54%), the fraction of THg that is MeHg, occurred concurrently with the highest salinity (i.e., 5.54 ppt) in the late summer season (September 2019; $p <0.001$) in PDW. There was no significant difference in PDW between other seasons.

There are some possible explanations for the high levels of MeHg in the surface water of PDW in September 2019. One explanation would be the second-highest mean tide levels (i.e., 0.365 m) of 2019 in North Inlet Estuary station, which is approximately 6 km away from PDW (data retrieved from 8662245 Oyster Landing, North Inlet Estuary, South Carolina; https://tidesandcurrents.noaa.gov/). I speculated that the high tides in September brought enormous saltwater, consisting of a high amount of sulfate (i.e., 74.75 mg/L), from the Winyah Bay to the PDW. The concentration of salinity was also at the peak (i.e., 5.54 ppt). A sealed microcosm study that mixed freshwater sediment with the seawater (both collected from the same location as the current study) showed that after three-week incubation at 5 ppt salinity (53.55 mg/L sulfate) resulted in FMeHg level of 3.8 ng/L, which is close to our observed field values (Ku et al., unpublished).

Similarly, Myrbo et al. (2017) reported that the highest surface water % MeHg occurred with sulfate levels of 59 and 93 mg/L in the mesocosm study. However, Orem et al. (2014) reported optimal sulfate levels (2 and 10 - 15 mg/L), which results in the peak levels of MeHg in the water column in Everglades. Another explanation may be the

anoxic water conditions, as it is generally considered hot spots for mercury methylation (Paranjape & Hall, 2017). Since there was no precipitation (based on the Myrtle Beach, SC Weather History data retrieved from https://www.wunderground.com/history/monthly/us/sc/myrtle-beach/KMYR/date/2018-3) for the entire week right before the sampling day, the water column was stable, and the DO level was the lowest (i.e., 1.75 mg/L) in PDW compared to previous DO measurements. Hence, it provided an optimum condition for Hg methylation and results in an increase in MeHg in September 2018 at PDW.

Generally, FMeHg in surface water of saltmarsh (n = 8) exhibited consistently low levels in all seasons (except August 2018). In August of 2018, I observed the highest levels of FMeHg values (i.e., 3.85 ng/L). However, it should be noted that surface water was completely dry; thus, I had to dig a small canal to collect water samples, which represents porewater rather than surface water. Many other studies showed elevated MeHg levels in porewater because of water level fluctuations (Eckley et al., 2017; Evers et al., 2007; Selch et al., 2007) and suggested that the reason could be partly due to a phenomenon called sulfate re-cycling mechanism. FMeHg concentrations were similar to a study conducted in southern Louisiana and the Gulf of Mexico (Hall et al., 2008). In this study, the highest surface THg and MeHg concentrations occurred in summer, and late summer could be partially due to season as MeHg production increases through warm weather (Hall et al., 2008; Barringer et al., 2010) and elevated salinities in PDW.

*Aqueous mercury concentrations and temporal variation in groundwater*

Mean levels of groundwater (all seasons combined) FTHg were similar in the FW (3.03 ± 2.05 ng/L; n = 8) and PDW (3.13 ± 2.38 ng/L; n = 8), but SM (1.14 ± 0.54 ng/L; n = 8) values were significantly lower than both FW and PDW ($p = 0.019$). However, there was no statistically significant difference in average groundwater FMeHg levels between the sites (Appendix B, Table S3). Mean groundwater FMeHg levels were generally lower than those surface water and were 0.06 ± 0.04 ng/L, 0.12 ± 0.13 ng/L, and 0.02 ± 0.03 ng/L in the order of FW, PDW, and SM for all sites. In the PDW, average MeHg concentrations in groundwater were noticeably higher in March and August of 2018 compared to all sites and seasons (Figure 2.2 E). This could be because of optimal

$SO_4^{2-}$ levels (3.90 and 17.93 mg/L) in water column during March and August of 2018 (Orem et al., 2014). Besides, FMeHg values showed an inverse relationship ($r^2 = 0.739$, $p = 0.028$) with the dissolved oxygen levels in the PDW as usually anoxic environments are considered a crucial condition for Hg methylation (Compeau & Bartha, 1985).

*Relationship of Hg and dissolved organic carbon*

In surface water, there were strong, positive relationships ($p < 0.001$, $r^2 = 0.83$, combination of all sites) between THg and DOC concentrations (Figure 2.3 A) which is comparable to many studies conducted in coastal areas (Barringer et al., 2010; Hall et al., 2008; Tsui et al., 2020). Similarly, FMeHg levels also showed a positive relationship

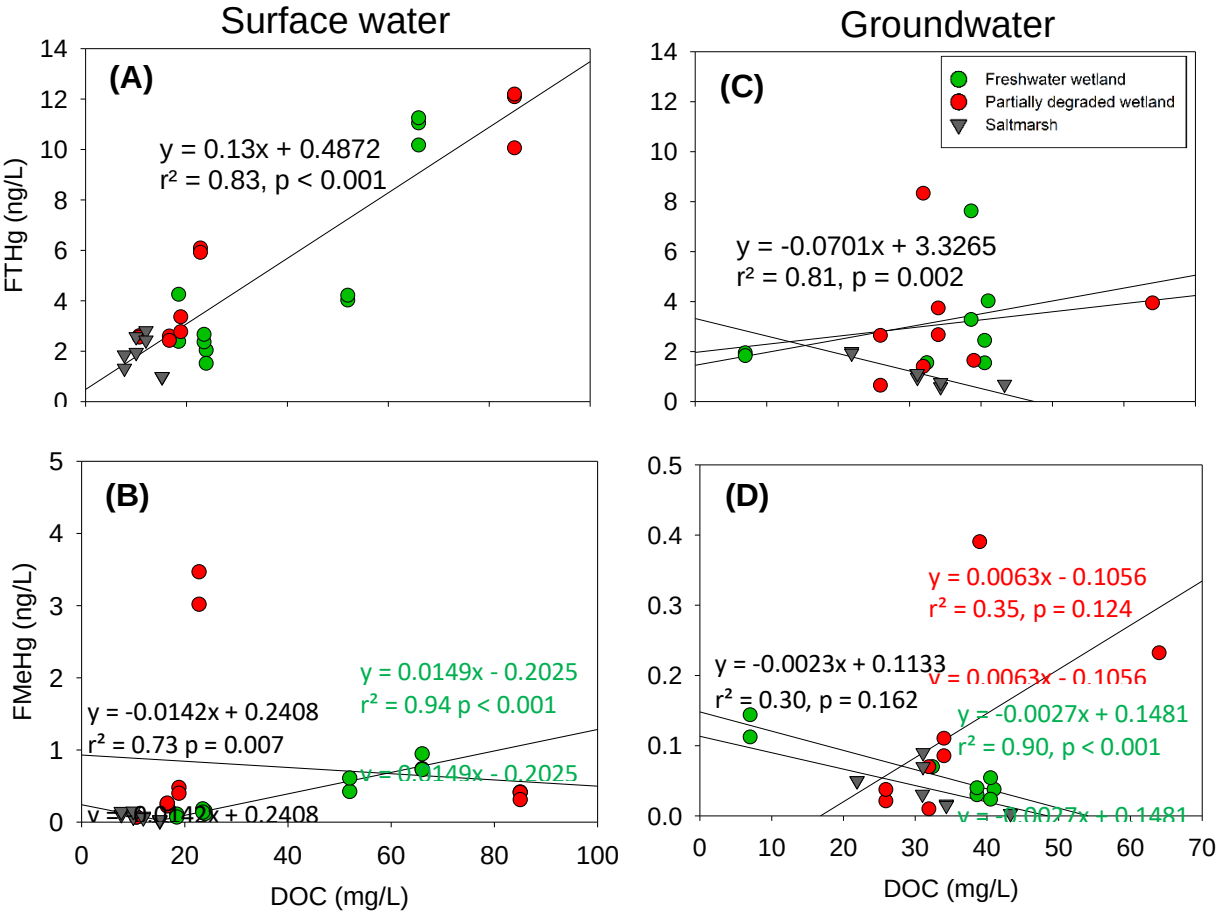


Figure 2. 3: Filtered mercury and dissolved organic carbon (DOC) relationship in surface water, (A) Filtered Total-Hg (FTHg) and DOC, (B) filtered methylmercury (FMeHg) and DOC and in groundwater, (C) FTHg and DOC, (D) FMeHg and DOC, in freshwater wetland, partially degraded wetland and saltmarsh.

($p < 0.001$) with DOC in FW ($r^2 = 0.94$) and negative relationship with SM ($r^2 = 0.73$) but not in PDW (Figure 2.3 B). Although FTHg and DOC concentrations in groundwater did not show a relationship in FW and PDW, in SM, a strong inverse relationship ($r^2 = 0.81$, $p = 0.002$) was observed between FTHg and DOC levels (Figure 2.3 C). Interestingly, a strong inverse relationship ($r^2 = 0.90$, $p < 0.001$) was also observed between FMeHg and DOC levels in FW. Nonetheless, PDW showed a weak positive correlation between FTHg and DOC, and there was no correlation between FMeHg and DOC in SM.

Moreover, I normalized average MeHg levels with DOC (MeHg/DOC) to evaluate probable MeHg production that is not influenced by DOC in all sites. In surface water, PDW showed the highest MeHg/DOC ratios (0.14 ± 0.01 ng MeHg/ mg DOC) in late summer (September 2019), which further indicates that salinity may perhaps be the main reason behind the peak of MeHg levels in this wetland (Figure 2.4 A). These results suggest that elevated surface water Hg methylation in PDW (in March and September 2019) was because of constituents (i.e., salinity) other than DOC.

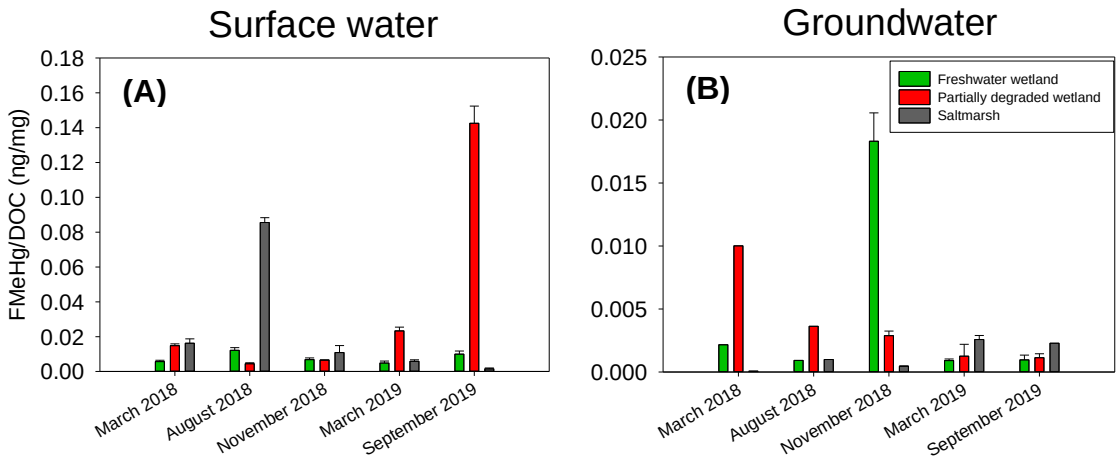


Figure 2. 4: Normalization of average mercury levels to dissolved organic carbon (DOC) levels in surface water (A) total Hg (FMeHg) to DOC and groundwater (B) FMeHg to DOC in freshwater wetland, partially degraded wetland, and saltmarsh.

Coastal freshwater wetlands are the primary sources of DOC for the adjacent estuaries (Ardón et al., 2016), and since there is a strong relationship between Hg and DOC

(Ravichandran, 2004), I suggest that these saltwater experienced wetlands may export high amount of Hg to nearby waters (i.e., Winyah Bay and the Atlantic Ocean).

*Sediment THg and MeHg concentrations*

THg and MeHg analyses results for sediment are based on dry mass of sediment (dry wt.), and all findings are exhibited in Figure 2.5 and Appendix B (Table S4). All seasons combined mean THg concentrations in sediment samples were similar in FW (294.17 ± 111.88 ng/g, n = 25) and PDW (209.14 ± 75.13 ng/g, n = 25) but both significantly higher ($p < 0.001$) than SM (87.33 ± 31.47 ng/g, n = 23). Seasonal THg concentrations

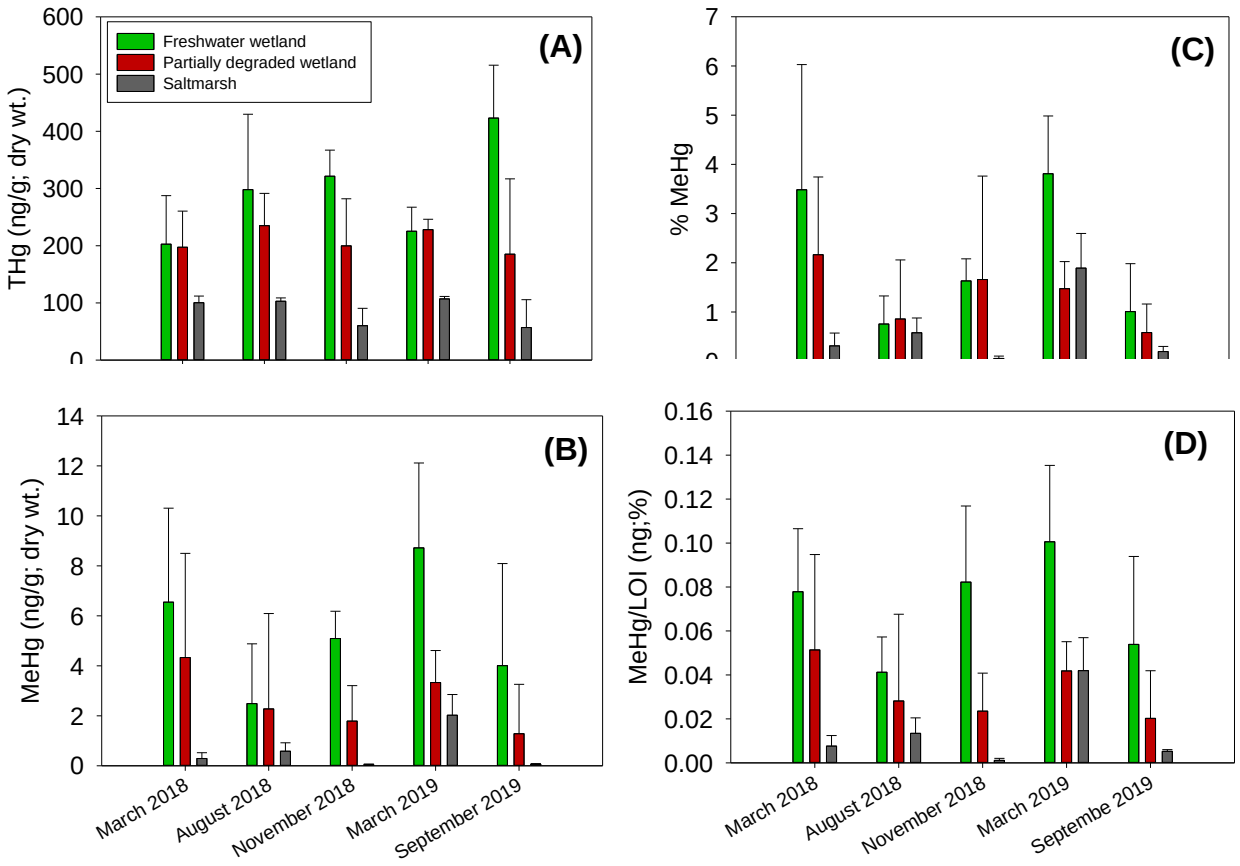


Figure 2. 5: Sediment THg (A), MeHg (B) % MeHg (C), and MeHg/OM (D) concentrations in freshwater wetland, partially degraded wetland, and saltmarsh in different seasons. Error bars represents standard deviation. n = 5, for all seasons and sites except saltmarsh in September 2019 9 (n = 3).

in sediment samples were comparable in the FW (except September 2019; p = 0.048) and PDW but consistently low in SM. However, in SM, THg levels in March 2019 was significantly higher than in November 2018 (P = 0.036) and September 2019 (P =

0.027) (Figure 2.5 A). Interestingly, overall mean MeHg levels significantly decreased ($p < 0.001$) with increasing salinities and were 5.37 ± 3.60 ng/g (n = 25), 2.60 ± 2.79 ng/g, (n = 25), and 0.64 ± 0.86 ng/g, (n = 23), in FW, PDW, and SM, respectively. Although MeHg content was generally similar in each wetland in different seasons, SM sediment MeHg level level in March 2019 were significantly higher than other seasons in SM. This could be due to the highest amount of OM (i.e., 48.01 ± 1.29 %) that existed in that season (Figure 2.5 B).

While a significantly high amount of MeHg production in FW could be because of this site's conducive environment in PDW, salinity could be the critical factor to inhibit MeHg production. Inhibition of MeHg production in PDW and SM could be due to; **(1)** increasing salinities in the order of FW, PDW, and SM, which reduces MeHg production: Previously, few incubation laboratory studies have illustrated that increasing salinities decreases MeHg production in estuarine and coastal sediment. For instance, Blum and Bartha (1980) demonstrated that low salinity (i.e., 1 ppt) levels stimulated Hg methylation while, in general, there was an inverse relationship increasing salinity in estuarine sediment. Similarly, Campeau and Bartha (1987) demonstrated that increasing salinity in incubated estuarine sediments reduced the MeHg levels. However, there are minimal field studies (Boyd et al., 2017) illustrating a negative relationship between MeHg and salinity. On the contrary, Hollweg et al. (2009) and Wu et al. (2011) showed a positive relationship between salinity and sediment MeHg levels in estuaries. **(2)** Elevated $Cl^-$ concentration in the order of FW, PDW, and SM (i.e.,16.6 mg/L, 941.8 mg/L, and 2,813.5 mg/L, respectively): Park et al. (2018) found that elevated levels of $Cl^-$ ions may decrease Hg adsorption from the sediment. This reduction in mercury adsorption is due to the formation of soluble Hg-Cl complexes with a low affinity to freshwater marsh sediment as the soil is mostly negatively charged. Besides, the availability of negatively charged mercuric chloride species $HgCl_3^-$ and $HgCl_4^{2-}$, are limited to the bacteria (Barkay et al., 1997), causing reduced MeHg production in saltwater-affected wetlands. **(3)** High sulfide levels in PDW and SM: High sulfide levels in sediment can form strong ionic bonds with inorganic Hg, therefore, reducing the bioavailability of inorganic Hg to methylating microbes (Lei et al., 2019; Ravichandran, 2004). **(4)** Decreasing primary productivity and tree diversity: The lower amount of

MeHg concentrations in PDW than FW could be due to decreasing tree species allowing more light penetrations and causing photodegradation of MeHg in this site as previously reported (Seller et al., 1996). However, in an area nearby the study site, Tsui et al. (2020) reported that MeHg is less likely to be photodegraded from the ultraviolet (UV) due to the elevated DOM concentrations in the water column in the study conducted at blackwater river. I also checked the % MeHg of sediment samples to find methylation potential of available THg in three wetlands (Figure 2.5 C). Percent MeHg levels were highest in FW during the spring seasons (March of 2018 and 2019). However, PDW and SM showed lower methylation rates, presumably because of the reasons indicated above.

The MeHg produced in coastal areas could significantly contribute to increased Hg levels in bordering marine ecosystems (Chen et al., 2008). Hence, the findings of this study for sediment samples suggest that saltwater intrusion lowers Hg methylation in sediment in PDW and SM, which may ultimately reduce bioaccumulation of MeHg in biota. Even though several laboratory experiment studies demonstrated how increasing salinities reduces MeHg levels in sediment(Blum and Bartha, 1980; Compeau & Bartha, 1987; Gilmour & Henry 1991; Dongmei et al., 2020), to our knowledge, our study is the first to demonstrate the impact of salinity on MeHg production in natural environments.

*Relationship of mercury and organic matter in sediment*

All sites combined, I found a weak, but significant positive relationship ($r^2 = 0.30$, $p < 0.001$; Figure 2.6 A) between THg and OM, consisted to prior studies (Buckman et al., 2017; Tsui et al., 2020). Likewise, MeHg concentrations showed a significant positive relationship with the OM ($r^2 = 0.45$, $p < 0.001$; Fig 2.6 B). Other studies have also reported a significant positive correlation with OM (Tsui et al., 2020; Morris et al., 2014). Interestingly, MeHg and OM relationship differ between sites. FW shows slightly stronger and significant correlation ($r^2 = 0.50$, $p < 0.001$) than PDW ($r^2 = 0.21$, $p = 0.02$) and SM ($r^2 = 0.34$, $p = 0.004$). Weak, but significant relationships observed in both PDW and SM could be due to the reasons speculated above (i.e., High $S^{2-}$ and $Cl^-$). I also normalized the concentration of sediment MeHg to OM to separate mercury methylation due to OM. MeHg levels of sediment in FW still exhibited the highest MeHg levels than

PDW and SM, emphasizing the inhibition of Hg methylation in PDW and SM (Figure 2.5 D). These results suggest that methylation activity inhibited by the presence of elevated salinity (or $SO_4^{2-}$, or $Cl^-$) in PDW, saltwater experienced freshwater wetlands, and SM, may reduce export of THg and MeHg to surrounding water (i.e., Winyah Bay).

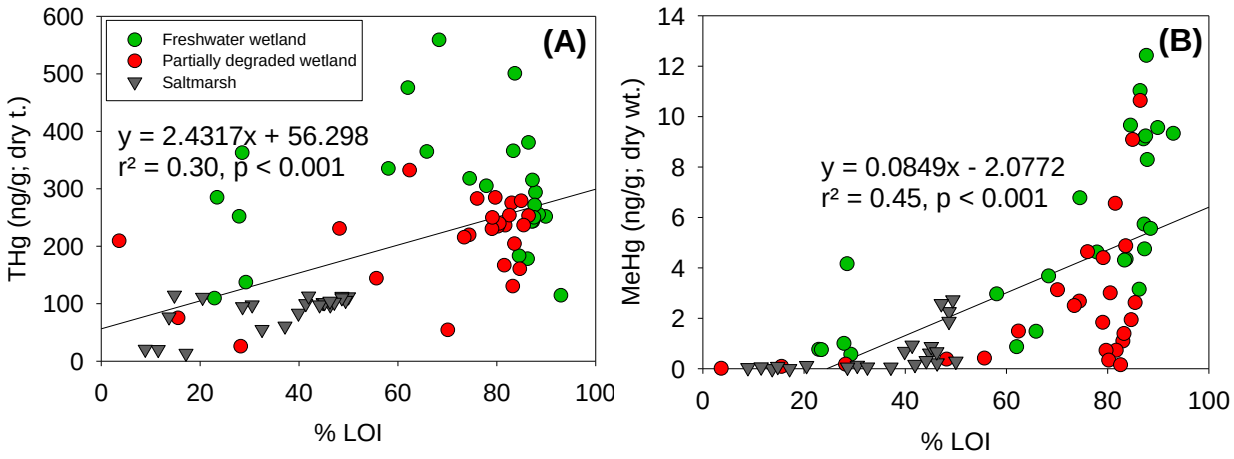


Figure 2. 6: Relationship between THg (A), MeHg (B) concentrations and loss on ignition (LOI) freshwater wetland, partially degraded wetland, and saltmarsh.

*Relationship of water salinity and mercury levels in water and sediment*

During the sampling times, water salinity levels in FW were extremely stable as it has never experienced saltwater intrusion, while PDW and SM showed variation in both surface and groundwater in different seasons (Appendix, Table S1). Generally, surface water and groundwater salinity were positively correlated ($r^2 = 0.69$, $p < 0.001$) except for SM in each wetland. Here, I have shown, overall (sites and seasons combined), groundwater salinity (Figure 2.7) relationship with the mercury levels in sediment samples.

Sediment THg levels were inversely correlated (r2 = 0.49, $p < 0.001$) with the groundwater salinity levels across the sites. Comparably, MeHg levels of sediment showed a weak but significant negative relationship (r2 = 0.18, $p < 0.001$) with surface water salinity levels.

However, when I plot groundwater salinity with sediment MeHg concentrations, the association between the two parameters becomes stronger (i.e., $r^2 = 0.26$, $p < 0.001$), which shows the influence of groundwater salinity larger than surface water salinity on sediment MeHg values (Figure 2.7 B).

In contrast to our findings, Wu et al. (2011) reported a significant positive correlation between MeHg and salinity, while de Oliveira et al. (2015) reported no relationship between MeHg formation and pore water salinity in sediment.

Salinization of wetlands has intensified impacting Hg cycling in coastal environments across the world due to global climate change. These areas are subject to Hg pollution in both the land and water. Therefore, it is vital to assess Hg cycling in saltwater experienced wetlands.

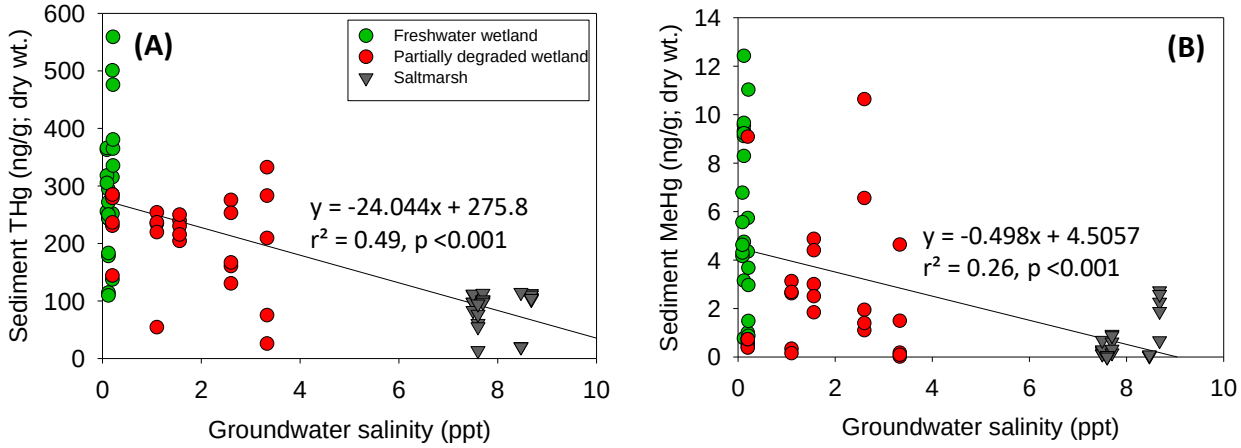


Figure 2.7: Relationship between groundwater salinity and total mercury (A), MeHg levels (B) of sediment in freshwater wetland, partially degraded wetland, and saltmarsh.

Although I found a positive relationship ($r^2 = 0.69$) between salinity and surface water MeHg levels in PDW, the water sample size was not large enough to suggest the association between the two parameters. Perhaps, a more frequent sample collection would be required to better understand the water MeHg and salinity relationship.

In terms of sediment MeHg, our results showed a significant decreasing trend of MeHg concentrations with increasing water salinity levels. I suggest that increasing salinity

levels (i.e., surface and groundwater) can significantly mitigate MeHg levels in sediment and, ultimately, reduce MeHg accumulation in biota.

# CHAPTER III: IMPACT OF HURRICANES ON MERCURY METHYLATION AND ITS TRANSFER TO ADJACENT WATERS


## Abstract

Because of the warming of ocean surface, the frequency and intensity of Atlantic hurricanes are foreseen to rise in the next few decades. Category 4 hurricanes or higher are becoming a more frequent danger to many coastal zones of the southeast United States. In late summer of 2018 and 2019, Hurricane Florence and Dorian caused extensive damages to the North Carolina coast due to storm surge and extensive rainfall. Nevertheless, little is known about the temporal changes, cycling, and transport of mercury (Hg) after the passage of hurricanes. I collected surface water samples from Point Peter (PP) site (i.e., open water, saltmarsh, partially degraded wetland, and freshwater wetland), along the salinity gradient, and relatively more inland site, Timberlake Observatory for Wetland Restoration, (i.e., T-North, T-Middle, and T-South) site before and after hurricanes. I found that while elevated salinities ultimately reduced THg and MeHg levels by reducing dissolved organic carbon (DOC) levels, dissolved oxygen (DO) and sulfate/chloride ($SO^{2-}_4/Cl^-$) ratio are important determinants for MeHg production in water column after the hurricanes in coastal wetlands. Also, stable carbon isotopes ($\delta^{13}C$ - DOC) values of water samples indicated that wetlands in the PP site were the main source of Hg to open water (i.e., Pamlico Sound) and wetland derived $\delta^{13}C$ - DOC persisted in open water for more than two months after Hurricane Florence.


## Introduction

Ongoing global climate change has resulted in increasing global sea level since the past century. According to Nerem et al. (2018), the global mean sea level (GMSL) may increase 65 ± 12 cm by the end of this century compared with 2005. However, relative sea-level (RSL), (i.e., the difference between the sea surface and seafloor's mean height), could be even more than GMSL. For example, estimations from different models suggest that North Carolina (NC) will be experiencing RSL rise in the range of 24 -132 cm by 2100 (Kopp et al., 2015).

Extreme weather events such as hurricanes, tornadoes, and droughts also receive more attention across the world as they occur more frequently (Coumou and Rahmstorf 2012; Trenberth, 2011). Several hurricanes (e.g., Hurricanes Joaquin - 2015, Matthew - 2016, Harvey and Irma - 2017, Florence - 2018, and Dorian - 2019) occurred just within the last five years in the southeast and Gulf coast of the United States. Unfortunately, the frequency and intensity of Atlantic hurricanes are expected to increase in the next few decades (Bender et al., 2010) because of elevated sea surface temperature that is positively correlated with the frequency of hurricanes in the Atlantic Ocean (Hosseini et al., 2018).

Coastal wetlands provide numerous ecosystem services (e.g., storm protection, habitat, water, and food source) and are among the most productive ecosystems on the earth (Nicholls, 2004; Zedler 2003). However, they have been exposed to many chronic (i.e., sea-level rise) and acute (i.e., hurricane, storm surge, and drought) environmental stressors because of their location in the landscape (Cahoon, 2006; White and Kaplan, 2017).

A combination of these factors exacerbates landward saltwater intrusion leading to elevated salinities in low-lying coastal regions (Barendregt & Swarth, 2013). Such events affect freshwater ecosystems (i.e., swamp forests and freshwater marshes) the most because they are incredibly prone to salinity changes in coastal areas (Herbert et al., 2015). The overlap of climate-related stressors further increases salinity levels in these coastal areas. For instance, in North Carolina, this study shows that the 2018 Hurricane Florence brought an enormous amount of saltwater to coastal freshwater wetlands causing more than 50-fold increase in salinity levels.

Hurricanes significantly alter biogeochemical and nutrient cycling in coastal plain wetlands (Michener et al., 1997). However, due to safety reasons and limited access to sampling sites during extreme weather events, only few studies were conducted during, before, and after hurricanes. For instance, Majidzadeh et al. (2017) illustrated that DOC and dissolved organic nitrogen (DON) mobilization increased following Hurricanes Joaquin (2015) and Matthew (2016) in South Carolina. Similarly, Osburn et al. (2019)

showed a significant wetland carbon transfer to adjacent coastal waters because of Hurricane Matthew (2016) in North Carolina. Other studies have focused on the effect of SLR or drought-driven salinity on nutrient cycling in coastal freshwater wetlands (e.g., Ardón et al., 2013; Ardón et al., 2016; Liu et al., 2017).

Aside from hurricanes increasing carbon (C) and nitrogen (N) transfer to nearby waters, mobilization of toxic metals (e.g., mercury) may also pose a potential risk for the environment (Du Laing et al., 2008; Wong et al., 2013). Generally, the speciation and transport of Hg are strongly controlled by dissolved organic matter (DOM) in coastal wetlands (Ravichandran, 2004), where the environmental conditions are ideal for converting inorganic Hg (Hg II) to more toxic and highly bioaccumulative methylmercury (MeHg) (Hall et al., 2008). Thus, extreme weather events (i.e., hurricane, storm surge, and flood) may mobilize Hg from the coastal wetlands (Guentzel 2009; Tsui et al., 2020). However, to our knowledge, only two studies have assessed the impact of hurricanes (storm surge/flooding) on Hg. Liu et al. (2009) investigated how the aftermath of Hurricanes Katrina and Rita (2005) affected sediment Hg biogeochemistry. Tsui et al. (2020), on the other hand, evaluated variation and isotopic compositions of water Hg in the Waccamaw River of South Carolina during the Hurricanes Joaquin (2015) and Matthew (2016). It is crucial to understand Hg cycling in coastal plain wetlands, which is generally considered an important source of MeHg to surrounding waters (Hall et al., 2008) and food webs, especially under extreme weather events such as hurricanes.

Many common fish species already contain high Hg concentrations that surpass the consumption advisory action level (i.e., 0.4 ng/g; wet weight) of North Carolina. Although many fish species are under statewide advisory for Hg, to our knowledge, there has been no study on Hg biogeochemistry and the effects of hurricanes in the coastal regions of North Carolina. Since August 2018, I started collecting water samples to examine SLR and drought-induced salinity impact on Hg cycling from five wetlands located in the coastal zone. Nevertheless, Hurricanes Florence in 2018 and Dorian in 2019 presented an interesting and unique opportunity to investigate before and

aftereffect of the hurricanes (i.e., storm surge) on Hg biogeochemistry over the subsequent year. Our primary goal was to examine the biogeochemical cycling of Hg in wetlands affected by saltwater incursions from hurricane (Florence and Dorian) storm surges in coastal plain wetlands of North Carolina. I hypothesized that MeHg concentration would increase in freshwater wetlands due to salinization after the major hurricane events.

## Materials and Methods

*Study site*

Our sites, Point Peter (PP) and Timberlake Observatory for Wetland Restoration (TOWeR) are in the coastal plain of North Carolina on the Albemarle - Pamlico Peninsula (Figure 3.1). Albemarle-Pamlico Sound is the second-largest estuarine system with no astronomical tides of the Atlantic Ocean because of the barrier islands' protection (Giese et al., 1985; Corbett et al., 2007). In certain areas, the land elevation is one meter (m) under sea level (Poulter and Halpin, 2008), making it vulnerable to storms, sea levels rise, and hurricanes. PP sites are located at the Alligator River Wildlife Refuge in Manns Harbor and include a small forest marsh transect (2.5 km), freshwater wetland (FW), partially degraded wetland (PDW), saltmarsh (SM), and open water (OW; sound). These sites are regularly exposed to extensive saltwater intrusion due to droughts, storm surge, and the proximity of the sites to the open water (Pamlico Sound). TOWeR sites consist of 420 ha mature forested wetland, 787 ha of forested wetland, 57.2 ha of the drained shrub, and 440 ha former agricultural fields that underwent stream and wetland restoration (Ardón et al., 2010). However, our work centers on 440 ha former agricultural fields (Figure 3.1). These sites are more inland compared to PP sites. I established 3 subsites, T-North, T-Middle, and T-South (along a decreasing salinity gradient) based on the water salinity levels and locations. These wetlands have waters with low dissolved oxygen (DO) (e.g., 0.10 - 3.83 mg/L) and elevated DOC (e.g., 4 - 120 mg/L), have been exposed to saltwater intrusion episodically for a long time. This may lead to degradation of freshwater wetland or dynamic changes in ecosystem biogeochemical cycling (Ardón et al., 2013).

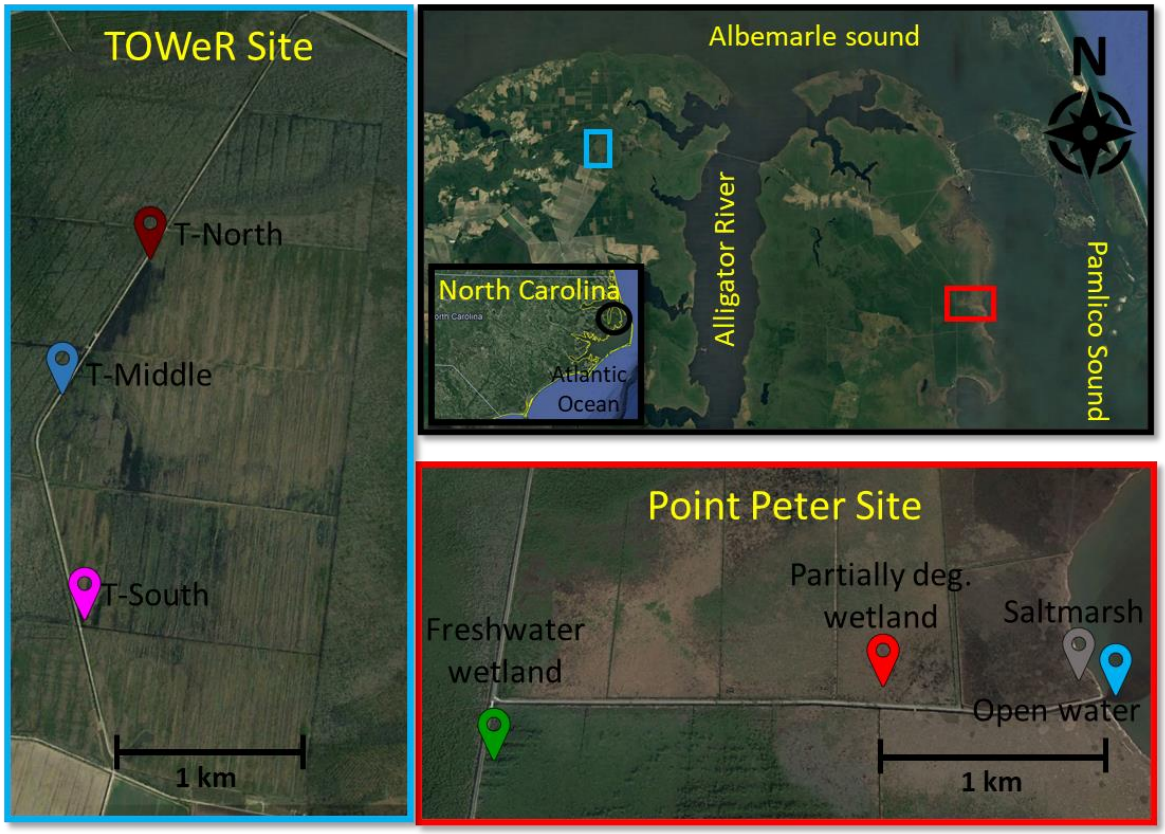


Figure 3. 1: Map of the sample collection locations of Point Peter site (freshwater wetland, partially degraded wetland, saltmarsh, and open water) and Timberlake Observatory for Wetland Restoration (TOWeR; T-North, T-Middle, and T-South) site.

*Sample collection and measurement*

Sample collection was performed 15 times for each site (6 locations plus open water) for a year (June 2018 - December 2019), which included 2 major hurricanes (i.e., Hurricanes Florence and Dorian). To analyze total Hg (THg), methylmercury (MeHg), DOC, stable carbon isotopes ($\delta^{13}C$), and other water quality data (e.g., sulfate, chlorine, dissolved oxygen, conductivity, temperature, and pH), surface water (n = 182) samples were collected with acid-washed Teflon bottles and immediately placed into a cooler.

During each water sampling time, water quality parameters such as dissolved oxygen (DO), conductivity (mS/cm), and temperature (℃) were conducted with a handheld YSI probe (PRO 2030). The whole water samples were filtered (Whatman GF/F, 0.7 µm), subsampled, and preserved for THg, MeHg, and water quality analysis in the ecotoxicology and biogeochemistry laboratory at the University of North Carolina, Greensboro (UNCG). Subsamples were sent to North Carolina State University (NCSU) for water quality, anions, and stable carbon isotope analysis.

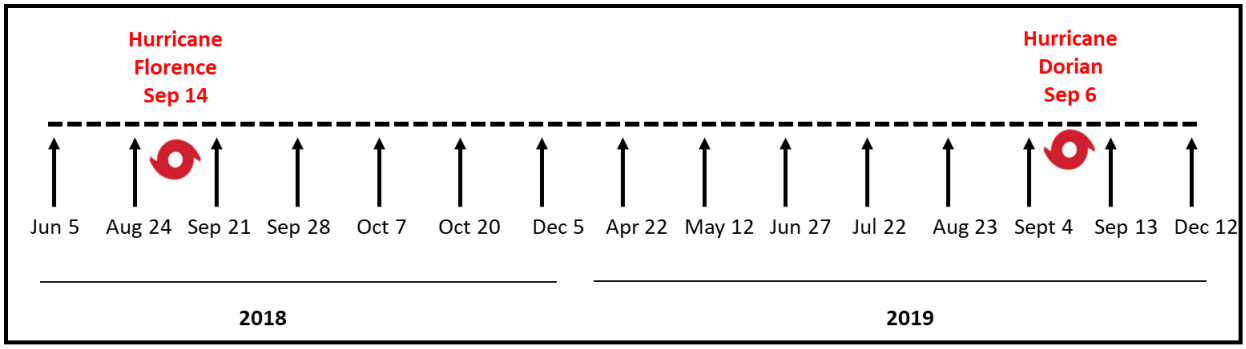


Figure 3. 2: Timeline of water sampling in Point Peter and TOWeR sites.

*Processing and analysis of samples for THg and MeHg*

Water THg and MeHg processing, digestion, and analysis techniques are described in the method section of chapter II.

*Sample processing and analyses of water $SO_4^{2-}$, $Cl^-$, DOC, and $\delta^{13}C$ - DOC*

Water $SO_4^{2-}$, $Cl^-$, and DOC were analyzed on a Metrohm 930 Flex Ion Chromatograph using chemical suppression and conductivity detection (EPA 300.1) and on a Teledyne Tekmar Torch TOC combustion analyzer with a total nitrogen module at North Carolina State University's Department of Forestry and Environmental Resources.

*Statistical analyses*

Data analyses were performed by using SigmaPlot 12.5 (Systat) software and the significance were tested $\alpha = 0.05$.

## Result and Discussion

*Surface water quality parameters*

All the water quality illustrations are shown in Appendix C (Table S1). Conductivity (which is a proxy for salinity) levels were dynamic and showed substantial variations across the sites and seasons. Overall, both SM and PDW conductivity levels were significantly higher than freshwater wetland ($p = < 0.001$). Temporal variations of conductivity were also sharp and influenced by the hurricanes (Florence and Dorian) and droughts. For example, during June and August (2018), average conductivity levels were 0.13 (mS/cm) in freshwater wetland (Table S1). However, a month later (21 September), conductivity levels increased 60-fold (7.99 mS/cm) due to Hurricane Florence (Appendix C; Table S1). Both $SO_4^{2-}$ and $Cl^-$, levels were well correlated ($r^2 = 0.90$ and 0.93) with all three wetlands' conductivity values. However, sharp increases were observed in DO levels after the hurricanes. DO levels were similar and low during the spring and summer in three wetlands.

*Surface water THg and MeHg levels*

Generally, Point Peter sites' (OW, SM, PDW, and FW) THg and MeHg levels were high and showed high variation in summer and fall seasons. THg and MeHg levels did not indicate a significant difference among the wetlands (SM, PDW, and FW) in both seasons, but OW site recorded a significantly lower THg and MeHg levels than the wetlands (Figure 3.3 A, B, E, and F).

In winter, THg and MeHg (except OW) values were similar across the wetlands (SM, PDW, and FW). While THg levels in the spring season were highest in FW, MeHg levels were similar among the wetlands but lowest in OW (Figure 3.3 D H). The high variations of THg and MeHg in water samples (figure 3.3 A, B, E, and F) could be due to increased saltwater intrusion in summer and fall compared to winter and spring (see details in subtitle "Association of salinity, DOC, and Hg"; figure 3.9 A)

I also looked at the temporal variation of Hg levels across the seasons for each wetland by using One Way Repeated Measures Analysis of Variance for each site. THg and MeHg levels were similar among the seasons in both OW and FW sites. However, the highest THg and MeHg occurred in summer, while other seasons showed no significant difference in both PDW and SM except for spring MeHg in SM (Figure 3.3).

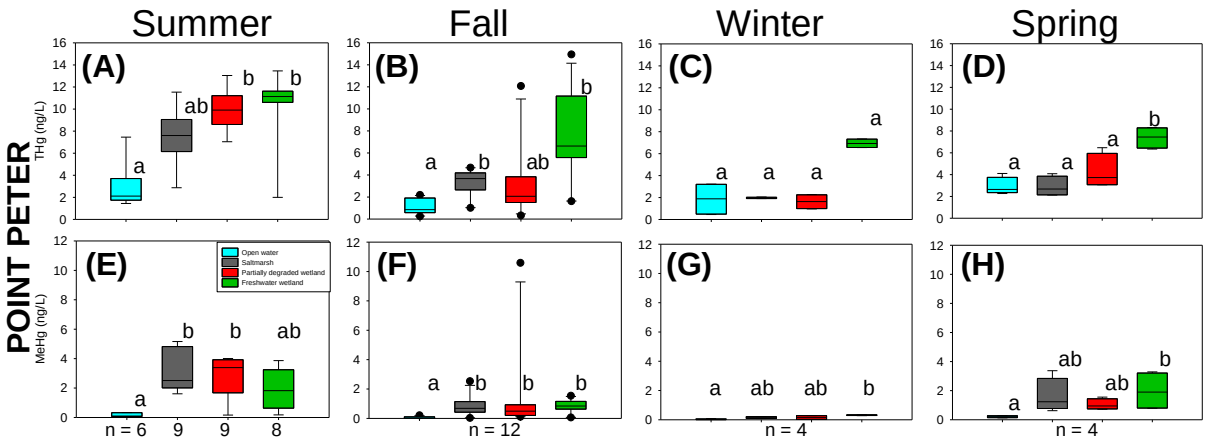


Figure 3. 3: Boxplots of water total mercury (THg) and methylmercury (MeHg) concentrations in summer (A & E), fall (B & F), winter (C & G), spring (D & H) in Point Peter site. Blue, grey, red, and green colors represent open water, saltmarsh, partially degraded wetland, and freshwater wetland, respectively. Different letters indicates significant difference between the bars in each figure ($p < 0.05$).

In the TOWeR site, there were no statistically significant differences in THg levels among the sites (Figure 3.4). Similarly, MeHg values were similar in summer and winter seasons among the sites, but in the fall season, the T-North site recorded a significantly higher MeHg value than T-Middle and T-South. The highest MeHg levels (0.82 ng/L) in T-North site occurred with the highest salinity (2.13 mS/cm) and DOC levels (28.24 mg/L). In spring, T-South was significantly lower than T-North and T-Middle. Temporal

variation of THg and MeHg in each wetland revealed no statistically significant difference among the seasons (Figure 3.4).

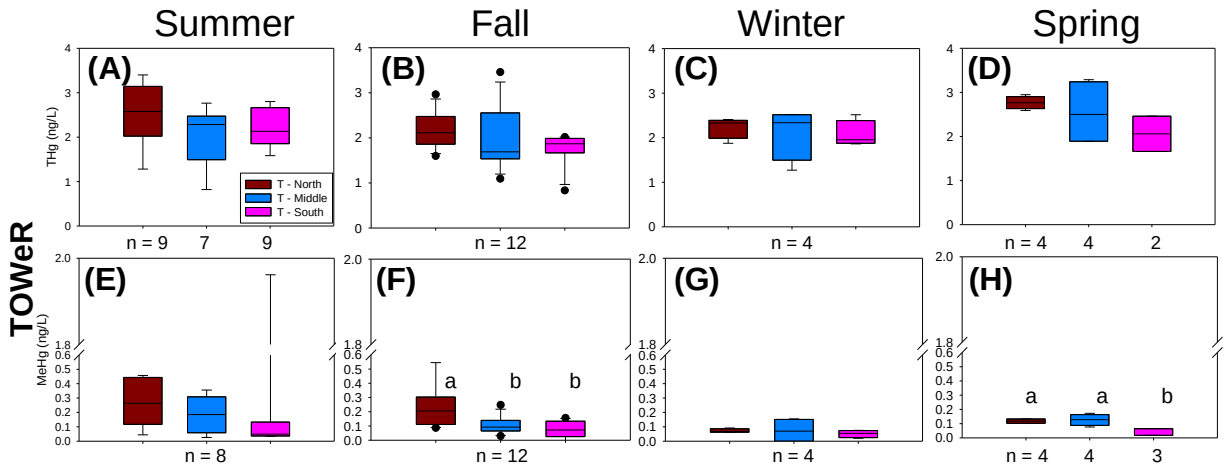


Figure 3. 4: Boxplots of water total mercury (THg) and methylmercury (MeHg) concentrations in summer (A & E), fall (B & F), winter (C & G), spring (D & H) in TOWeR site. Brown, blue, and purple colors represent T-North, T-Middle, and T-South, respestively.Different letters indicates significant difference between the bars in each figure ($p < 0.05$).

*Relationship between mercury and dissolved organic carbon*

Concentrations of DOC showed high variation in each site, and the highest DOC levels ($p < 0.001$) were detected in the freshwater wetland at the Point Peter site (Figure 3.5.A). The high variation of DOC concentrations in these sites could be due to salinity changes influenced by tides, winds, droughts, and hurricanes. The low levels of DOC in PDW and SM may be due to vegetation degradation (based on observation) in these areas. Although THg levels were positively correlated with DOC levels (Figure 3.5.C; $r^2 = 0.51$, $p < 0.001$), MeHg levels revealed no correlation with DOC at PP sites.
Unlike the PP sites, DOC concentrations showed less variation in each wetland of TOWeR site (Figure 3.5.B), and our mean DOC values corresponded with a long-term study in the same area (Ardón et al., 2016). THg levels indicated a weak but

significantly positive relationship ($r^2 = 0.13$, $p < 0.001$) while there was no significant correlation between MeHg and DOC (Figure 3.5.D). The positive relationship between THg and DOC levels were also observed in many other studies (Tsui et al., 2020; Tsui & Finlay, 2011) and generally attributed to instances where Hg is originated and released from wetlands and soils (Ravichandran, 2004). It is somewhat surprising that no relationship was found between MeHg and DOC, which may be due to various parameters (i.e., DO, salinity, and sulfate) that control Hg methylation.

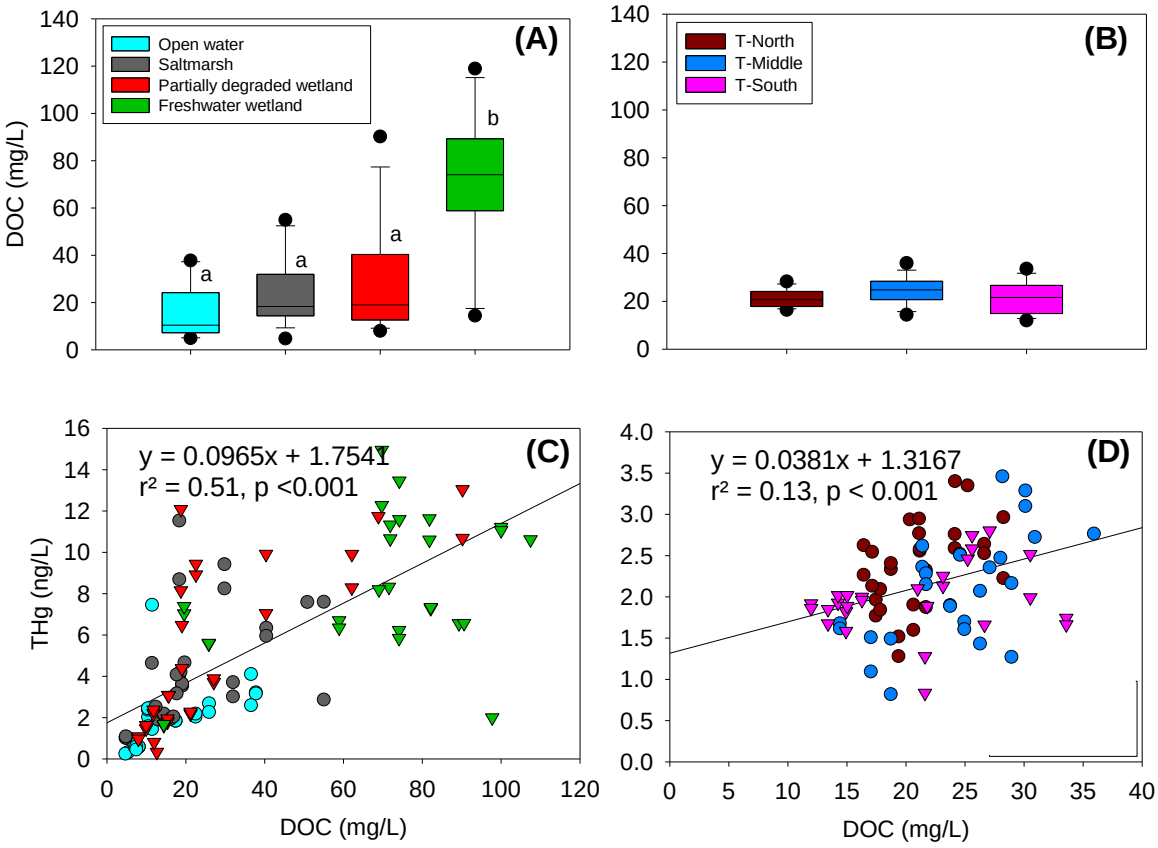


Figure 3. 5: Water dissolved organic carbon (DOC) levels in Point Peter site (A), TOWeR site (B) and total mercury (THg) and dissolved organic carbon relationship in Point Peter (C) and TOWeR (D) sites.

*Impact of Hurricanes Florence and Dorian on mercury cycling and its transport to adjacent waters*

I used $SO^{2-}_4/Cl^-$ (normalization of sulfate by chloride levels) ratios and DO concentrations to understand the source of saltwater, indication of sulfate reductions, and their effects on MeHg before and after the passage of the hurricanes.

DO levels drastically rose right after Hurricanes Florence and Dorian in all sites (Figure 3.6). This is supported by a prior study that reported increased DO values in water column following hurricane Katrina in coastal areas of Gulf of Mexico (Smith et al., 2009). Generally, anoxic environments are considered hot spots for Hg methylation (Compeau & Bartha, 1985). Thus, increases in DO levels that usually follows hurricanes may suppress MeHg production in water and sediment.

Moreover, the observed increment in $SO^{2-}_4/Cl^-$ ratios after hurricanes indicates less sulfate reduction during these times. Ardón et al. (2013) suggested that during the saltwater intrusion, $Cl^-$ were transferred further upstream (further landward) than $SO^{2-}_4$ levels in coastal wetlands. This mainly happens as a result of conservative movement of $Cl^-$ and microbial usage of $SO^{2-}_4$, and therefore the ratio of $SO^{2-}_4/Cl^-$ generally diminishes with increasing distance from the source of saltwater (Ardón et al., 2013). For example, the mean $SO^{2-}_4/Cl^-$ ratio in Point Peter sites decreased from the source, open water, (0.13 ± 0.01) landward in order of SM (0.08 ± 0.03), PDW (0.06 ± 0.03), and FW (0.044 ± 0.02).

One of the indicators of $SO^{2-}_4$ reduction is the decrease in the ratio of $SO^{2-}_4/Cl^-$(Alpers et al., 2014) as $SO^{2-}_4$ is reduced to $H_2S$ by sulfate reducing bacteria (SRB). In all sites (except open water) $SO^{2-}_4/Cl^-$ ratios were boosted right after hurricane Florence made the landfall (Sept.14.2018) in NC (Figure 3.6). Opposite trend was reported after Hurricane Dorian except for SM, PDW, and T-South sites. As I mentioned earlier in the introduction part (chapter I), inorganic mercury is converted to organic mercury (MeHg) during the metabolism of organic matter by SRB. Hence, decreasing $SO^{2-}_4/Cl^-$ ratios generally implies MeHg production in these coastal zones.

Although I hypothesized that MeHg levels in water column will increase due to sulfate that is brought by storm surge, the decrease in MeHg levels in SM, PDW, T-South, while FW and T-North sites showed no difference after hurricane Florence (Figure 3.6). Similarly, increases of water MeHg values in the T-Middle site may be due to low DO and high $SO^{2-}_4/Cl^-$ content. Interestingly, after Hurricane Dorian MeHg levels appeared to be elevated in SM, PDW, T-North, T-Middle, and T-South but not FW.

Variations in water MeHg levels could be attributed to shifts in DO concentrations influencing sulfate reducing activity as SRB (obligated anaerobes) thrive in anoxic environment. For instance, after Hurricane Florence, MeHg concentrations were declining as DO level were rising, however, in the same wetland after Hurricane Dorian, MeHg values escalated with the existence of low DO values. Historic amounts of torrential rainfall and winds after Hurricane Florence could be the cause for high levels of DO (Kunkel & Champion, 2019) as generally rainfall is positively correlated with the DO levels. Therefore, I suggested that the amount of DO and $SO^{2-}_4/Cl^-$ brought by hurricanes are important determinants for MeHg production in water columns in coastal waters.

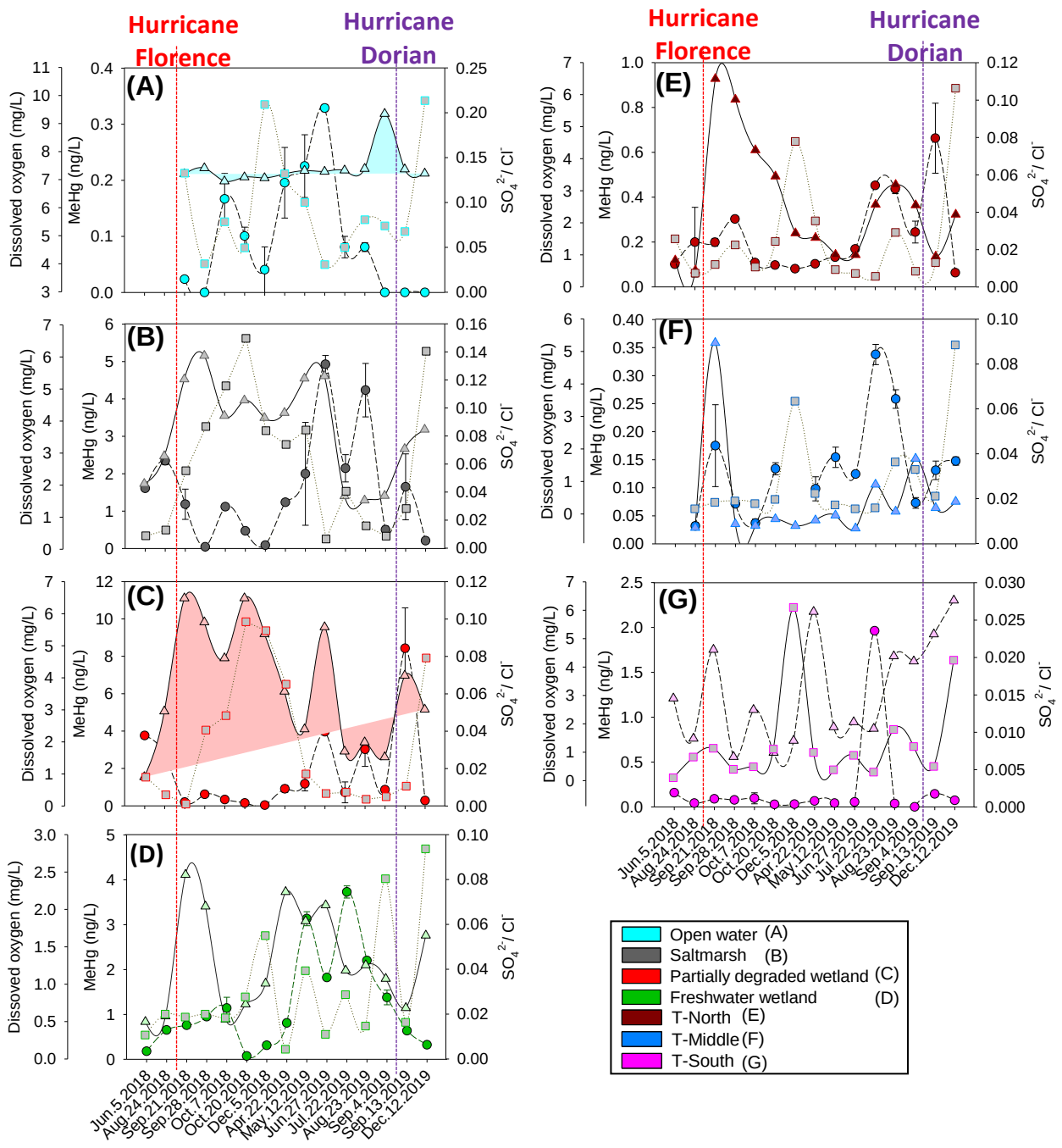


Figure 3. 6: Water methylmercury (circle), sulfate/chloride (triangle), and dissolved oxygen (square) concentrations in open water (A), saltmarsh (B), partially degraded wetland (C), and freshwater wetland (D) and T-North (E), T-Middle (F), and T-South (G).

*Understanding of Hg transport to nearby waters by utilizing carbon isotopes of water*

Water samples for $\delta^{13}C$ - DOC analysis were collected before (Jun. and Aug 2018) and after hurricane Florence (Sep., Oct., and Dec 2018) in all wetlands, except open water (only in Sep., Oct., and Dec 2018) site (Figure 3.7 C and F). I have exploited $\delta^{13}C$ - DOC values to confirm that wetlands are the main source of Hg to adjacent waters (e.g., Pamlico sound) at least in our study system.

Generally, $\delta^{13}C$ - DOC values of C3 plants range from -32 to -19 ‰ while C4 plants range from -16 to -10 ‰ (Xia et al., 2021). On the other hand, marine derived organic carbon (e.g., phytoplankton) varies between -18 and -22‰ (Kelley et al., 1998). Our $\delta^{13}C$ - DOC values range between -28.83 to -26.27 ‰, with an average value of -27.64 ± 0.79‰ (n = 22) in all wetlands at PP site (Figure 3.7 A and B). Interestingly, mean $\delta^{13}C$ - DOC value of open water site (Pamlico sound) was -27.57 ± 0.82 (n = 4) suggesting $\delta^{13}C$ values are terrigenous wetland derived $\delta^{13}C$ - DOC for more than two months after Hurricane Florence which suggested that wetland derived $\delta^{13}C$ - DOC persisted in these waters for a while. Although I do not have any prior $\delta^{13}C$ - DOC data for the OW site (i.e., Pamlico Sound) before Hurricane Florence, Osburn et al. (2019) reported a mean $\delta^{13}C$ - DOC level of -24.6 ± 0.8 ‰ indicating lack of wetland derived DOC in the Pamlico Sound. In TOWeR site (Figure 3.7 D and E), I did not observe any variation of $\delta^{13}C$ - DOC values (except T-North, Sep. 21) as the mean $\delta^{13}C$ - DOC values were -28.91 ± 0.37 (n = 16).

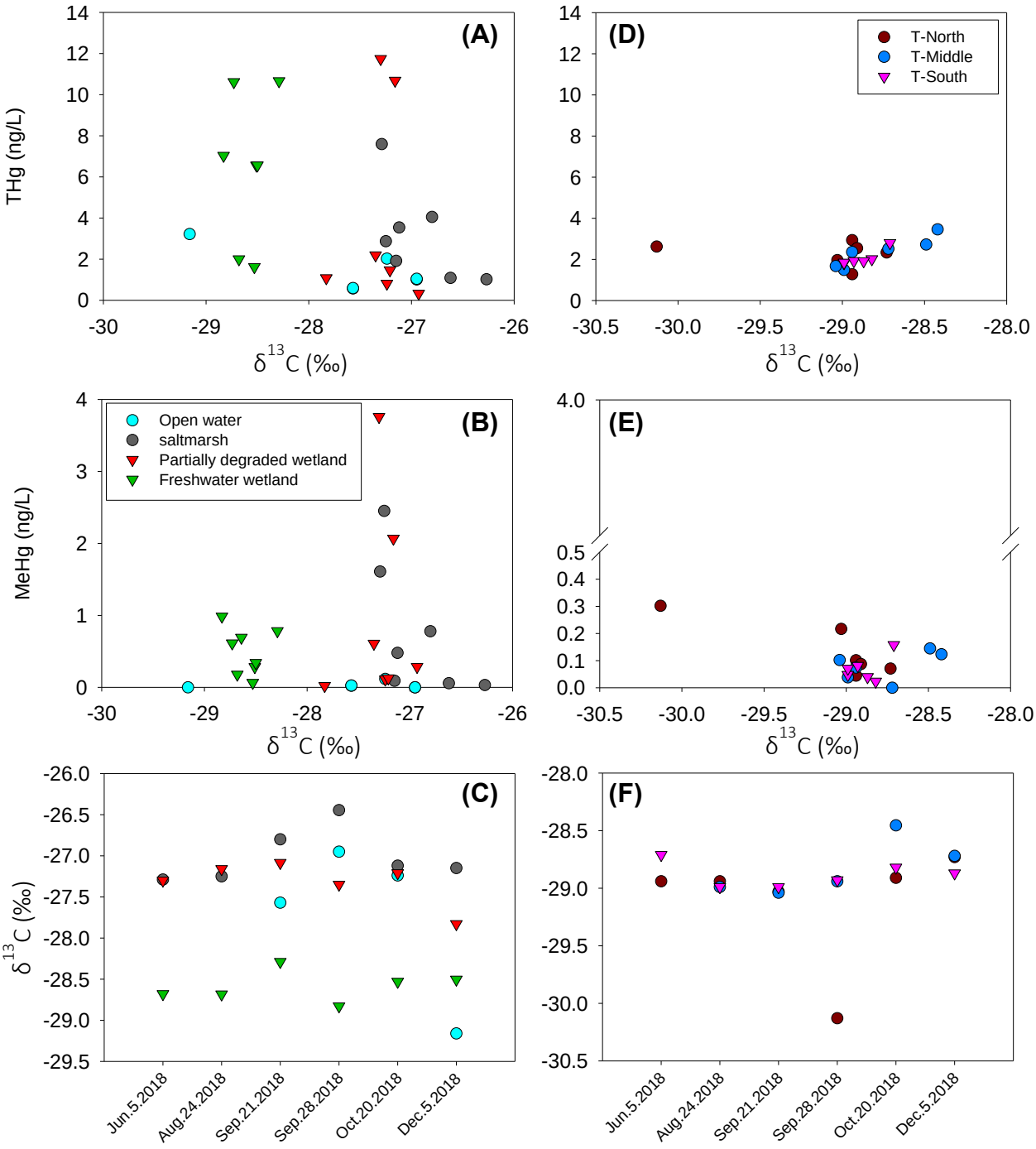


Figure 3. 7: Relationship between THg and δ13C in Point Peter site (A) and TOWeR site (D), MeHg and δ13C in Point Peter site (B), and TOWeR site (E), and δ13C levels in different dates in Point Peter (C) and TOWeR (F) sites.

*Association of salinity, DOC, and Hg*

I report a strong influence of salinity (a proxy of conductivity) on DOC levels in the Point Peter site in this study. There was a significant negative relationship ($r^2 = 0.29$, $p < 0.001$) between DOC and salinity levels in these wetlands and open water (Figure 3.8 A). Ardón et al. (2016) conducted a long-term field and laboratory studies on the combination of drought and increased salinity impact on DOC in the TOWeR sites. Both the field, and microcosm experiments suggested that DOC levels declined in response to drought and salinity. I did not observe any relationship between these two parameters in the TOWeR sites (Figure 3.8 B). This could be mainly because of the low salinity values (generally < 1 mS/cm) recorded in these wetlands during the study period.

In the PP sites, while there was a strong positive relationship between THg and DOC levels (Figure 3.5 C), DOC levels showed a strong negative relationship with salinity (Figure 3.8 A).

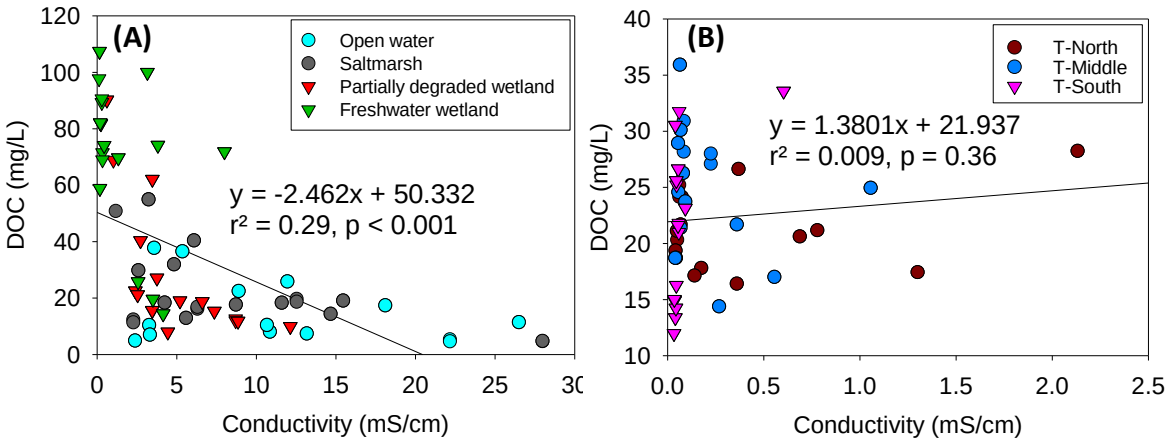


Figure 3. 8: Relationship between dissolved organic carbon (DOC) and conductivity levels in Point Peter (A) and TOWeR (B) sites.

Comparably, THg, and MeHg also displayed a negative relationship with salinity in these wetlands. On the other hand, I did not observe any relationship between THg and salinity levels in the TOWeR site (Figure 3.9 C), while a positive correlation was found between MeHg and salinity (Figure 3.9 D).

Overall, increasing salinity indirectly altered THg and MeHg levels by reducing DOC levels in these wetlands (Figure 16C, 17B, 18A, and 18B).

Climate change can cause temperatures to rise in the ocean surface. Hence, frequency and intensity of Atlantic hurricanes is expected to grow and alter biogeochemistry of coastal wetlands in this century. For example, in 2018 and 2019 Hurricanes Florence and Dorian generated extensive ecological damages and long-term consequences of damages are still unknown. Here I explored the temporal changes, cycling, and transport of mercury (Hg) after the passage of hurricanes.

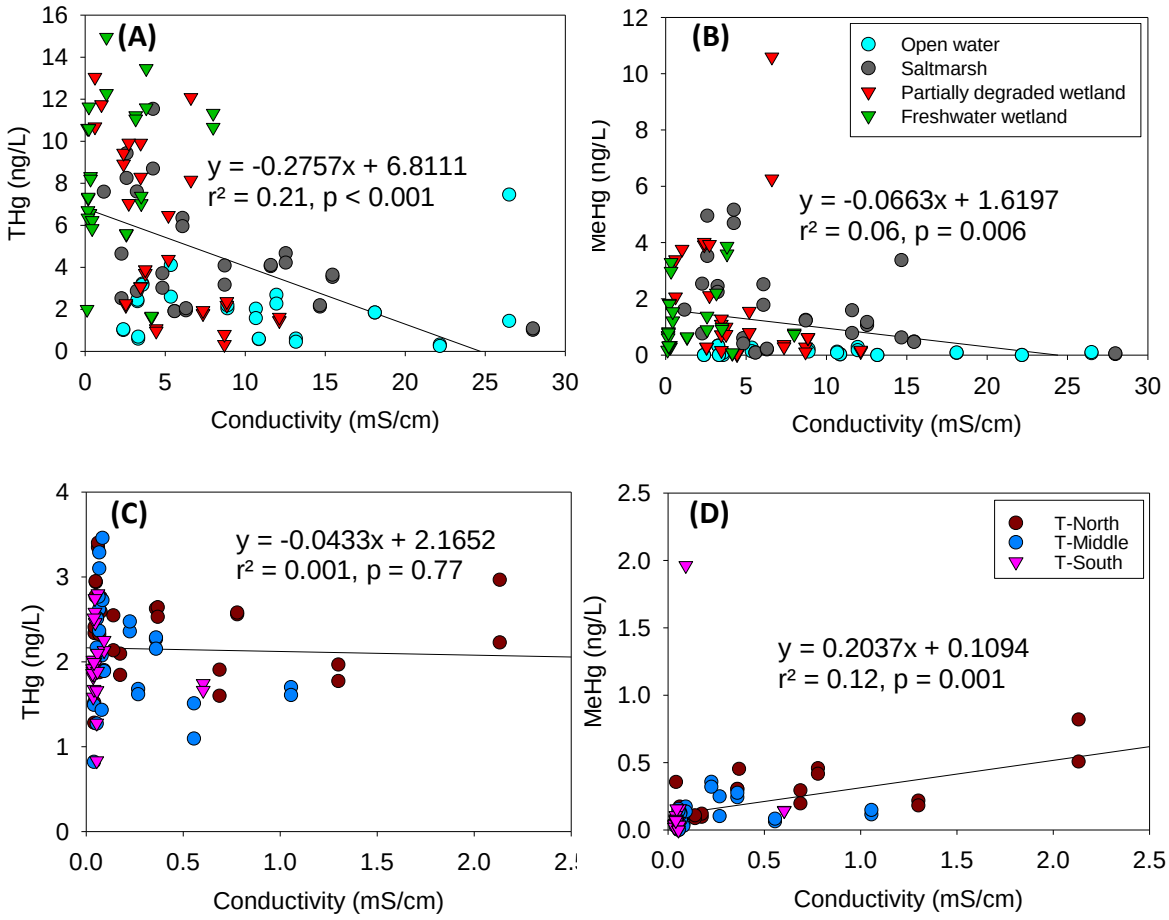


Figure 3. 9: Relationship between total mercury (THg), methylmercury (MeHg) and conductivity levels in Point Peter (A and B) and TOWeR (C and D) sites, respectively.

I found that regular saltwater intrusion (PP sites) increases water overall THg and MeHg levels compared to episodic saltwater intrusions (TOWeR sites). Specifically, our findings suggested that storm driven elevated salinities ultimately lessened water THg and MeHg levels by reducing DOC levels, while, generally, DO and $SO^{2-}_4/Cl^-$ ratio was a

crucial element to predict MeHg production in water column after the passage of hurricanes in coastal wetlands. Moreover, water $\delta^{13}C$ - DOC levels revealed that wetlands in PP site were the major source of Hg to neighboring open water (i.e., Pamlico sound).

# CHAPTER IV: UTILIZATION OF STABLE ISOTOPES TO ASSESS BIOACCUMULATION AND TROPHIC TRANSFER OF MERCURY IN SALTWATER AFFECTED COASTAL WETLANDS


## Abstract

Concentrations of THg, MeHg, and stable isotope ratios ($\delta^{13}C$, $\delta^{15}N$, and $\delta^{34}S$) were assessed in sediment, plant, and multiple organisms (e.g., fish, crayfish, crab, shrimp, and dragonfly larvae) from a coastal plain wetland food web at Georgetown, South Carolina. I studied the salinity effect on Hg bioaccumulation in food web in the natural forest-marsh salinity gradient. I collected plant and invertebrate samples five times in different seasons (i.e., spring, summer, and fall) in freshwater wetland (FW), partially degraded wetland (PDW) and saltmarsh (SM). Sediment THg and MeHg concentrations were negatively associated with $\delta^{13}C$ values (THg: $r^2 = 0.16$, $p = 0.005$; MeHg: $r^2 = 0.1551$, $p = 0.007$), while no correlations were found in $\delta^{15}N$ values in all sites. $\delta^{13}C$ values of sediment were similar in FW and PDW but different in SM. I detected a declining trend and large difference in median values of fish THg and MeHg levels in FW, PDW, and SM, respectively. However, average MeHg levels (FW, 241.35 ng/g; PDW, 153.77 ng/g; SM, 42.98 ng/g) were not different in FW and PDW, but both sites were significantly higher than SM. There was also a significant negative relationship between salinity (surface and groundwater) and MeHg levels both in fish and crayfish. Generally, $\delta^{13}C$ and $\delta^{15}N$ values well separated carbon source and trophic levels among the sites. Log MeHg levels and $\delta^{13}C$ values were negatively correlated while MeHg was positively correlated with $\delta^{15}N$ in invertebrates across the wetlands.

## Introduction

The most critical step of Hg cycling is bioaccumulation and biomagnification in the food web. This step is controlled by various biogeochemical, physical, and ecological processes, which leads to the dissimilarity in Hg levels between regions and individuals (Chen et al., 2008). The concentrations of Hg in biota have been related to a variety of environmental factors, including water parameters, MeHg bioavailability, the structure of the food web, and the age and size of the organism (Lange et al., 1993; Munthe et al., 2007; Selch et al., 2007; Sherman & Blum, 2013). Both inorganic Hg and MeHg are bioconcentrated by plankton and transferred to primary consumers and food web through consumption (Chen et al., 2012).

The structure of the food web alters MeHg; therefore, the combination of the stable isotopes is commonly used to evaluate MeHg accumulation in the aquatic and terrestrial food webs. Thus far, numerous studies have used stable isotopes (e.g., sulfur, carbon, and nitrogen) to trace organic matter flow and trophic relations in the food web (Fry, 2002; Fry & Chumchal, 2012; Peterson et al., 1985). The ratio of stable carbon isotopes ($^{13}C$ / $^{12}C$ or $\delta^{13}C$) provide information to understand energy source as $\delta^{13}C$ values shift ~ +0.4 ‰ per trophic level in the food web (Chételat et al., 2020).

Besides, the differences in stable isotope ratios of carbon in C3 plants (i.e., upland plants) and C4 plants (i.e., *Spartina alterniflora*) allows the understanding of the energy source of the food web. In contrast, nitrogen stable isotope ratios ($^{15}N/^{14}N$ or $\delta^{15}N$) are utilized to understand the trophic level of species in the food web (Peterson et al., 1985) because $\delta^{15}N$ tend to increase approximately 3 to 4‰ per each trophic level.

Sulfur stable isotope ratios ($^{34}S/^{32}S$ or $\delta^{34}S$) are generally used as an extra tool to distinguish energy flow in estuaries (with variations of salinity) when it is used along with C and N isotopes (Tiunov, 2007).

Although previous studies have investigated MeHg availability or bioaccumulation in freshwater ecosystems, there are fewer research investigating bioaccumulation of MeHg in saltwater affected coastal wetlands. For example, Barkay et al. (1987)

conducted a laboratory experiment and suggested that negatively charged Hg(II) species are less available for the bacteria therefore less accumulation of MeHg occurs in estuarine biota than freshwater (Barkay et al., 1997). Another laboratory study concluded that dietary uptake and elimination of Hg(II) as well as MeHg was not impacted by salinity while aqueous uptake would be significantly affected by salinity in *Oreochromis niloticus* (Wang & Wang, 2010). Nevertheless, there are only few works that investigated MeHg bioaccumulation in saltwater impacted natural ecosystems.

In this chapter, I aimed to address the bioaccumulation of MeHg in saltwater affected coastal wetlands, (i.e., FW, PDW and SM) in Winyah Bay, South Carolina. I hypothesized that MeHg bioaccumulation would be the highest in saltwater impacted freshwater wetland (i.e., PDW).

## Materials and Methods

### *Study sites*

Invertebrate sampling locations (forest-marsh transect) is described in the method section of chapter II. These wetland sites are located at Georgetown, South Carolina, which includes a freshwater wetland, partially degraded wetland, and saltmarsh (Figure 2.1).

### *Field sampling and sample processing*

All field sampling was conducted five times in 2018 (March, August, and November) and 2019 (March and September). During the field trips, basic water quality parameters such as dissolved oxygen (DO), conductivity (as a proxy for salinity), and temperature were measured in-situ (YSI probe, PRO 2030).

Mosquitofish (*Gambusia affinis*), Crayfish (*Procambarus troglodytes*), Dragonfly larvae (*Anax Junius; Epicordulia sp.*), Fiddler crab (*Ocypodidae*), and White shrimp (*Litopenaeus setiferus*) were collected by using a rectangular style kick-net and handpicking with non-powder gloves to decrease inadvertent contamination from three sites. In subsequent sampling, invertebrate samples were thoroughly rinsed with

deionized water in the field and transported on ice in a cooler to the analytical laboratory at UNCG. Before analysis, invertebrate and fish samples were lyophilized (VirTis benchtop K) and ground with agate mortar and pestle. Homogenized samples were stored in 50 ml polypropylene centrifuge tubes (Falcon) for subsequent THg, MeHg, and stable C, N, and S isotope analysis.

*Sample digesting and analysis for THg and MeHg*

Homogenized invertebrate and fish samples were weighed (~0.01 g) into 40 mL borosilicate glass vials before the addition of trace metal grade $HNO_3$ and $H_2O_2$ in a ratio of 4:1, respectively. This step was followed by heating at 80 ℃ in a water bath overnight.

THg analyses were performed by adding the desired amount (based on the Hg content; 0.1 - 1 ml) of digested samples into a glass bubbler filled with ~100 mL nanopure water. Subsequently, 200 µL of 20% Tin(II) chloride ($SnCl_2$; Alfa Aesar) was added to the bubbler to reduce Hg(II) to elemental Hg(0). Finally, Hg(0) was purged together with Hg-free nitrogen ($N_2$) gas for 15 min to concentrate Hg(0) into a gold trap. Hg(0) was then heat-desorbed and measured using the Brooks Rand Model III cold vapor atomic fluorescence spectrometer (CVAFS) (USEPA, 2002).

For MeHg analysis, I added approximately 0.01 g of homogenized invertebrate samples into 15 mL polypropylene centrifuge tubes (Falcon). Extraction of MeHg was performed by adding 6 mL of dilute $HNO_3$ (4.6 M) at 60 °C water bath for 12 h (Hammerschmidt and Fitzgerald, 2005) for subsequent MeHg analysis.

To analyze MeHg in biota samples, digested aliquots (10 - 500 µL) were transferred into 100 ml of nanopore water in glass bubblers after the addition of 200 µL $CH_3COONa$. To neutralize aliquots of the acid digests, KOH was used, and finally, samples were ethylated via an ice-cold 1% NaB(Et)4 for 25 minutes. Quantification of MeHg was performed by Brooks Rand Model III CVAFS with an isothermal GC separation and pyrolysis, as described above. The average of standard reference materials (SRM; ng/g) recoveries with certified values for each batch is included below.

Table 1: Average standard reference materials (ng/g) with certified values.

| SRM | Description | THg | n | MeHg | n |
|---|---|---|---|---|---|
| DORM 4 | National Research Council of Canada (THg 410±55) | 371.51±13.66 | 7 | NA | NA |
| TORT 2 | National Research Council of Canada (MeHg 152±13) | NA | NA | 148.12±9.55 | 12 |

*$\delta^{13}C$ and $\delta^{15}N$ analysis for sediment and invertebrate (plus $\delta^{34}S$) samples*

Selected sediment and invertebrate samples were homogenized and freeze-dried before being weighed into tin capsules and encapsulated for stable isotope analysis. Biota samples were analyzed using gas isotope-ratio mass spectrometry at Colorado Plateau Stable Isotope Laboratory at Northern Arizona University, and and using PDZ Europa ANCA-GSL elemental analyzer interfaced to a PDZ Europa 20-20 isotope ratio mass spectrometer (Sercon Ltd., Cheshire, UK) at the University of California, Davis Stable Isotope Facility for $\delta^{13}C$, $\delta^{15}N$, and $\delta^{34}S$. Sediment samples were analyzed with Isotope Ratio Mass Spectrometer Delta-V at Swiss Federal Institute for Forest, Snow and Landscape Research for $\delta^{13}C$ and $\delta^{15}N$.

*Statistical analyses*

All statistical analyses were performed using SigmaPlot 12.5 (Systat) software.

## Result and Discussion

*Mercury levels in macroinvertebrate and fish samples*

To compare Hg levels in boxplot graphs, I included only mosquitofish and crayfish (both dry weight) as both were ubiquitous throughout all the sites. However, crayfish inhabits only freshwater and brackish ecosystems (FW, PDW); thus, I collected crabs (mud crab and fiddler crab) in SM to substitute crayfish Hg levels as they are all crustaceans. MeHg concentration in mosquitofish samples varied (34.68 ± 15.5 and 252.82 ± 56.9

ng/g) among the sites. THg levels (a proxy of MeHg) of mosquitofish reported in the Florida Everglades (i.e., 68 ± 54 and 100 ± 90; wet weight; dry and wet season) (Liu et al., 2008) and Okefenokee Swamp (i.e., < 70 ng/g; wet weight) (Beganyi & Batzer, 2011). I observed a decreasing trend and large difference in median values of fish THg and MeHg levels in the order of FW, PDW, and SM. However, THg and MeHg levels were statistically similar in FW and PDW, but both sites were significantly higher than SM (Figure 4.1 A and B; $p < 0.001$, indicated with asterisk symbol). Decreasing MeHg concentrations in the fish tissue could reflect sediment MeHg levels, which were also declined in the same order due to saltwater intrusion (chapter II). Another explanation could be the formation of mercuric chloride (Hg-Cl) complexes (i.e., $HgCl^{-}_{3}$, $HgCl_4^{2-}$) in saltwater experienced wetlands (PDW and SM). Generally, uncharged Hg-Cl complexes (i.e., $HgCl_2$) are more available than anionic Hg-Cl forms for the methylating bacteria (Ullrich et al., 2001). Therefore, the accumulation of MeHg in biota tissues was highest at FW and lowest in SM. Likewise, average crayfish tissue THg and MeHg levels in both FW and PDW were similar, but crab tissue THg and MeHg levels in SM were significantly lower ($p = < 0.001$; Figure 4.1 A and B) than both FW and PDW. Percent MeHg levels showed a decreasing trend with increasing salinities in the order of FW, PDW, and SM, however, there was no statistically significant difference for mosquitofish and crayfish but was significant for crab samples (Figure 4.1 C). These results may suggest that fish MeHg content is strongly influenced by the sediment as well as Hg-Cl forms, and sediment MeHg could be the primary source of MeHg for the food web across the sites.

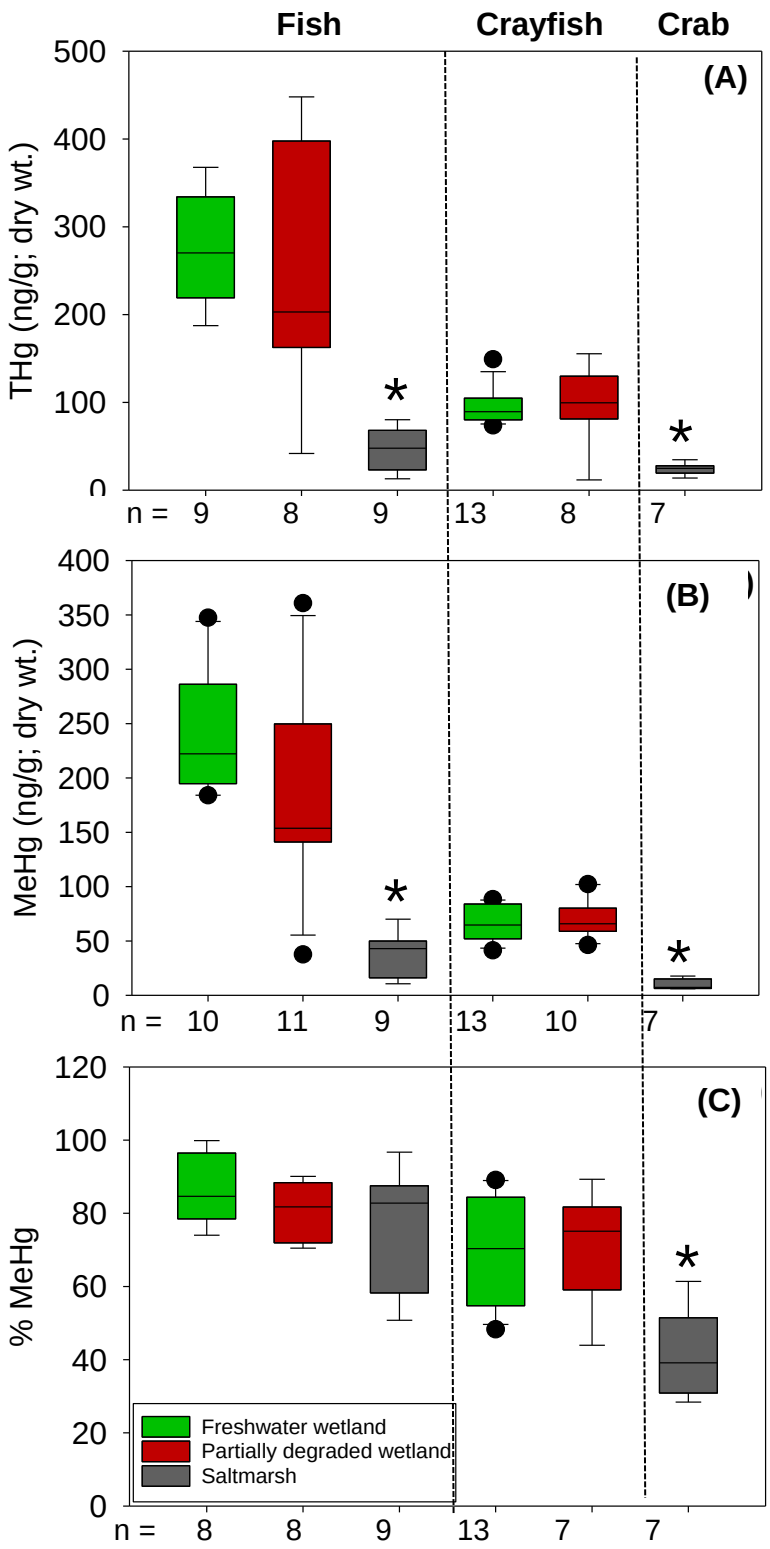


Figure 4. 1: (A) Total mercury (THg), (B) methylmercury (MeHg) and (C) percent methylmercury (% MeHg) concentrations of mosquitofish, crayfish, and crab (dry weight) samples collected from freshwater wetland, partially degraded wetland, and saltmarsh.

*Composition of $\delta^{13}C$ and $\delta^{15}N$ and their relationship with Hg in sediment samples*

I utilized isotope ratios of stable $\delta^{13}C$, $\delta^{15}N$ in sediment samples to evaluate organic matter flow and the food web (Peterson et al., 1985) and predict the MeHg source in the food web.

Mean $\delta^{13}C$ values, in both bulk sediment and dominant plant species (-31.84 ± 1.14, n = 4 and -29.77 ± 1.75, n = 5) samples were similar in FW (-28.29 ± 0.51, n = 15 and -31.84 ± 1.14, n = 4) and PDW (-28.63 ± 0.57, n = 17 and -29.77 ± 1.75, n = 5), respectively. Nevertheless, mean $\delta^{13}C$ values of sediment (-26.89 ± 0.95, n = 14) and plant tissues (-27.19 ± 0.43, n = 4) in SM were significantly ($p < 0.001$) enriched (Figure 4.2 A). Sediment $\delta^{15}N$ values showed a positive correlation with $\delta^{13}C$ in all sites (Figure 4.2 B; $r^2 = 0.44$, $p < 0.001$).

Previous study (Goñi et al., 2000) investigated macro-organic and humus fractions of sediment $\delta^{13}C$ in forest and saltmarsh ecosystem and also showed similar $\delta^{13}C$ values in forest ecosystem (~ -28‰) but more enriched in *Spartina* dominated wetland (OM, 17 to -22‰ and humus, -23 ‰). Likewise, dominant plant (pine) tissue values of $\delta^{13}C$ were similar (-27.1 to -29.9 ‰ in forest site but more enriched *Spartina* values (-13.3 to -13.4 ‰) compared to our *Spartina* site (SM).

FW and PDW sites are dominated by $C_3$ (e.g., bald cypress and water tupelo) plants, while the SM site is dominated by $C_4$ plants (e.g., saltmarsh grass). Despite the lack of significant difference in $\delta^{13}C$ values in FW and PDW, there was more positive shift in $\delta^{13}C$ values in PDW which could be due to reduced stomatal conductance because of elevated salinity (especially in PDW and SM). Increased salinity triggers more $CO_2$ entering the leaf, which causes less isotope fractionation and eventually increases plant $\delta^{13}C$ values (Khan et al., 2015). Interestingly, mean $\delta^{15}N$ in sediment were comparable in FW (2.22 ± 0.58‰, n = 13) and SM (2.17 ± 1.00 ‰, n = 14) while PDW (0.05 ± 0.78 ‰, n = 16) was significantly lower (Figure 4.2 A, $p < 0.001$). Plant $\delta^{15}N$ values were 1.72 ± 2.57 ‰, -0.18 ± 2.75 ‰, and 4.49 ± 0.96 ‰ in FW, PDW, and SM, respectively. The high variation in $\delta^{15}N$ values in FW and PDW could be due to difference in plant species as well as different N cycling in these three habitats.

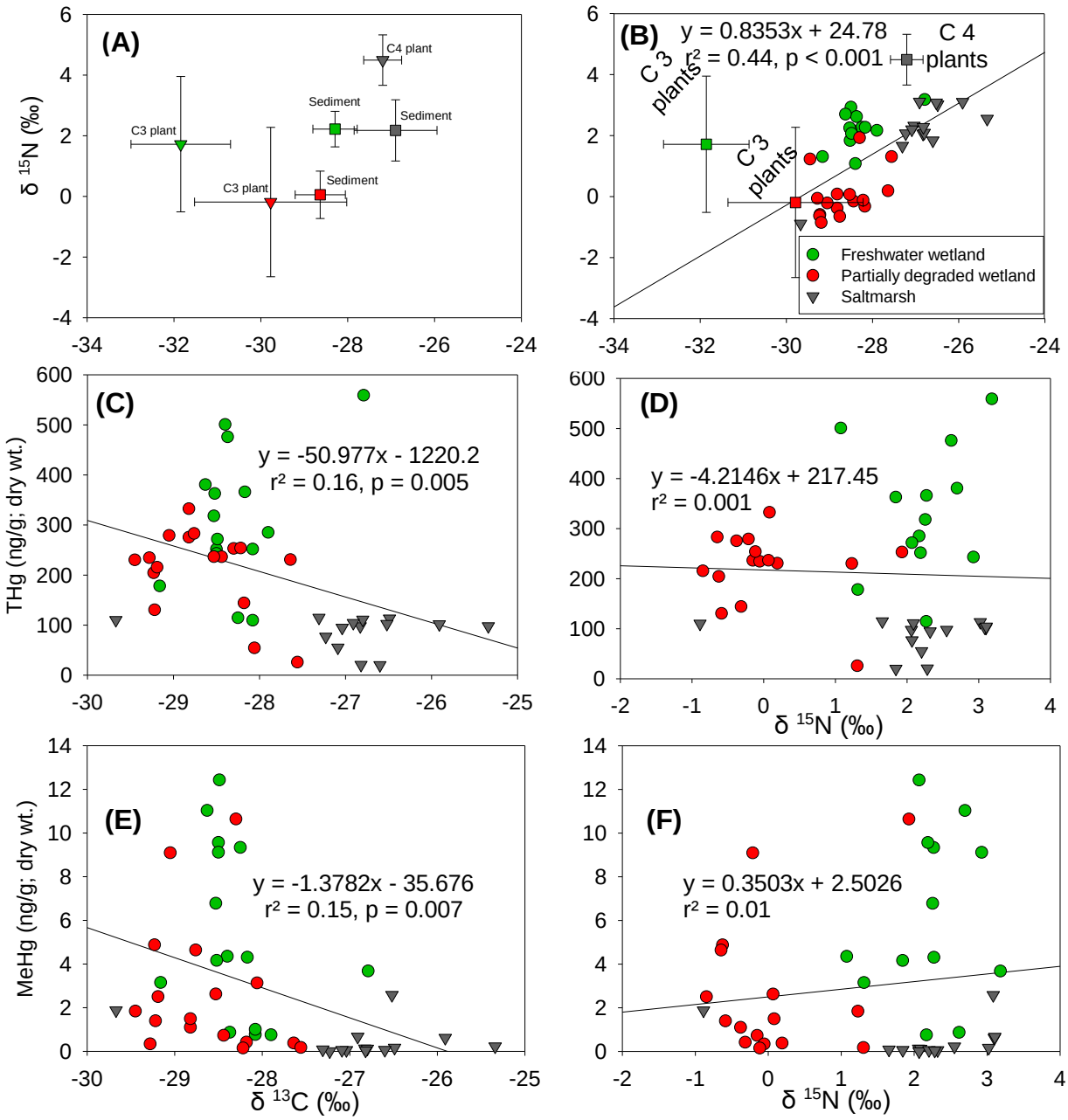


Figure 4. 2: Relationship between $\delta^{13}C$ and $\delta^{15}N$ (A and B); THg and $\delta^{13}C$ (C), THg and $\delta^{15}N$ (D), MeHg and $\delta^{13}C$ (E), MeHg and $\delta^{15}N$ (F). Square scatter plots with error bar (B) does not included in regression and represents dominant vegetation types in each wetland.

THg and MeHg levels were negatively correlated with $\delta^{13}C$ values (THg: $r^2 = 0.16$, $p = 0.005$; MeHg: $r^2 = 0.1551$, $p = 0.007$), while no correlations were detected in $\delta^{15}N$ values in all sites (Figure 4.2 A, B, C and D). Based on $\delta^{13}C$ values of sediment and their

relationship with Hg (Figure 4.2 A and C), I speculate that the source of carbon is similar in FW and PDW but not in SM. These results indicated that the differences in THg and MeHg levels in FW and PDW (chapter II) are not simply due to difference in vegetation type, which further emphasizes the impacts of salinity in these wetlands.

*Assessment of stable isotopes and Hg values in food web*

I have used composite and individual samples to investigate energy source and trophic position of macroinvertebrates in our coastal wetland system. Although incorporating individual samples are important to examine stable isotope variation, using composite samples would provide sufficient biomass for analysis, and be more cost-effective (Fry et al., 2008).

There was a strong and negative relationship ($r^2 = 0.51$, $p < 0.001$) between the $\delta^{15}N$ and $\delta^{13}C$ in FW and PDW among all organisms while positive relationship ($r^2 = 0.69$, $p < 0.01$) was observed only in fish samples of SM (Figure 4.3 B) A scatterplot of log MeHg and $\delta^{13}C$ values showed a negative correlation in invertebrates and fish across the wetlands ($r^2 = 0.32$, $p < 0.001$). The $\delta^{13}C$ values of invertebrate and fish samples displayed differences and were significantly ($p = < 0.001$) enriched in the order of FW (-33.66 to -26.88 ‰), PDW (-31.30 to -25.46 ‰), and SM (-28.17 to -22.45 ‰), which suggest that dominant vegetation type (FW, -31.84 ± 1.14; PDW, -29.77 ± 1.75: and SM, -27.19 ± 0.43) is the basal food source in each wetland (Figure 4.3 A). For instance, the $\delta^{13}C$ values of mosquitofish samples collected from 3 wetlands reflected dominant plant species in wetlands and were between -33.55 to -28.54 ‰, -30.52 to 28.02 ‰, and -28.16 to -25.81‰ in FW, PDW, and SM, respectively (Figure 4.3 B).

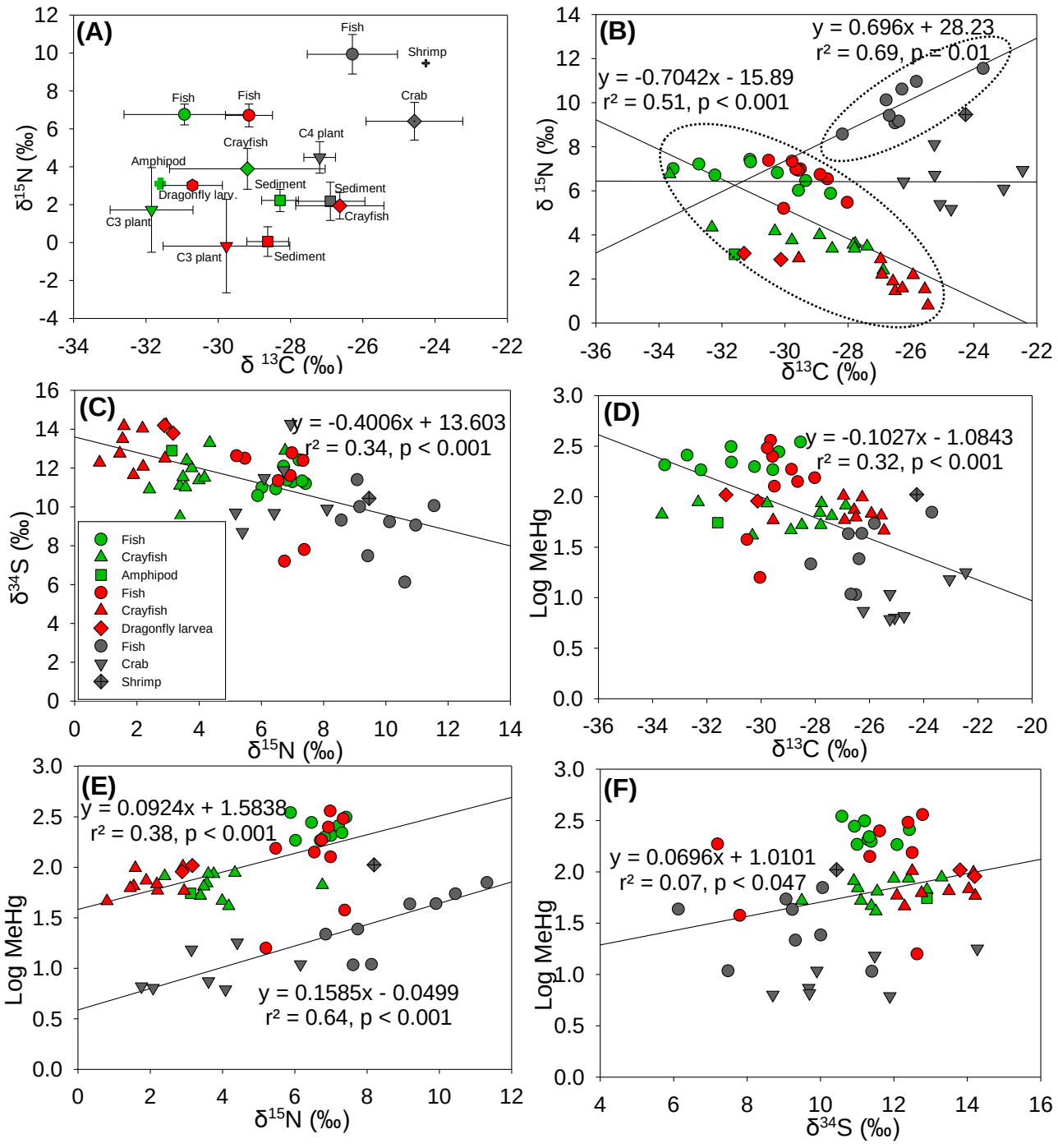


Figure 4. 3: Relationship between $\delta^{15}N$ and $\delta^{13}C$ in sediment and biota (A), $\delta^{15}N$ and $\delta^{13}C$ (B), $\delta^{34}S$ and $\delta^{15}N$ (C), Log MeHg and $\delta^{13}C$ (D), Log MeHg and $\delta^{15}N$ (E), Log MeHg and $\delta^{34}S$ of fish and invertebrates in freshwater wetland (green), partially degraded wetland (red), and saltmarsh (gray). Error bars represent standard deviation.

These results indicated that foraging behavior of all invertebrates was llimited to their habitat (e.g., saltmarsh). In figure 4.3 A and B, mean $\delta^{15}N$ values of all organisms were similar in FW and PDW (5.08 ± 1.71 ‰, 4.15 ± 2.40 ‰, respectively) but significantly higher in SM (8.36 ± 2.02 ‰). Interestingly, invertebrate and fish $\delta^{15}N$ results distinguished FW and PDW from SM revealed that data divided to two groups. The $\delta^{15}N$ values of FW and PDW were between 0.80 and 7.42 ‰, while that of SM was between 5.17 and 11.54 ‰. The higher $\delta^{15}N$ in SM indicate higher trophic levels in this wetland in comparison to FW and PDW.

I observed high variation in $\delta^{15}N$ values of plant tissues in FW (1.72 ± 2.58 ‰, n = 4) and PDW (-0.18 ± 2.75‰, n = 5) while small variation existed in SM (4.49 ± 0.96 ‰, n = 4). Variation in plant $\delta^{15}N$ values could be due to multiple factors including deposited N signature, total N obtained from symbiotic fixation, and the form of N (Craine et al., 2015).

I also examined $\delta^{34}S$ isotopes in invertebrate, fish, and plant tissues in all sites. Mean $\delta^{34}S$ values of invertebrates and fish samples were similar in FW and PDW (11.55 ± 0.88 ‰ and 12.28 ±1.91 ‰) and were lower in SM (9.92 ± 1.84 ‰). Mean plant $\delta^{34}S$ values were similar in PDW and SM (13.84 ± 2.5, 10.42 ±1.56 ‰) but more depleted in FW (7.9 ± 0.86 ‰). Depleted invertebrate and fish $\delta^{34}S$ values could be associated with reducing environment in sediment (Harper et. al., 2018). I found no correlation between log MeHg and $\delta^{34}S$ values in invertebrates and fish samples (Figure 4.3 F).

Overall, I found that $\delta^{13}C$ and $\delta^{15}N$ values are good predictors of MeHg levels in invertebrates and fish in comparison to $\delta^{34}S$ values.

*Relationship between water salinity and mercury levels in macroinvertebrates*

Here, I have shown, overall (sites and seasons combined), groundwater salinity (Figure 4.4 a and B) relationship with the mercury levels in surface water, sediment, mosquitofish, and crayfish samples.

In terms of biota samples, I found a significant negative relationship between surface water salinity and average MeHg levels in mosquitofish samples ($r^2 = 0.50$, $p < 0.001$) in

all sites. Similarly, crayfish samples (FW and PDW) and crab samples (SM) showed a negative relationship ($r^2 = 0.38$, $p < 0.001$) with the salinity. Interestingly, groundwater salinity levels exhibited stronger negative relationship with MeHg levels both in mosquitofish ($r^2 = 0.58$, $p < 0.001$) and Crayfish/Crab ($r^2 = 0.65$, $p < 0.001$) samples (Figure 4.4 A & B). To our knowledge, this is the very first study that showed a negative relationship between salinity and MeHg levels. In recent years, some studies (Buckman et al., 2017; Reinhart et al., 2018) found no significant relationship between salinity and MeHg concentrations in fish. Nevertheless, they reported an increase in Hg levels in Grass Shrimp and Chironomids with increasing salinity levels.

The global prevalence of wetland salinization has been exacerbated by climate change, and the consequences are widely unknown on Hg biogeochemistry in coastal zones. Coastal wetlands are considered favorable environment for mercury methylation and Hg source to adjacent ecosystems that create a vital link among atmosphere, land, water, fish, and finally human. Based on this study, I suggest that increasing salinity levels (i.e., surface and groundwater) can significantly mitigate MeHg levels in sediment and, eventually, accumulation in biota in saltwater experienced coastal plain wetlands. Although I found a positive relationship ($r^2 = 0.69$) between salinity and surface water MeHg levels in PDW, the water sample size was not sufficient to suggest the association between two parameters. Maybe, frequent, and more sample collection would be required to understand the water MeHg and salinity relationship.

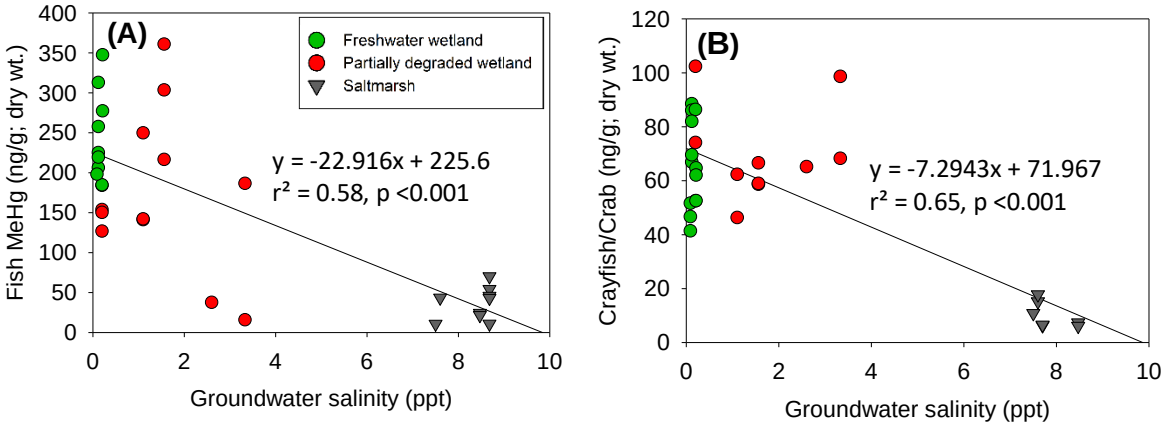


Figure 4. 4: Relationship between groundwater salinity and methylmercury (MeHg) levels in fish (A) and crayfish/crab (B) in freshwater wetland, partially degraded wetland, and saltmarsh.

# CHAPTER V: CONCLUSION

The overall goal of this dissertation was to identify saltwater impact (chronic and acute) on mercury cycling in coastal plain wetlands of North and South Carolina. I accomplished the main goal of this study by answering the following questions.

**Question 1 (Chapter II)**

**How does saltwater intrusion (gradual) influence MeHg concentrations along the salinity gradient in coastal freshwater wetlands?**

To answer this question, I collected 5 seasons of field data from coastal wetlands along the salinity gradient. Although a strong positive relationship ($r^2 = 0.69$, $p < 0.001$) between surface water salinity and water MeHg levels in partially degraded wetland, water sample size (n = 12) was not adequate to suggest saltwater intrusion increases water MeHg levels in coastal wetlands. I found that the highest water MeHg levels occurred with the highest salinity in the partially degraded wetland. I also found that water THg levels were well correlated with DOC across the wetlands which suggests that saltwater experienced wetlands may export higher amount of Hg to nearby waters (e.g., Winyah Bay).

In sediment samples, I found that MeHg levels indicate a significant negative relationship with water salinity levels (surface and groundwater) which suggest increasing salinities in coastal wetlands may suppress methylation of mercury in these ecosystems.

**Question 2 (Chapter III)**

**How does hurricane-induced (episodic) storm surge affect aqueous MeHg levels and its transfer to adjacent waters in coastal wetlands?**

To disentangle this question, I have collected water samples along with field water quality measurements before and after hurricanes over fifteen times.

Overall, I found that hurricane driven storm surge increased salinity across the wetlands. However, high quantity of salinity reduced DOC levels, which was followed by decline in Hg levels as Hg levels are positively correlated with DOC, generally. Besides, DO, $SO^{2-}_4/Cl^-$ ratio was the key component of MeHg production in water column after the passage of hurricanes. Generally, elevated $SO^{2-}_4/Cl^-$ ratio is associated with high MeHg production in coastal freshwater wetlands; however, cooccurrence of high levels of $SO^{2-}_4/Cl^-$ with high DO values created oxic environment which limited MeHg production in these ecosystems. I also demonstrated that Hg in OW was mainly originated from PP sites as water $\delta^{13}$C-DOC concentrations in OW (Pamlico Sound) were derived from the PP sites

**Question 3 (Chapter IV)**

**How does food web MeHg accumulation vary among coastal wetlands along a salinity gradient?**

I collected 5 seasons of field data from the coastal wetlands along the salinity gradient and leveraged stable isotopes to solve this question. Sediment THg and MeHg concentrations were negatively associated with $\delta^{13}$C values (THg: $r^2 = 0.16$, $p = 0.005$; MeHg: $r^2 = 0.1551$, $p = 0.007$), while no correlations was found in $\delta^{15}$N values in all sites. Based on $\delta^{13}$C values of sediment and their relationship with Hg, I suggest that carbon source is similar in FW and PDW but different in SM. These results further suggest that the differences in Hg levels in FW and PDW (chapter II) are not because of vegetation type but salinity levels in these wetlands.

MeHg concentration in fish, crayfish, and crab tissue indicated a negative relationship with the groundwater salinity levels. However, despite the large differences in median values, fish MeHg levels (FW, 241.35; PDW, 153.77; SM, 42.98) were statistically similar in FW and PDW, but significantly different in SM.

Log MeHg levels and $\delta^{13}$C values were negatively correlated in invertebrates across the wetlands ($r^2 = 0.32$, $p < 0.001$). Since invertebrate $\delta^{13}$C values were significantly ($p = < 0.001$) enriched in the order of FW (-33.66 to -26.88 ‰) PDW (-31.30 to -25.46 ‰), and

SM (-28.17 to -22.45 ‰) I can suggest that dominant vegetation type (FW, -31.84 ± 1.14; PDW, -29.77 ± 1.75: and SM, -27.19 ± 0.43) was the basal food source in each wetland.

*Overall Conclusion*

I found a strong empirical evidence that salinity controls MeHg levels in sediment and its bioaccumulation in food web in coastal wetlands as it shown in Figure 5.1. My findings suggest that increasing salinity levels (i.e., surface and groundwater) can significantly reduce MeHg levels in sediment and attenuate its accumulation in biota in coastal plain wetlands. However, although I reported increases of water MeHg levels in saltwater experienced freshwater wetlands, I cannot conclude that salinity elevates MeHg levels in surface water due to limited sample size.

The world is already experiencing climate change linked ecological alterations in many ecosystems due to extreme weather events. MeHg is already one of the major global problems impacting the population worldwide; therefore, it is crucial to understand the biogeochemical cycling of MeHg under extreme weather events.

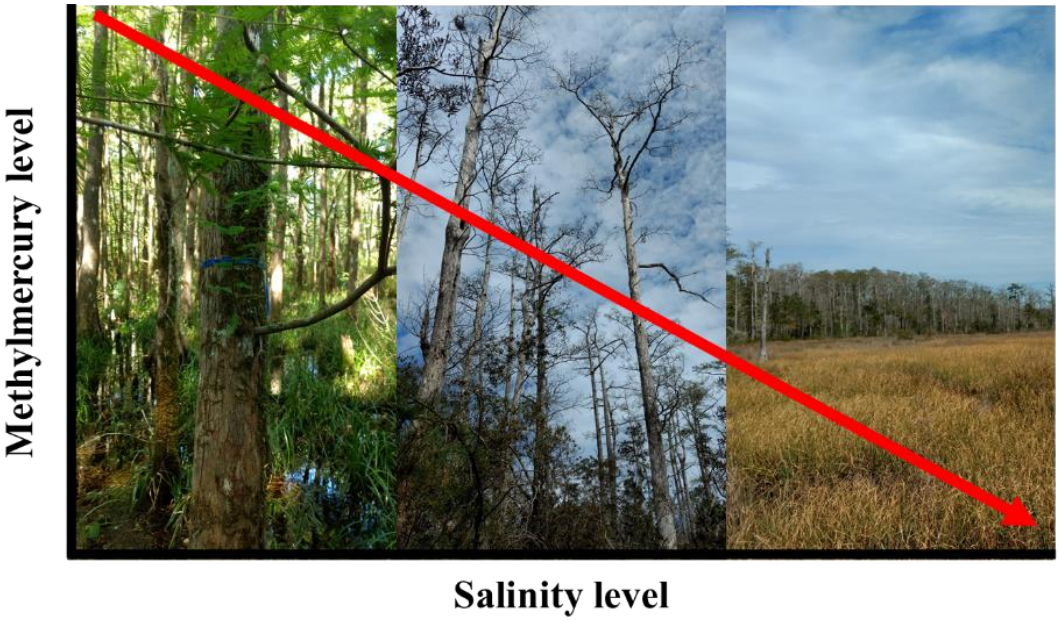


Figure 5. 1: Conceptual model of sediment methylmercury levels with increasing salinities in coastal wetlands.

# REFERENCES


Alpers, C. N., Fleck, J. A., Marvin-DiPasquale, M., Stricker, C. A., Stephenson, M., & Taylor, H. E. (2014). Mercury cycling in agricultural and managed wetlands, Yolo Bypass, California: Spatial and seasonal variations in water quality. *Science of The Total Environment*, *484*, 276–287. https://doi.org/10.1016/j.scitotenv.2013.10.096

Al-Reasi, H. A., Ababneh, F. A., & Lean, D. R. (2007). Evaluating mercury biomagnification in fish from a tropical marine environment using stable isotopes (δ13C and δ15N). *Environmental Toxicology and Chemistry*, *26*(8), 1572. https://doi.org/10.1897/06-359R.1

Amos, H. M., Jacob, D. J., Kocman, D., Horowitz, H. M., Zhang, Y., Dutkiewicz, S., Horvat, M., Corbitt, E. S., Krabbenhoft, D. P., & Sunderland, E. M. (2014). Global biogeochemical implications of mercury discharges from rivers and sediment burial. *Environmental Science & Technology*, *48*(16), 9514–9522. https://doi.org/10.1021/es502134t

Ardón, M., Helton, A. M., & Bernhardt, E. S. (2016). Drought and saltwater incursion synergistically reduce dissolved organic carbon export from coastal freshwater wetlands. *Biogeochemistry*, *127*(2–3), 411–426. https://doi.org/10.1007/s10533-016-0189-5

Ardón, M., Morse, J. L., Colman, B. P., & Bernhardt, E. S. (2013). Drought-induced saltwater incursion leads to increased wetland nitrogen export. *Global Change Biology*, *19*(10), 2976–2985. https://doi.org/10.1111/gcb.12287

Ardón, M., Morse, J. L., Doyle, M. W., & Bernhardt, E. S. (2010). The water quality consequences of restoring wetland hydrology to a large agricultural watershed in the southeastern coastal plain. *Ecosystems*, *13*(7), 1060–1078. https://doi.org/10.1007/s10021-010-9374-x

Bank, M. S., Chesney, E., Shine, J. P., Maage, A., & Senn, D. B. (2007). Mercury bioaccumulation and trophic transfer in sympatric snapper species from the Gulf of Mexico. *Ecological Applications*, *17*(7), 2100–2110. https://doi.org/10.1890/06-1422.1

Barendregt, A., & Swarth, C. W. (2013). Tidal freshwater wetlands: variation and changes. *Estuaries and Coasts*, *36*(3), 445–456. https://doi.org/10.1007/s12237-013-9626-z

Barkay, T., Gillman, M., & Turner, R. R. (1997). Effects of dissolved organic carbon and salinity on bioavailability of mercury. *Applied and Environmental Microbiology*, *63*(11), 4267–4271. https://doi.org/10.1128/AEM.63.11.4267-4271.1997

Barringer, J. L., Riskin, M. L., Szabo, Z., Reilly, P. A., Rosman, R., Bonin, J. L., Fischer, J. M., & Heckathorn, H. A. (2010). Mercury and Methylmercury Dynamics in a Coastal Plain Watershed, New Jersey, USA. *Water, Air, & Soil Pollution*, *212*(1–4), 251–273. https://doi.org/10.1007/s11270-010-0340-1

Beganyi, S. R., & Batzer, D. P. (2011). Wildfire induced changes in aquatic invertebrate communities and mercury bioaccumulation in the Okefenokee Swamp. *Hydrobiologia*, *669*(1), 237–247. https://doi.org/10.1007/s10750-011-0694-4

Bender, M. A., Knutson, T. R., Tuleya, R. E., Sirutis, J. J., Vecchi, G. A., Garner, S. T., & Held, I. M. (2010). Modeled impact of anthropogenic warming on the frequency of intense Atlantic hurricanes. *Science*, *327*(5964), 454–458. https://doi.org/10.1126/science.1180568

Bindoff, N. L., Willebrand, J., Artale, V., Cazenave, A., Gregory, J. M., Gulev, S., Quéré, C. L., Levitus, S., Nojiri, Y., Shum, C. K., Talley, L. D., Unnikrishnan, A. S., Antonov, J., Curry, R., Emerson, S., Feely, R., Garcia, H., González-Davíla, M., Gruber, N., … Wratt, D. (2007). Observations: oceanic climate change and sea level. 48.

Blum, J. E., & Bartha, R. (1980). Effect of salinity on methylation of mercury. *Bulletin of Environmental Contamination and Toxicology*, *25*(1), 404–408. https://doi.org/10.1007/BF01985546

Boening, D. W. (2000). Ecological effects, transport, and fate of mercury: A general review. *Chemosphere*, *40*(12), 1335–1351.

Boyd, E. S., Yu, R.-Q., Barkay, T., Hamilton, T. L., Baxter, B. K., Naftz, D. L., & Marvin-DiPasquale, M. (2017). Effect of salinity on mercury methylating benthic microbes and their activities in Great Salt Lake, Utah. *Science of The Total Environment*, *581–582*, 495–506. https://doi.org/10.1016/j.scitotenv.2016.12.157

Busbee, W. S., Conner, W. H., Allen, D. M., & Lanham, J. D. (2003). Composition and aboveground productivity of three seasonally flooded depressional forested wetlands in coastal South Carolina. *Southeastern Naturalist*, *2*(3), 335–346. https://doi.org/10.1656/1528-7092(2003)002[0335:CAAPOT]2.0.CO;2

Cahoon, D. R. (2006). A review of major storm impacts on coastal wetland elevations. *Estuaries and Coasts*, *29*(6), 889–898. https://doi.org/10.1007/BF02798648

Carpenter, L. J., & Liss, P. S. (2000). On temperate sources of bromoform and other reactive organic bromine gases. *Journal of Geophysical Research: Atmospheres*, *105*(D16), 20539–20547. https://doi.org/10.1029/2000JD900242

Chakraborty, P., Jayachandran, S., Lekshmy, J., Padalkar, P., Sitlhou, L., Chennuri, K., Shetye, S., Sardar, A., & Khandeparker, R. (2019). Seawater intrusion and resuspension of surface sediment control mercury (Hg) distribution and its bioavailability in water column of a monsoonal estuarine system. *Science of The*

*Total Environment*, *660*, 1441–1448. https://doi.org/10.1016/j.scitotenv.2018.12.477

Chambers, L. G., Reddy, K. R., & Osborne, T. Z. (2011). Short-term response of carbon cycling to salinity pulses in a freshwater wetland. *Soil Science Society of America Journal*, *75*(5), 2000–2007. https://doi.org/10.2136/sssaj2011.0026

Chen, C., Amirbahman, A., Fisher, N., Harding, G., Lamborg, C., Nacci, D., & Taylor, D. (2008). Methylmercury in marine ecosystems: spatial patterns and processes of production, bioaccumulation, and biomagnification. *EcoHealth*, *5*(4), 399–408. https://doi.org/10.1007/s10393-008-0201-1

Chételat, J., Ackerman, J. T., Eagles-Smith, C. A., & Hebert, C. E. (2020). Methylmercury exposure in wildlife: A review of the ecological and physiological processes affecting contaminant concentrations and their interpretation. *Science of The Total Environment*, *711*, 135117. https://doi.org/10.1016/j.scitotenv.2019.135117

Chow, A. T., Dai, J., Conner, W. H., Hitchcock, D. R., & Wang, J.-J. (2013). Dissolved organic matter and nutrient dynamics of a coastal freshwater forested wetland in Winyah Bay, South Carolina. *Biogeochemistry*, *112*(1–3), 571–587. https://doi.org/10.1007/s10533-012-9750-z

Compeau, G. C., & Bartha, R. (1987). Effect of salinity on mercury-methylating activity of sulfate-reducing bacteria in estuarine sediments. *Applied and Environmental Microbiology, 53(2), 261-265.*

Corbett, D. R., Vance, D., Letrick, E., Mallinson, D., & Culver, S. (2007). Decadal-scale sediment dynamics and environmental change in the Albemarle Estuarine System, North Carolina. *Estuarine, Coastal and Shelf Science*, *71*(3–4), 717–729. https://doi.org/10.1016/j.ecss.2006.09.024

Coumou, D., & Rahmstorf, S. (2012). A decade of weather extremes. *Nature Climate Change*, *2*(7), 491–496. https://doi.org/10.1038/nclimate1452

Craine, J. M., Brookshire, E. N. J., Cramer, M. D., Hasselquist, N. J., Koba, K., Marin-Spiotta, E., & Wang, L. (2015). Ecological interpretations of nitrogen isotope ratios of terrestrial plants and soils. *Plant and Soil*, *396*(1–2), 1–26. https://doi.org/10.1007/s11104-015-2542-1

Day, J. W., Christian, R. R., Boesch, D. M., Yáñez-Arancibia, A., Morris, J., Twilley, R. R., Naylor, L., Schaffner, L., & Stevenson, C. (2008). Consequences of climate change on the ecogeomorphology of coastal wetlands. *Estuaries and Coasts*, *31*(3), 477–491. https://doi.org/10.1007/s12237-008-9047-6

de Oliveira, D. C. M., Correia, R. R. S., Marinho, C. C., & Guimarães, J. R. D. (2015). Mercury methylation in sediments of a Brazilian mangrove under different

vegetation covers and salinities. *Chemosphere*, *127*, 214–221. https://doi.org/10.1016/j.chemosphere.2015.02.009

Dongmei, Z., Shiwei, Z., Huanchi, M., & Huiying, L. (2020). Simulation of methylmercury content and SRB methylation in phragmites australis soil under different salinity conditions. *Water, Air, & Soil Pollution*, *231*(1), 18. https://doi.org/10.1007/s11270-019-4382-8

Driscoll, C. T., Han, Y.-J., Chen, C. Y., Evers, D. C., Lambert, K. F., Holsen, T. M., Kamman, N. C., & Munson, R. K. (2007). Mercury contamination in forest and freshwater ecosystems in the northeastern United States. *BioScience*, *57*(1), 17–28. https://doi.org/10.1641/B570106

Du Laing, G., De Vos, R., Vandecasteele, B., Lesage, E., Tack, F. M. G., & Verloo, M. G. (2008). Effect of salinity on heavy metal mobility and availability in intertidal sediments of the Scheldt estuary. *Estuarine, Coastal and Shelf Science*, *77*(4), 589–602. https://doi.org/10.1016/j.ecss.2007.10.017

Eckley, C. S., Luxton, T. P., Goetz, J., & McKernan, J. (2017). Water-level fluctuations influence sediment porewater chemistry and methylmercury production in a flood-control reservoir. *Environmental Pollution*, *222*, 32–41. https://doi.org/10.1016/j.envpol.2017.01.010

Ericksen, J. A., Gustin, M. S., Schorran, D. E., Johnson, D. W., Lindberg, S. E., & Coleman, J. S. (2003). Accumulation of atmospheric mercury in forest foliage. *Atmospheric Environment*, 10.

Evers, D. C., Han, Y.-J., Driscoll, C. T., Kamman, N. C., Goodale, M. W., Lambert, K. F., Holsen, T. M., Chen, C. Y., Clair, T. A., & Butler, T. (2007). Biological mercury hotspots in the northeastern United States and southeastern Canada. *BioScience*, *57*(1), 29–43. https://doi.org/10.1641/B570107

Fitzgerald, W. F., Lamborg, C. H., & Hammerschmidt, C. R. (2007). Marine biogeochemical cycling of mercury. *Chemical Reviews*, *107*(2), 641–662. https://doi.org/10.1021/cr050353m

Fry, B, & Chumchal, M. M. (2012). Mercury bioaccumulation in estuarine food webs. *Ecological Applications*, *22*(2), 606–623. https://doi.org/10.1890/11-0921.1

Fry, B, Cieri, M., Hughes, J., Tobias, C., Deegan, L., & Peterson, B. (2008). Stable isotope monitoring of benthic–planktonic coupling using salt marsh fish. *Marine Ecology Progress Series*, *369*, 193–204. https://doi.org/10.3354/meps07644

Fry, B. (2002). Conservative mixing of stable isotopes across estuarine salinity gradients: A conceptual framework for monitoring watershed influences on downstream fisheries production. *Estuaries*, *25*(2), 264–271. https://doi.org/10.1007/BF02691313

Gilmour, C., Orem, W., Krabbenhoft, D., & Mendelssohn, I. (2007). Preliminary assessment of sulfur sources, trends and effects in the Everglades. 2007 South Florida Environmental Report, Appendix 3B-3. *West Palm Beach, FL: South Florida Water Management District, 83.*

Glover, J. B., Domino, M. E., Altman, K. C., Dillman, J. W., Castleberry, W. S., Eidson, J. P., & Mattocks, M. (2010). Mercury in South Carolina fishes, USA. *Ecotoxicology*, *19*(4), 781–795. https://doi.org/10.1007/s10646-009-0455-6

Goñi, M. A., Thomas, K. A., & Goni, M. A. (2000). Sources and Transformations of Organic Matter in Surface Soils and Sediments from a Tidal Estuary (North Inlet, South Carolina, USA). *Estuaries*, *23*(4), 548. https://doi.org/10.2307/1353145

Gornitz, V. M., Daniels, R. C., White, T. W., & Birdwell, K. R. (1994). The development of a coastal risk assessment database: vulnerability to sea-level rise in the US Southeast. *Journal of Coastal Research*, 327-338.

Guentzel, J. L. (2009). Wetland influences on mercury transport and bioaccumulation in South Carolina. *Science of The Total Environment*, *407*(4), 1344–1353. https://doi.org/10.1016/j.scitotenv.2008.09.030

Hackney, C. T., Avery, G. B., Leonard, L. A., Posey, M., & Alphin, T. (2007). Biological, chemical, and physical characteristics of tidal freshwater swamp forests of the Lower Cape Fear River/Estuary, North Carolina. In W. H. Conner, T. W. Doyle, & K. W. Krauss (Eds.), *Ecology of Tidal Freshwater Forested Wetlands of the Southeastern United States* (pp. 183–221). Springer Netherlands. https://doi.org/10.1007/978-1-4020-5095-4_8

Hall, B. D., Aiken, G. R., Krabbenhoft, D. P., Marvin-DiPasquale, M., & Swarzenski, C. M. (2008). Wetlands as principal zones of methylmercury production in southern Louisiana and the Gulf of Mexico region. *Environmental Pollution*, 11.

Hammerschmidt, C. R., & Fitzgerald, W. F. (2004). Geochemical controls on the production and distribution of methylmercury in near-shore marine sediments. *Environmental Science & Technology*, *38*(5), 1487–1495. https://doi.org/10.1021/es034528q

Harper, A., Landing, W., & Chanton, J. P. (2018). Controls on the Variation of Methylmercury Concentration in Seagrass Bed Consumer Organisms of the Big Bend, Florida, USA. *Estuaries and Coasts*, *41*(5), 1486–1495. https://doi.org/10.1007/s12237-017-0355-6

Herbert, E. R., Boon, P., Burgin, A. J., Neubauer, S. C., Franklin, R. B., Ardón, M., Hopfensperger, K. N., Lamers, L. P. M., & Gell, P. (2015). A global perspective on wetland salinization: Ecological consequences of a growing threat to freshwater wetlands. *Ecosphere*, *6*(10), art206. https://doi.org/10.1890/ES14-00534.1

Hollweg, T. A., Gilmour, C. C., & Mason, R. P. (2009). Methylmercury production in sediments of Chesapeake Bay and the mid-Atlantic continental margin. *Marine Chemistry*, *114*(3–4), 86–101. https://doi.org/10.1016/j.marchem.2009.04.004

Horvat, M., Bloom, N. S., & Liang, L. (1993). Comparison of distillation with other current isolation methods for the determination of methyl mercury compounds in low level environmental samples: Part 1. Sediments. *Analytica Chimica Acta*, *281*(1), 135–152. https://doi.org/10.1016/0003-2670(93)85348-N

Hossaini, R., Chipperfield, M. P., Saiz-Lopez, A., Harrison, J. J., Glasow, R., Sommariva, R., Atlas, E., Navarro, M., Montzka, S. A., Feng, W., Dhomse, S., Harth, C., Mühle, J., Lunder, C., O'Doherty, S., Young, D., Reimann, S., Vollmer, M. K., Krummel, P. B., & Bernath, P. F. (2015). Growth in stratospheric chlorine from short-lived chemicals not controlled by the Montreal Protocol. *Geophysical Research Letters*, *42*(11), 4573–4580. https://doi.org/10.1002/2015GL063783

Hosseini, S. R., Scaioni, M., & Marani, M. (2018). On the influence of global warming on Atlantic hurricane frequency. In *2018 ISPRS TC III Mid-Term Symposium on Developments, Technologies and Applications in Remote Sensing* (Vol. 42, No. 3, pp. 527-532). International Society for Photogrammetry and Remote Sensing. https://doi.org/10.5194/isprs-archives-XLII-3-527-2018

Hsu-Kim, H., Kucharzyk, K. H., Zhang, T., & Deshusses, M. A. (2013). Mechanisms regulating mercury bioavailability for methylating microorganisms in the aquatic environment: a critical review. *Environmental science & technology*, *47*(6), 2441-2456. https://doi.org/10.1021/es304370g

Jiang, T., Skyllberg, U., Björn, E., Green, N. W., Tang, J., Wang, D., Gao, J., & Li, C. (2017). Characteristics of dissolved organic matter (DOM) and relationship with dissolved mercury in Xiaoqing River-Laizhou Bay estuary, Bohai Sea, China. *Environmental Pollution*, *223*, 19–30. https://doi.org/10.1016/j.envpol.2016.12.006

Joye, S. B., & Hollibaugh, J. T. (1995). Influence of sulfide inhibition of nitrification on nitrogen regeneration in sediments. *Science*, *270*(5236), 623–625. https://doi.org/10.1126/science.270.5236.623

Kemp, A. C., & Horton, B. P. (2013). Contribution of relative sea-level rise to historical hurricane flooding in New York City. *Journal of Quaternary Science*, *28*(6), 537–541. https://doi.org/10.1002/jqs.2653

Kendrick, M. A. (2018). Halogens in seawater, marine sediments and the altered oceanic lithosphere. In The role of halogens in terrestrial and extraterrestrial geochemical processes (pp. 591-648).Springer International Publishing. https://doi.org/10.1007/978-3-319-61667-4_9

King, J. K., Harmon, S. M., Fu, T. T., & Gladden, J. B. (2002). Mercury removal, methylmercury formation, and sulfate-reducing bacteria profiles in wetland

mesocosms. *Chemosphere*, *46*(6), 859–870. https://doi.org/10.1016/S0045-6535(01)00135-7

Kopp, R. E. (2013). Does the mid-Atlantic United States sea level acceleration hot spot reflect ocean dynamic variability?. *Geophysical Research Letters*, *40*(15), 3981-3985.https://doi.org/10.1002/grl.50781

Kopp, R. E., Horton, B. P., Kemp, A. C., & Tebaldi, C. (2015). Past and future sea-level rise along the coast of North Carolina, USA. *Climatic Change*, *132*(4), 693–707. https://doi.org/10.1007/s10584-015-1451-x

Krauss, K. W., Duberstein, J. A., Doyle, T. W., Conner, W. H., Day, R. H., Inabinette, L. W., & Whitbeck, J. L. (2009). Site condition, structure, and growth of baldcypress along tidal/non-tidal salinity gradients. *Wetlands*, *29*(2), 505–519. https://doi.org/10.1672/08-77.1

Ku, P., Tsui, M. T.-K., Nie, X., Chen, H., Hoang, T. C., Blum, J. D., Dahlgren, R. A., & Chow, A. T. (2018). Origin, reactivity, and bioavailability of mercury in wildfire ash. *Environmental science & technology, 52(24), 14149-14157.*

Kunkel, K. E., & Champion, S. M. (2019). An assessment of rainfall from Hurricanes Harvey and Florence relative to other extremely wet storms in the United States. *Geophysical Research Letters*, *46*(22), 13500–13506. https://doi.org/10.1029/2019GL085034

Lange, T. R., Royals, H. E., & Connor, L. L. (1993). Influence of water chemistry on mercury concentration in largemouth bass from Florida lakes. *Transactions of the American Fisheries Society*, *122*(1), 74-84.

Laturnus, F., Haselmann, K. F., Borch, T., & Grøn, C. (2002). Terrestrial natural sources of trichloromethane (chloroform, CHCl 3)–An overview. *Biogeochemistry*, *60*(2), 121-139.

Lei, P., Zhong, H., Duan, D., & Pan, K. (2019). A review on mercury biogeochemistry in mangrove sediments: Hotspots of methylmercury production? *Science of The Total Environment*, *680*, 140–150. https://doi.org/10.1016/j.scitotenv.2019.04.451

Li, P., Du, B., Chan, H. M., & Feng, X. (2015). Human inorganic mercury exposure, renal effects and possible pathways in Wanshan mercury mining area, China. *Environmental Research*, *140*, 198–204. https://doi.org/10.1016/j.envres.2015.03.033

Li, X., Bellerby, R., Craft, C., & Widney, S. E. (2018). Coastal wetland loss, consequences, and challenges for restoration. *Anthropocene Coasts*, 1–15. https://doi.org/10.1139/anc-2017-0001

Liu, B., Schaider, L. A., Mason, R. P., Bank, M. S., Rabalais, N. N., Swarzenski, P. W., Shine, J. P., Hollweg, T., & Senn, D. B. (2009). Disturbance impacts on mercury

dynamics in northern Gulf of Mexico sediments: DISTURBANCE IMPACTS ON MERCURY DYNAMICS. *Journal of Geophysical Research: Biogeosciences*, *114*(G2), n/a-n/a. https://doi.org/10.1029/2008JG000752

Liu, G., Cai, Y., Philippi, T., Kalla, P., Scheidt, D., Richards, J., Scinto, L., & Appleby, C. (2008). Distribution of total and methylmercury in different ecosystem compartments in the Everglades: Implications for mercury bioaccumulation. *Environmental Pollution*, *153*(2), 257–265. https://doi.org/10.1016/j.envpol.2007.08.030

Liu, X., Ruecker, A., Song, B., Xing, J., Conner, W. H., & Chow, A. T. (2017). Effects of salinity and wet–dry treatments on C and N dynamics in coastal-forested wetland soils: Implications of sea level rise. *Soil Biology and Biochemistry*, *112*, 56–67. https://doi.org/10.1016/j.soilbio.2017.04.002

Luo, M., Huang, J.-F., Zhu, W.-F., & Tong, C. (2019). Impacts of increasing salinity and inundation on rates and pathways of organic carbon mineralization in tidal wetlands: A review. *Hydrobiologia*, *827*(1), 31–49. https://doi.org/10.1007/s10750-017-3416-8

Majidzadeh, H., Uzun, H., Ruecker, A., Miller, D., Vernon, J., Zhang, H., Bao, S., Tsui, M. T. K., Karanfil, T., & Chow, A. T. (2017). Extreme flooding mobilized dissolved organic matter from coastal forested wetlands. *Biogeochemistry*, *136*(3), 293–309. https://doi.org/10.1007/s10533-017-0394-x

Marvin-DiPasquale, M., Agee, J., Bouse, R., & Jaffe, B. (2003). Microbial cycling of mercury in contaminated pelagic and wetland sediments of San Pablo Bay, California. *Environmental Geology*, *43*(3), 260–267. https://doi.org/10.1007/s00254-002-0623-y

Michener, W. K., Blood, E. R., Bildstein, K. L., Brinson, M. M., & Gardner, L. R. (1997). Climate change, hurricanes and tropical storms, and rising sea level in coastal wetlands. *Ecological Applications*, *7*(3), 770–801. https://doi.org/10.1890/1051-0761(1997)007[0770:CCHATS]2.0.CO;2

Morris, J. T., Sundareshwar, P. V., Nietch, C. T., Kjerfve, B., & Cahoon, D. R. (2002). Responses of coastal wetlands to rising sea level. *Ecology*, *83*(10), 2869–2877. https://doi.org/10.1890/0012-9658(2002)083[2869:ROCWTR]2.0.CO;2

Munthe, J., Bodaly, R. A. (Drew), Branfireun, B. A., Driscoll, C. T., Gilmour, C. C., Harris, R., Horvat, M., Lucotte, M., & Malm, O. (2007). Recovery of mercury-contaminated fisheries. *AMBIO: A Journal of the Human Environment*, *36*(1), 33–44. https://doi.org/10.1579/0044-7447(2007)36[33:ROMF]2.0.CO;2

Myrbo, A., Swain, E. B., Johnson, N. W., Engstrom, D. R., Pastor, J., Dewey, B., Monson, P., Brenner, J., Dykhuizen Shore, M., & Peters, E. B. (2017). Increase in nutrients, mercury, and methylmercury as a consequence of elevated sulfate reduction to sulfide in experimental wetland mesocosms. *Journal of Geophysical*

*Research: Biogeosciences*, *122*(11), 2769–2785. https://doi.org/10.1002/2017JG003788

Nerem, R. S., Beckley, B. D., Fasullo, J. T., Hamlington, B. D., Masters, D., & Mitchum, G. T. (2018). Climate-change–driven accelerated sea-level rise detected in the altimeter era. *Proceedings of the National Academy of Sciences*, *115*(9), 2022–2025. https://doi.org/10.1073/pnas.1717312115

Neubauer, S. C., Franklin, R. B., & Berrier, D. J. (2013). Saltwater intrusion into tidal freshwater marshes alters the biogeochemical processing of organic carbon. *Biogeosciences*, *10*(12), 8171–8183. https://doi.org/10.5194/bg-10-8171-2013

Noh, S., Choi, M., Kim, E., Dan, N. P., Thanh, B. X., Ha, N. T. V., Sthiannopkao, S., & Han, S. (2013). Influence of salinity intrusion on the speciation and partitioning of mercury in the Mekong River Delta. *Geochimica et Cosmochimica Acta*, *106*, 379–390. https://doi.org/10.1016/j.gca.2012.12.018

O'Driscoll, N. J., Canário, J., Crowell, N., & Webster, T. (2011). Mercury speciation and distribution in coastal wetlands and tidal mudflats: Relationships with sulphur speciation and organic carbon. *Water, Air, & Soil Pollution*, *220*(1–4), 313–326. https://doi.org/10.1007/s11270-011-0756-2

Olund, S. D., DeWild, J. F., Olson, M.L., & Tate, M. T. (2004). Methods for the preparation and analysis of solids and suspended solids for total mercury (No. 5-A8).

Orem, W., Gilmour, C., Axelrad, D., Krabbenhoft, D., Scheidt, D., Kalla, P., McCormick, P., Gabriel, M., & Aiken, G. (2011). Sulfur in the South Florida ecosystem: distribution, sources, biogeochemistry, impacts, and management for restoration. *Critical Reviews in Environmental Science and Technology*, *41*(sup1), 249–288. https://doi.org/10.1080/10643389.2010.531201

Osburn, C. L., Rudolph, J. C., Paerl, H. W., Hounshell, A. G., & Van Dam, B. R. (2019). Lingering carbon cycle effects of Hurricane Matthew in North Carolina's coastal waters. *Geophysical Research Letters*, *46*(5), 2654–2661. https://doi.org/10.1029/2019GL082014

Paranjape, A. R., & Hall, B. D. (2017). Recent advances in the study of mercury methylation in aquatic systems. *FACETS*, *2*(1), 85–119. https://doi.org/10.1139/facets-2016-0027

Peterson, B. J., Howarth, R. W., & Garritt, R. H. (1985). Multiple stable isotopes used to trace the flow of organic matter in estuarine food webs. *Science*, *227*(4692), 1361–1363. https://doi.org/10.1126/science.227.4692.1361

Pezeshki, S. R., Delaune, R. D., & Patrick, W. H. (1990). Flooding and saltwater intrusion: Potential effects on survival and productivity of wetland forests along

the U.S. Gulf Coast. *Forest Ecology and Management*, *33–34*, 287–301. https://doi.org/10.1016/0378-1127(90)90199-L

Post, D. M. (2002). Using stable isotopes to estimate trophic position: models, methods and assumptions. *Ecology*, *83*(3), 703–718. https://doi.org/10.1890/0012-9658(2002)083[0703:USITET]2.0.CO;2

Poulter, B., & Halpin, P. N. (2008). Raster modelling of coastal flooding from sea-level rise. *International Journal of Geographical Information Science*, *22*(2), 167–182. https://doi.org/10.1080/13658810701371858

Ravichandran, M. (2004). Interactions between mercury and dissolved organic matter—a review. *Chemosphere*, *55*(3), 319–331. https://doi.org/10.1016/j.chemosphere.2003.11.011

Rysgaard, S., Thastum, P., Dalsgaard, T., Christensen, P. B., Sloth, N. P., & Rysgaard, S. (1999). Effects of salinity on NH 4+ adsorption capacity, nitrification, and denitrification in Danish estuarine sediments. *Estuaries*, *22*(1), 21. https://doi.org/10.2307/1352923

Schwesig, D., & Matzner, E. (n.d.). Dynamics of mercury and methylmercury in forest floor and runoff of a forested watershed in Central Europe. *Biogeochemistry, 53(2), 181-200.*

Selch, T. M., Hoagstrom, C. W., Weimer, E. J., Duehr, J. P., & Chipps, S. R. (2007). Influence of fluctuating water levels on mercury concentrations in adult Walleye. *Bulletin of Environmental Contamination and Toxicology*, *79*(1), 36–40. https://doi.org/10.1007/s00128-007-9229-0

Selin, N. E. (2009). Global biogeochemical cycling of mercury: a review. *Annual review of environment and resources*, *34*.

Sherman, L. S., & Blum, J. D. (2013). Mercury stable isotopes in sediments and largemouth bass from Florida lakes, USA. *Science of The Total Environment*, *448*, 163–175. https://doi.org/10.1016/j.scitotenv.2012.09.038

Smith, L. M., Macauley, J. M., Harwell, L. C., & Chancy, C. A. (2009). Water quality in the near coastal waters of the Gulf of Mexico affected by Hurricane Katrina: before and after the storm. *Environmental Management*, *44*(1), 149–162. https://doi.org/10.1007/s00267-009-9300-1

South Carolina Department of Health and Environmental Control (SCDHEC). 2018. South Carolina fish consumption advisories Columbia, SC.

Stammer, D., Cazenave, A., Ponte, R. M., & Tamisiea, M. E. (2013). Causes for contemporary regional sea level changes. *Annual Review of Marine Science*, *5*(1), 21–46. https://doi.org/10.1146/annurev-marine-121211-172406

Titus, J. G. (1998). Sea level rise and wetland loss: an overview. *Titus, JG Greenhouse Effect, Sea Level Rise, and Coastal Wetlands. US Environmental Protection Agency. Washington, DC*, *186*.

Tiunov, A. V. (2007). Stable isotopes of carbon and nitrogen in soil ecological studies. *Biology Bulletin*, *34*(4), 395–407. https://doi.org/10.1134/S1062359007040127

Trenberth, K. (2011). Changes in precipitation with climate change. *Climate Research*, *47*(1), 123–138. https://doi.org/10.3354/cr00953

Tsui, M. T. K., & Finlay, J. C. (2011). Influence of dissolved organic carbon on methylmercury bioavailability across Minnesota stream ecosystems. *Environmental Science & Technology,* 45(14), 5981-5987.

Tsui, M. T. K., Uzun, H., Ruecker, A., Majidzadeh, H., Ulus, Y., Zhang, H., ... & Chow, A. T. (2020). Concentration and isotopic composition of mercury in a blackwater river affected by extreme flooding events. *Limnology and Oceanography,* 65(9), 2158-2169.

Tsui, M.T.K., Liu, S., Brasso, R. L., Blum, J. D., Kwon, S. Y., Ulus, Y., Nollet, Y. H., Balogh, S. J., Eggert, S. L., & Finlay, J. C. (2019). Controls of methylmercury bioaccumulation in forest floor food webs. *Environmental Science & Technology*, *53*(5), 2434–2440. https://doi.org/10.1021/acs.est.8b06053

Ullrich, S. M., Tanton, T. W., & Abdrashitova, S. A. (2001). Mercury in the aquatic environment: a review of factors affecting methylation. *Critical Reviews in Environmental Science and Technology*, *31*(3), 241–293. https://doi.org/10.1080/20016491089226

Valle-Levinson, A., Dutton, A., & Martin, J. B. (2017). Spatial and temporal variability of sea level rise hot spots over the eastern United States. *Geophysical Research Letters*, *44*(15), 7876-7882. https://doi.org/10.1002/2017GL073926

Wang, J.-J., Jiao, Y., Rhew, R. C., & Chow, A. T. (2016). Haloform formation in coastal wetlands along a salinity gradient at South Carolina, United States. *Environmental Chemistry*, *13*(4), 745. https://doi.org/10.1071/EN15145

Wang, R., & Wang, W. X. (2010). Importance of speciation in understanding mercury bioaccumulation in tilapia controlled by salinity and dissolved organic matter. Environmental science & technology, 44(20), 7964-7969.

Whitacre, D. M. (Ed.). (2014). *Reviews of Environmental Contamination and Toxicology* (Vol. 229). Springer International Publishing. https://doi.org/10.1007/978-3-319-03777-6

Willacker, J. J., Eagles-Smith, C. A., & Ackerman, J. T. (2017). Mercury bioaccumulation in estuarine fishes: Novel insights from sulfur stable isotopes.

*Environmental Science & Technology*, *51*(4), 2131–2139. https://doi.org/10.1021/acs.est.6b05325

Zillioux, E. J., Porcella, D. B., & Benoit, J. M. (1993). Mercury cycling and effects in freshwater wetland ecosystems. *Environmental Toxicology and Chemistry*, *12*(12), 2245–2264. https://doi.org/10.1002/etc.5620121208

APPENDIX A. PICTURES OF SAMPLE COLLECTION SITES


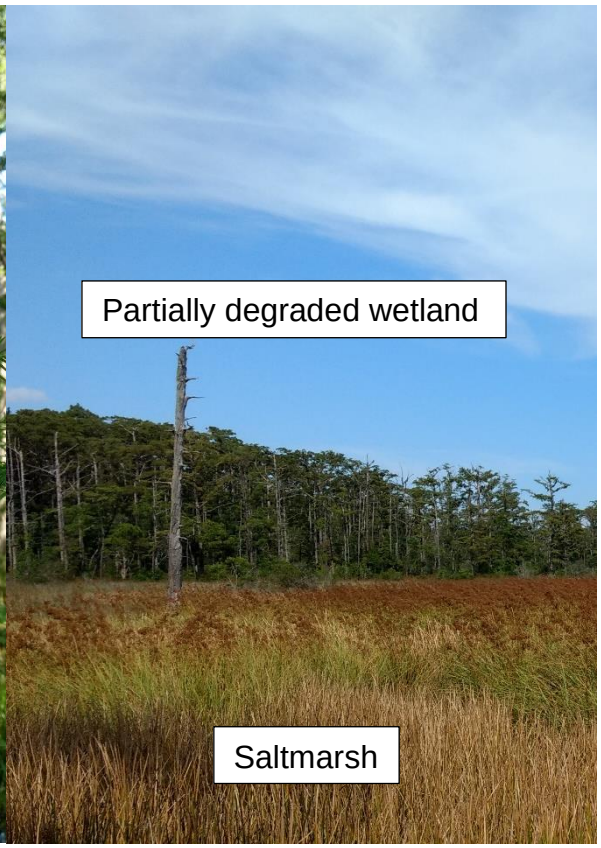

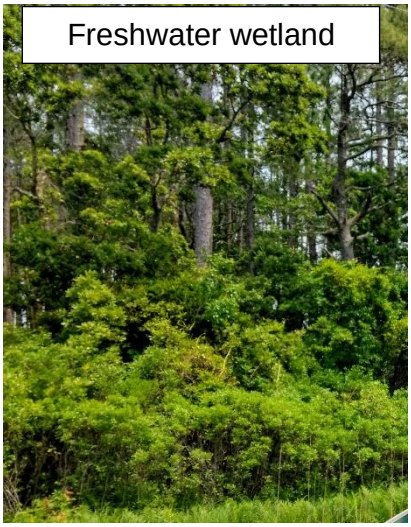
Freshwater wetland


Partially degraded wetland

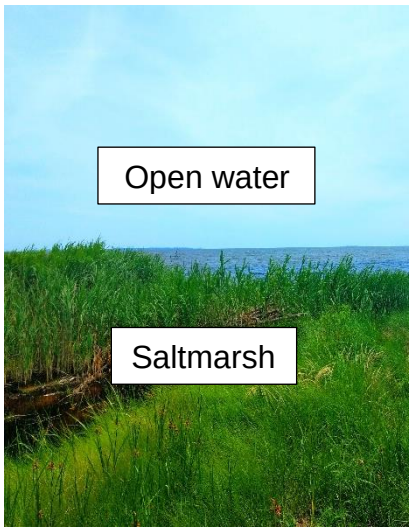
Open water
Saltmarsh


T-North


T-Middle

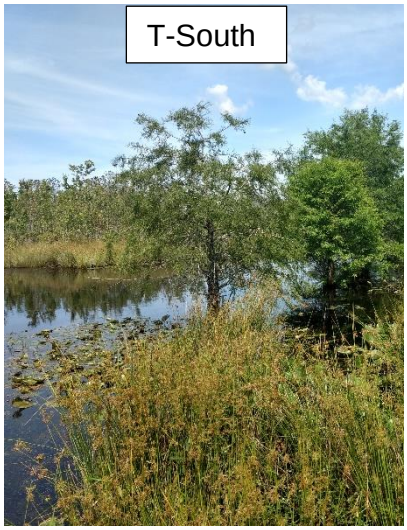
T-South

# APPENDIX B. SEASONAL WATER AND SEDIMENT QUALITY DATA

Table S1: Seasonal surface water quality data, dissolved organic carbon (DOC), sulfate ($SO^{2-}_4$), chlorine ($Cl^-$), nitrogen (N), salinity (ppt), dissolved oxygen (DO), and temperature (℃) in the freshwater wetland (FW), partially degraded wetland (PDW), and saltmarsh (SM) at Georgetown, South Carolina

| Date | Site | DOC (mg/L) | Sulfate (mg/L) | Cl- (mg/L) | N (mg/L) | Salinity (ppt) | DO (mg/L) | Temp (℃) |
|---|---|---|---|---|---|---|---|---|
| Mar 18 | FW-S | 23.90 | 0.20 | 21.30 | 0.50 | 0.10 | 1.32 | 8.90 |
| Aug 18 | FW-S | 66.00 | 0.37 | 8.19 | 1.44 | 0.08 | 1.32 | 25.60 |
| Nov 18 | FW-S | 23.46 | 0.28 | 20.19 | 3.02 | 0.15 | 2.20 | 12.40 |
| Mar 19 | FW-S | 18.43 | 0.20 | 17.83 | 0.80 | 0.17 | 1.79 | 18.30 |
| Sep 19 | FW-S | 51.96 | 0.20 | 15.96 | 1.72 | 0.09 | 1.66 | 19.50 |
| Mar 18 | PDW-S | 16.60 | 121.70 | 2574.90 | 0.40 | 2.64 | 3.94 | 12.60 |
| Aug 18 | PDW-S | 85.00 | 0.89 | 14.87 | 1.50 | 0.10 | 2.28 | 25.00 |
| Nov 18 | PDW-S | 10.62 | 79.74 | 586.20 | 0.67 | 0.75 | 5.70 | 10.80 |
| Mar 19 | PDW-S | 18.85 | 1.68 | 121.10 | 0.69 | 0.29 | 1.83 | 18.00 |
| Sep 19 | PDW-S | 22.75 | 74.75 | 1412.32 | 0.88 | 5.54 | 1.75 | 22.50 |
| Mar 18 | SM-S | 7.70 | 199.00 | 4068.60 | <MRL | 6.00 | 9.52 | 12.00 |
| Aug 18 | SM-S | 45.00 | 53.66 | 3011.48 | 2.08 | 9.20 | ND | ND |
| Nov 18 | SM-S | 10.01 | 119.43 | 895.39 | 0.81 | 2.00 | 7.10 | 11.30 |
| Mar 19 | SM-S | 11.95 | 106.72 | 936.64 | 0.65 | 4.31 | 6.60 | 19.40 |
| Sep 19 | SM-S | 15.15 | 549.49 | 5155.43 | 1.38 | 9.39 | 0.48 | 25.90 |

| Date | Site | DOC (mg/L) | Sulfate (mg/L) | Cl- (mg/L) | N (mg/L) | Salinity (ppt) | DO (mg/L) | Temp. (℃) |
|---|---|---|---|---|---|---|---|---|
| Mar 18 | FW-G | 32.40 | 0.30 | 31.40 | 1.00 | 0.12 | 1.48 | 10.80 |
| Aug 18 | FW-G | 41.00 | 0.39 | 8.63 | 1.30 | 0.20 | 0.44 | 22.60 |
| Nov 18 | FW-G | 7.00 | 0.58 | 7.04 | 0.40 | 0.09 | 1.97 | 15.30 |
| Mar 19 | FW-G | 38.62 | 0.31 | 34.12 | 1.18 | 0.12 | ND | 17.30 |
| Sep 19 | FW-G | 40.51 | 1.19 | 35.82 | 1.84 | 0.21 | 1.14 | 20.80 |
| Mar 18 | PDW-G | 39.00 | 3.90 | 684.20 | 0.80 | 2.60 | ~0 | 12.80 |
| Aug 18 | PDW-G | 64.00 | 17.93 | 1061.84 | 1.62 | 0.20 | 0.23 | 24.30 |
| Nov 18 | PDW-G | 34.01 | 30.14 | 817.52 | 1.99 | 1.10 | 3.50 | 15.00 |
| Mar 19 | PDW-G | 31.90 | 9.88 | 739.53 | 1.45 | 1.56 | ND | 16.60 |
| Sep 19 | PDW-G | 25.90 | 136.97 | 2559.39 | 1.11 | 3.33 | 2.78 | 22.20 |
| Mar 18 | SM-G | 43.30 | 34.80 | 3638.0 | 1.20 | 7.50 | 5.40 | 14.70 |
| Aug 18 | SM-G | 31.00 | 174.95 | 4110.79 | 5.52 | 7.70 | ND | ND |

| | | | | | | | | |
|---|---|---|---|---|---|---|---|---|
| Nov 18 | SM-G | 34.33 | 71.05 | 4132.91 | 1.97 | 7.60 | 0.19 | 12.40 |
| Mar 19 | SM-G | 31.08 | 83.76 | 4115.80 | 1.27 | 8.68 | ND | 17.00 |
| Sep 19 | SM-G | 21.89 | 187.32 | 4817.99 | 3.59 | 8.47 | 0.50 | 24.80 |

Table S2: Surface water FTHg, FMeHg, and %MeHg concentrations of freshwater wetland (FW), partially degraded wetland (PDW), and saltmarsh (Saltmarsh)

| Date | Site | FTHg (ng/L) | FMeHg (ng/L) | % MeHg |
|---|---|---|---|---|
| Mar 2018 | FW-S-1 | 2.04 | 0.15 | 7.57 |
| | FW-S-2 | 1.52 | 0.12 | 7.61 |
| Aug 2018 | FW-S-1 | 11.06 | 0.74 | 6.68 |
| | FW-S-2 | 10.18 | 0.73 | 7.14 |
| | FW-S-3 | 11.26 | 0.95 | 8.40 |
| Nov 2018 | FW-S-1 | 2.37 | 0.18 | 7.71 |
| | FW-S-2 | 2.67 | 0.14 | 5.13 |
| Mar 2019 | FW-S-1 | 4.26 | 0.11 | 2.58 |
| | FW-S-2 | 2.39 | 0.07 | 2.93 |
| Sept 2019 | FW-S-1 | 4.03 | 0.42 | 10.51 |
| | FW-S-2 | 4.22 | 0.61 | 14.44 |
| **Average (±std)** | **N =11** | **5.09 (±3.80)** | **0.38 (±0.31)** | **7.33 (±3.30)** |
| March 2018 | PDW-S-1 | 2.60 | 0.22 | 8.58 |
| | PDW-S-2 | 2.43 | 0.25 | 10.45 |
| | PDW-S-3 | ND | 0.26 | ND |
| Aug 2018 | PDW-S-1 | 10.07 | 0.42 | 4.14 |
| | PDW-S-2 | 12.10 | 0.41 | 3.40 |
| | PDW-S-3 | 12.20 | 0.31 | 2.55 |
| Nov 2018 | PDW-S-1 | 2.62 | 0.07 | 2.65 |
| | PDW-S-2 | 2.56 | 0.07 | 2.73 |
| March 2019 | PDW-S-1 | 3.37 | 0.48 | 14.26 |
| | PDW-S-2 | 2.77 | 0.40 | 14.43 |
| Sep 2019 | PDW-S-1 | 6.09 | 3.47 | 56.92 |
| | PDW-S-2 | 5.92 | 3.02 | 50.98 |
| **Average (±std)** | **N = 12** | **5.70 (±3.95)** | **0.78 (±1.16)** | **15.55 (±19.55)** |
| Mar 2018 | SM-S-1 | 1.85 | 0.11 | 5.71 |
| | SM-S-2 | 1.32 | 0.14 | 10.91 |
| Aug 2018 | SM-S-1 | 9.28 | 3.73 | 40.14 |
| | SM-S-2 | 10.14 | 3.98 | 39.21 |
| Nov 2018 | SM-S-1 | 2.57 | 0.07 | 2.69 |
| | SM-S-2 | 1.95 | 0.15 | 7.63 |
| Mar 2019 | SM-S-1 | 2.81 | 0.08 | 2.85 |
| | SM-S-2 | 2.44 | 0.06 | 2.46 |
| Sep 2019 | SM-S-1 | 0.98 | 0.02 | 1.62 |
| | SM-S-2 | 0.99 | 0.03 | 3.09 |
| **Average (±std)** | **N = 10** | **1.86 (±0.71)** | **0.08 (±0.04)** | **4.61 (±3.22)** |

ND represents no data. I didn't include water of FTHg, FMeHg, and % MeHg levels for SM (August 2018) in averages as they weren't representing surface water.

Table S3: Groundwater FTHg, FMeHg, and %MeHg concentrations of freshwater wetland (FW), partially degraded wetland (PDW), and saltmarsh (Saltmarsh)

| Date | Site | THg (ng/L) | MeHg (ng/L) | % MeHg |
|---|---|---|---|---|
| Mar 2018 | FW-G-1 | 1.56 | 0.07 | 4.50 |
| Aug 2018 | FW-G-1 | 4.03 | 0.04 | 0.94 |
| Nov 2018 | FW-G-1 | 1.95 | 0.14 | 7.37 |
| | FW-G-2 | 1.84 | 0.11 | 6.11 |
| Mar 2019 | FW-G-1 | 3.29 | 0.03 | 0.91 |
| | FW-G-2 | 7.63 | 0.04 | 0.52 |
| Sep 2019 | FW-G-1 | 2.45 | 0.02 | 0.96 |
| | FW-G-2 | 1.55 | 0.05 | 3.50 |
| **Average (±std)** | **N = 8** | **3.03 (±2.05)** | **0.06 (±0.04)** | **3.10 (±2.67)** |
| | | | | |
| Mar 2018 | PDW-G-1 | 1.65 | 0.39 | 23.65 |
| Aug 2018 | PDW-G-1 | 3.95 | 0.23 | 5.88 |
| Nov 2018 | PDW-G-1 | 2.68 | 0.09 | 3.19 |
| | PDW-G-2 | 3.75 | 0.11 | 2.95 |
| Mar 2019 | PDW-G-1 | 1.41 | 0.07 | 4.97 |
| | PDW-G-2 | 8.34 | 0.01 | 0.12 |
| Sep 2019 | PDW-G-1 | 0.65 | 0.02 | 3.23 |
| | PDW-G-2 | 2.65 | 0.04 | 1.42 |
| **Average (±std)** | **N = 8** | **3.13 (±2.38)** | **0.12 (±0.13)** | **5.67 (±7.48)** |
| | | | | |
| Mar 2018 | SM-G-1 | 0.69 | 0.00 | 0.44 |
| Aug 2018 | SM-G-1 | 1.12 | 0.03 | 2.75 |
| Nov 2018 | SM-G-1 | 0.59 | 0.02 | 2.83 |
| | SM-G-2 | 0.76 | 0.01 | 1.94 |
| Mar 2019 | SM-G-1 | 0.96 | 0.07 | 7.29 |
| | SM-G-2 | 1.12 | 0.09 | 8.03 |
| Sep 2019 | SM-G-1 | 2.00 | 0.01 | 0.25 |
| | SM-G-2 | 1.94 | 0.01 | 0.26 |
| **Average (±std)** | **N = 8** | **1.14 (±0.54)** | **0.02 (±0.03)** | **2.97 (±3.08)** |

Table S4: Sediment THg, MeHg, %MeHg, $\delta^{13}C$ (‰), $\delta^{15}N$ (‰), and C/N levels in of freshwater wetland (FW), partially degraded wetland (PDW), and saltmarsh (SM)

| Freshwater Wetland | THg ng/g) | MeHg (ng/g) | % MeHg | δ $^{13}$C (‰) | δ $^{15}$N (‰) | C/N |
|---|---|---|---|---|---|---|
| Mar_2018 | 114.63 | 9.34 | 8.15 | -28.25 | 2.27 | 16.58 |
| Mar_2018 | 251.78 | 9.56 | 3.80 | -28.50 | 2.19 | 16.41 |
| Mar_2018 | 109.68 | 0.77 | 0.70 | -28.08 | ND | ND |
| Aug_2018 | 251.89 | 1.01 | 0.40 | -28.08 | ND | ND |
| Aug_2018 | 285.09 | 0.76 | 0.27 | -27.90 | 2.17 | 13.64 |
| Aug_2018 | 500.77 | 4.35 | 0.87 | -28.40 | 1.08 | 15.50 |
| Nov_2018 | 362.81 | 4.17 | 1.15 | -28.52 | 1.84 | 13.94 |
| Nov_2018 | 318.05 | 6.78 | 2.13 | -28.53 | 2.25 | 14.07 |
| Nov_2018 | 366.11 | 4.31 | 1.18 | -28.17 | 2.27 | 15.50 |
| Mar_2019 | 271.73 | 12.43 | 4.58 | -28.49 | 2.07 | 15.94 |
| Mar_2019 | 178.28 | 3.16 | 1.77 | -29.16 | 1.31 | 19.72 |
| Mar_2019 | 243.19 | 9.12 | 3.75 | -28.50 | 2.93 | 16.78 |
| Sep_2019 | 559.16 | 3.68 | 0.66 | -26.79 | 3.18 | 15.19 |
| Sep_2019 | 475.92 | 0.87 | 0.18 | -28.37 | 2.62 | 15.40 |
| Sep_2019 | 380.68 | 11.03 | 2.90 | -28.63 | 2.70 | 13.55 |
| **Partially degraded wetland** | **THg (ng/g)** | **MeHg (ng/g)** | **% MeHg** | **δ $^{13}$C (‰)** | **δ $^{15}$N (‰)** | **C/N** |
| Mar_2018 | 275.65 | 1.10 | 0.40 | -28.82 | -0.38 | 17.40 |
| Mar_2018 | 253.09 | 10.64 | 4.20 | -28.30 | 1.93 | 15.68 |
| Mar_2018 | 130.60 | 1.40 | 1.07 | -29.22 | -0.59 | 15.60 |
| Aug_2018 | 144.31 | 0.42 | 0.29 | -28.18 | -0.32 | 19.83 |
| Aug_2018 | 230.77 | 0.38 | 0.17 | -27.64 | 0.19 | 16.37 |
| Aug_2018 | 279.24 | 9.09 | 3.26 | -29.05 | -0.21 | 16.16 |
| Aug_2018 | 236.51 | 0.74 | 0.31 | -28.44 | -0.15 | 16.20 |
| Nov_2018 | 234.65 | 0.34 | 0.15 | -29.28 | -0.06 | 16.65 |
| Nov_2018 | 253.94 | 0.16 | 0.06 | -28.22 | -0.12 | 17.10 |
| Nov_2018 | 236.69 | 2.63 | 1.11 | -28.53 | 0.07 | 15.27 |
| Nov_2018 | 54.40 | 3.13 | 5.76 | -28.06 | ND | ND |
| Mar_2019 | 230.29 | 1.84 | 0.80 | -29.45 | 1.23 | 17.29 |
| Mar_2019 | 204.45 | 4.88 | 2.39 | -29.23 | -0.63 | 15.37 |
| Mar_2019 | 215.57 | 2.50 | 1.16 | -29.19 | -0.85 | 19.72 |
| Sep_2019 | 332.45 | 1.50 | 0.45 | -28.82 | 0.08 | 15.85 |
| Sep_2019 | 283.09 | 4.64 | 1.64 | -28.76 | -0.65 | 17.23 |
| Sep_2019 | 209.47 | 0.02 | 0.01 | ND | ND | ND |
| Sep_2019 | 25.93 | 0.18 | 0.69 | -27.56 | 1.31 | 16.10 |
| **Saltmarsh** | **THg (ng/g)** | **MeHg (ng/g)** | **% MeHg** | **δ $^{13}$C (‰)** | **δ $^{15}$N (‰)** | **C/N** |
| Mar_2018 | 97.77 | 0.13 | 0.13 | -26.83 | 2.06 | 18.95 |
| Mar_2018 | 97.83 | 0.22 | 0.23 | -25.34 | 2.55 | 16.81 |
| Mar_2018 | 111.02 | 0.12 | 0.11 | -26.80 | 2.09 | 19.80 |

| | | | | | | |
|---|---|---|---|---|---|---|
| Aug_2018 | 101.68 | 0.62 | 0.61 | -25.91 | 3.10 | 15.21 |
| Aug_2018 | 113.17 | 0.17 | 0.15 | -26.49 | 3.02 | 16.17 |
| Nov_2018 | 76.92 | 0.00 | 0.00 | -27.23 | 2.07 | 22.91 |
| Nov_2018 | 94.77 | 0.06 | 0.06 | -27.04 | 2.32 | 19.77 |
| Nov_2018 | 55.11 | 0.06 | 0.12 | -27.09 | 2.20 | 18.05 |
| Mar_2019 | 110.15 | 1.88 | 1.71 | -29.67 | -0.89 | 16.58 |
| Mar_2019 | 102.50 | 2.58 | 2.52 | -26.52 | 3.08 | 16.51 |
| Mar_2019 | 104.30 | 0.67 | 0.64 | -26.91 | 3.11 | 15.16 |
| Sep_2019 | 20.65 | 0.04 | 0.18 | -26.82 | 2.28 | 19.50 |
| Sep_2019 | 20.23 | 0.07 | 0.33 | -26.60 | 1.84 | 28.49 |
| Sep_2019 | 114.76 | 0.09 | 0.07 | -27.31 | 1.66 | 20.27 |

## APPENDIX C. SEASONAL WATER QUALITY DATA

Table S1. Seasonal surface water quality data, dissolved organic carbon (DOC), sulfate ($SO^{2-}_4$), chlorine ($Cl^-$), nitrogen (N), salinity (ppt), dissolved oxygen (DO), and temperature (℃) in in Point Peter site and TOWeR site

| Sound Date | DOC (mg/L) | $SO_4^{2-}$ (mg/L) | DO (mg/L) | Cond. (mS/cm) | Temp. °C | pH | Cl- (mg/L) |
|---|---|---|---|---|---|---|---|
| 21 Sep 18 | 8.07 | 421.95 | 7.23 | 10.85 | 25.90 | 5.97 | 3202.18 |
| 28 Sep 18 | 4.90 | 1381.75 | 4.00 | 2.38 | 27.70 | 6.86 | 9985.26 |
| 7 Oct 18 | 22.48 | 343.98 | 5.50 | 8.89 | 27.30 | 6.47 | 2778.92 |
| 20 Oct 18 | 10.44 | 802.09 | 4.57 | 10.66 | 20.00 | 6.67 | 6252.89 |
| 5 Dec 18 | 37.76 | 114.85 | 9.68 | 3.58 | 11.00 | ND | 901.92 |
| 22 Apr 19 | 36.54 | 134.32 | 7.21 | 5.36 | 20.70 | ND | 1018.28 |
| 12 May 19 | 25.88 | 458.22 | 6.19 | 11.95 | 25.20 | 8.17 | 3381.24 |
| 27 Jun 19 | 10.42 | 149.52 | 3.97 | 3.27 | 29.70 | 7.34 | 1111.97 |
| 22 Jul 19 | 11.43 | 1057.92 | 4.58 | 26.50 | 29.70 | 7.34 | 7786.59 |
| 23 Aug 19 | 17.42 | 787.09 | 5.57 | 18.10 | 29.00 | 6.27 | 5716.96 |
| 4 Sep 19 | 5.35 | 739.66 | 5.35 | 22.17 | 29.00 | 6.37 | 3718.00 |
| 4 Sep 19 | 4.66 | 785.98 | 5.35 | 22.17 | 29.00 | 6.37 | 3987.97 |
| 13 Sep 19 | 7.00 | 477.93 | 5.15 | 3.31 | 25.40 | 6.33 | 3485.74 |
| 12 Dec 19 | 7.44 | 538.61 | 9.82 | 13.17 | 9.90 | ND | 4067.62 |
| **Saltmarsh Date** | **DOC (mg/L)** | **$SO_4^{2-}$ (mg/L)** | **DO (mg/L)** | **Cond. (mS/cm)** | **Temp. °C** | **pH** | **Cl- (mg/L)** |
| 5 Jun 18 | 50.83 | 20.72 | 0.42 | 1.17 | 27.80 | ND | 450.78 |
| 24 Aug 18 | 54.99 | 58.21 | 0.60 | 3.23 | 27.00 | ND | 886.00 |
| 21 Sep 18 | 18.34 | 472.71 | 2.45 | 11.59 | 24.60 | 5.71 | 3921.76 |
| 28 Sep 18 | 4.73 | 1242.14 | 3.83 | 27.98 | 27.50 | 5.86 | 9048.18 |
| 28 Sep 18 | 4.78 | 1490.74 | 3.83 | 27.98 | 27.50 | 6.03 | 10732.88 |
| 7 Oct 18 | 19.68 | 348.24 | 5.10 | 12.53 | 30.70 | 6.03 | 3686.17 |
| 7 Oct 18 | 18.66 | 352.52 | 5.10 | 12.53 | 30.70 | 6.04 | 3734.94 |
| 20 Oct 18 | 19.08 | 683.47 | 6.58 | 15.46 | 19.30 | 6.39 | 6479.85 |
| 5 Dec 18 | 12.94 | 192.25 | 3.70 | 5.58 | 11.20 | ND | 2067.45 |
| 22 Apr 19 | 17.67 | 226.23 | 3.27 | 8.72 | 22.60 | ND | 2342.36 |
| 12 May 19 | 14.40 | 527.78 | 3.72 | 14.67 | 28.90 | 7.70 | 4359.96 |
| 27 Jun 19 | 18.34 | 131.22 | 0.32 | 4.24 | 28.32 | 5.98 | 1068.34 |
| 22 Jul 19 | 40.40 | 57.10 | 1.81 | 6.08 | 34.30 | 7.28 | 1534.45 |
| 23 Aug 19 | 29.80 | 26.13 | 0.73 | 2.59 | 28.50 | 6.23 | 765.93 |
| 4 Sep 19 | 31.95 | 46.87 | 0.41 | 4.83 | 32.00 | 6.20 | 1252.92 |
| 13 Sep 19 | 12.35 | 28.72 | 1.27 | 2.27 | 26.10 | 6.25 | 405.54 |
| 13 Sep 19 | 11.38 | 33.99 | 1.27 | 2.27 | 26.10 | 6.25 | 435.75 |
| 12 Dec 19 | 16.21 | 220.70 | 6.18 | 6.30 | 9.10 | ND | 2607.99 |
| 12 Dec 19 | 16.85 | 226.47 | 6.18 | 6.30 | 9.10 | ND | 2690.43 |
| **PDW** | **DOC** | **$SO_4^{2-}$** | **DO** | **Cond.** | **Temp.** | **pH** | **Cl-** |

| Date | (mg/L) | (mg/L) | (mg/L) | (mS/cm) | °C | | (mg/L) |
|---|---|---|---|---|---|---|---|
| 5 Jun 18 | 68.86 | 4.22 | 0.90 | 1.02 | 27.50 | ND | 272.12 |
| 24 Aug 18 | 90.21 | 8.67 | 0.35 | 0.61 | 27.00 | ND | 171.10 |
| 21 Sep 18 | 12.64 | 294.08 | 0.06 | 8.70 | 24.10 | 3.64 | 2645.70 |
| 21 Sep 18 | 11.93 | 319.66 | 0.06 | 8.70 | 24.10 | 3.50 | 2846.64 |
| 28 Sep 18 | 11.80 | 248.65 | 2.37 | 8.85 | 27.20 | 3.82 | 2528.96 |
| 7 Oct 18 | 15.34 | 180.42 | 2.82 | 7.36 | 27.10 | 3.91 | 2281.88 |
| 20 Oct 18 | 9.92 | 585.51 | 5.75 | 12.13 | 16.40 | 4.75 | 5265.92 |
| 5 Dec 18 | 7.96 | 192.24 | 5.47 | 4.44 | 10.40 | ND | 2089.27 |
| 22 Apr 19 | 15.51 | 72.17 | 3.80 | 3.46 | 21.20 | ND | 1178.40 |
| 22 Apr 19 | 15.66 | 71.78 | 3.80 | 3.46 | 21.20 | ND | 1175.29 |
| 12 May 19 | 19.01 | 57.70 | 1.00 | 5.20 | 28.40 | 4.90 | 1404.63 |
| 27 Jun 19 | 22.54 | 78.45 | 0.39 | 2.40 | 26.03 | 4.94 | 819.74 |
| 22 Jul 19 | 62.10 | 27.39 | 0.43 | 3.46 | 30.40 | 6.21 | 938.28 |
| 23 Aug 19 | 40.33 | 24.03 | 0.21 | 2.72 | 28.30 | 5.41 | 704.51 |
| 4 Sep 19 | 27.09 | 21.50 | 0.29 | 3.75 | 28.00 | 5.60 | 821.74 |
| 13 Sep 19 | 18.74 | 42.14 | 0.62 | 6.61 | 26.00 | 5.48 | 603.75 |
| 12 Dec 19 | 21.18 | 50.75 | 4.62 | 2.54 | 9.10 | ND | 982.78 |

| FW Date | DOC (mg/L) | $SO_4^{2-}$ (mg/L) | DO (mg/L) | Cond. (mS/cm) | Temp. °C | pH | Cl- (mg/L) |
|---|---|---|---|---|---|---|---|
| 5 Jun 18 | 97.73 | 0.17 | 0.32 | 0.12 | 22.50 | ND | 10.43 |
| 24 Aug 18 | 107.41 | 0.20 | 0.60 | 0.15 | 26.00 | ND | 10.54 |
| 24 Aug 18 | 107.46 | 0.20 | 0.60 | 0.15 | 26.00 | ND | 10.68 |
| 21 Sep 18 | 71.87 | 28.16 | 0.56 | 8.00 | 23.50 | 3.06 | 342.87 |
| 28 Sep 18 | 19.58 | 65.71 | 0.60 | 3.50 | 25.10 | ND | 966.28 |
| 7 Oct 18 | 25.82 | 12.97 | 0.55 | 2.57 | 24.00 | 3.07 | 733.46 |
| 20 Oct 18 | 14.40 | 30.37 | 0.83 | 4.14 | 16.90 | 2.99 | 1243.78 |
| 5 Dec 18 | 89.29 | 2.00 | 1.65 | 0.29 | 9.00 | ND | 59.41 |
| 5 Dec 18 | 90.60 | 2.02 | 1.65 | 0.29 | 9.00 | ND | 59.78 |
| 22 Apr 19 | 58.87 | 2.37 | 0.13 | 0.17 | 16.80 | ND | 31.81 |
| 12 May 19 | 71.52 | 4.70 | 1.18 | 0.33 | 21.30 | 3.78 | 76.46 |
| 12 May 19 | 69.01 | 4.86 | 1.18 | 0.33 | 21.30 | 3.78 | 76.79 |
| 27 Jun 19 | 81.80 | 2.80 | 0.33 | 0.23 | 22.73 | 4.05 | 40.91 |
| 22 Jul 19 | 74.17 | 4.80 | 0.86 | 3.81 | 29.20 | 4.47 | 121.47 |
| 23 Aug 19 | 99.99 | 1.57 | 0.44 | 3.15 | 25.20 | 4.24 | 37.62 |
| 4 Sep 19 | 74.11 | 1.52 | 2.41 | 0.43 | 22.70 | 3.79 | 42.54 |
| 13 Sep 19 | 69.71 | 0.21 | 0.49 | 1.33 | 23.50 | 4.14 | 9.05 |
| 12 Dec 19 | 82.15 | 2.56 | 2.81 | 0.19 | 9.00 | ND | 46.55 |

| T-N Date | DOC (mg/L) | $SO_4^{2-}$ (mg/L) | DO (mg/L) | Cond. (mS/cm) | Temp. °C | pH | Cl- (mg/L) |
|---|---|---|---|---|---|---|---|
| 5 Jun 18 | 20.32 | 0.11 | 1.50 | 0.05 | 28.00 | ND | 7.40 |
| 24 Aug 18 | 19.36 | 0.06 | 0.43 | 0.04 | 27.00 | ND | 6.18 |
| 21 Sep 18 | 17.44 | 34.29 | 0.70 | 1.30 | 27.60 | 4.54 | 307.81 |
| 28 Sep 18 | 16.41 | 3.95 | 1.31 | 0.36 | 30.40 | 4.06 | 39.34 |
| 7 Oct 18 | 17.81 | 1.97 | 0.62 | 0.18 | 27.50 | 4.02 | 26.88 |

| | | | | | | | |
|---|---|---|---|---|---|---|---|
| 20 Oct 18 | 17.13 | 1.90 | 1.42 | 0.14 | 19.20 | 3.97 | 32.12 |
| 5 Dec 18 | 18.71 | 0.34 | 4.54 | 0.04 | 11.30 | ND | 11.78 |
| 22 Apr 19 | 21.12 | 0.29 | 2.06 | 0.05 | 21.30 | ND | 10.92 |
| 12 May 19 | 24.13 | 0.21 | 0.54 | 0.07 | 23.70 | 4.81 | 12.31 |
| 27 Jun 19 | 25.22 | 0.35 | 0.42 | 0.06 | 26.88 | 5.21 | 22.11 |
| 27 Jun 19 | 24.15 | 0.39 | 0.42 | 0.06 | 26.88 | 5.21 | 22.67 |
| 22 Jul 19 | 26.63 | 3.59 | 0.33 | 0.37 | 31.20 | 5.16 | 81.27 |
| 23 Aug 19 | 21.17 | 10.31 | 1.70 | 0.78 | 29.70 | 6.35 | 188.29 |
| 4 Sep 19 | 20.63 | 7.44 | 0.49 | 0.69 | 26.30 | 6.05 | 169.55 |
| 13 Sep 19 | 28.25 | 0.74 | 0.76 | 2.13 | 25.80 | 5.25 | 45.04 |
| 12 Dec 19 | 21.69 | 0.81 | 6.20 | 0.07 | 9.90 | ND | 20.88 |

| **T-Mid Date** | **DOC (mg/L)** | **$SO_4^{2-}$ (mg/L)** | **DO (mg/L)** | **Cond. (mS/cm)** | **Temp. °C** | **pH** | **Cl- (mg/L)** |
|---|---|---|---|---|---|---|---|
| 24 Aug 18 | 18.71 | 0.05 | 0.16 | 0.04 | 24.50 | ND | 6.81 |
| 21 Sep 18 | 14.40 | 6.52 | 0.36 | 0.27 | 24.00 | 6.42 | 72.88 |
| 28 Sep 18 | 21.38 | 0.11 | 0.40 | 0.07 | 25.70 | 4.34 | 12.83 |
| 7 Oct 18 | 26.27 | 0.12 | 0.32 | 0.08 | 25.60 | 4.32 | 15.24 |
| 20 Oct 18 | 28.17 | 0.21 | 0.45 | 0.08 | 17.70 | 4.59 | 19.20 |
| 20 Oct 18 | 30.91 | 0.20 | 0.45 | 0.08 | 17.70 | 4.65 | 20.13 |
| 5 Dec 18 | 24.58 | 0.11 | 3.47 | 0.06 | 10.50 | ND | 13.41 |
| 22 Apr 19 | 30.11 | 0.12 | 0.63 | 0.07 | 18.70 | ND | 11.93 |
| 12 May 19 | 23.74 | 0.15 | 0.28 | 0.09 | 21.90 | 5.42 | 11.71 |
| 27 Jun 19 | 35.92 | 0.11 | 0.16 | 0.06 | 25.05 | 5.15 | 16.77 |
| 22 Jul 19 | 27.09 | 1.34 | 0.19 | 0.23 | 29.90 | 5.44 | 50.97 |
| 22 Jul 19 | 28.00 | 1.40 | 0.19 | 0.23 | 29.90 | 5.44 | 52.27 |
| 23 Aug 19 | 21.69 | 1.27 | 1.60 | 0.36 | 28.50 | 6.23 | 88.94 |
| 4 Sep 19 | 17.02 | 4.52 | 1.37 | 0.56 | 27.30 | 5.60 | 119.29 |
| 13 Sep 19 | 24.95 | <0.2 | 0.55 | 1.06 | 25.10 | 5.05 | 11.97 |
| 12 Dec 19 | 28.94 | 0.51 | 5.20 | 0.05 | 9.30 | ND | 27.48 |

| **T-S Date** | **DOC (mg/L)** | **$SO_4^{2-}$ (mg/L)** | **DO (mg/L)** | **Cond. (mS/cm)** | **Temp. °C** | **pH** | **Cl- (mg/L)** |
|---|---|---|---|---|---|---|---|
| 5 Jun 18 | 27.09 | 0.14 | 0.10 | 0.06 | 27.50 | ND | 9.42 |
| 24 Aug 18 | 14.91 | 0.05 | 0.83 | 0.04 | 28.00 | ND | 4.91 |
| 21 Sep 18 | 13.39 | 0.14 | 1.14 | 0.04 | 25.30 | 5.43 | 6.41 |
| 28 Sep 18 | 14.24 | 0.05 | 0.40 | 0.04 | 29.20 | 5.84 | 6.69 |
| 7 Oct 18 | 16.27 | <0.1 | 0.49 | 0.05 | 26.00 | 4.68 | 7.61 |
| 20 Oct 18 | 15.02 | 0.06 | 1.11 | 0.04 | 17.00 | 4.75 | 7.97 |
| 5 Dec 18 | 11.96 | 0.07 | 6.10 | 0.03 | 10.10 | ND | 8.22 |
| 22 Apr 19 | 25.23 | 0.22 | 0.99 | 0.05 | 19.50 | ND | 8.58 |
| 12 May 19 | 26.65 | <0.1 | 0.38 | 0.05 | 22.40 | 5.09 | 9.26 |
| 27 Jun 19 | 25.61 | 0.11 | 0.89 | 0.05 | 26.84 | 4.88 | 10.03 |
| 22 Jul 19 | 23.14 | 0.10 | 0.30 | 0.09 | 30.30 | 5.58 | 9.63 |
| 23 Aug 19 | 21.00 | <0.2 | 1.80 | 0.06 | 29.00 | 5.60 | 9.86 |
| 23 Aug 19 | 21.81 | <0.2 | 1.80 | 0.06 | 29.00 | 5.60 | 10.36 |
| 4 Sep 19 | 21.61 | <0.2 | 1.20 | 0.05 | 27.30 | 5.24 | 10.21 |

| | | | | | | | |
|---|---|---|---|---|---|---|---|
| 13 Sep 19 | 33.58 | 0.22 | 0.50 | 0.60 | 24.90 | 4.52 | 9.43 |
| 12 Dec 19 | 30.53 | 0.28 | 4.24 | 0.04 | 9.10 | ND | 10.06 |
| **Ditch** | **DOC** | **$SO_4^{2-}$** | **DO** | **Cond.** | **Temp.** | **pH** | **Cl-** |
| **Date** | **(mg/L)** | **(mg/L)** | **(mg/L)** | **(mS/cm)** | **°C** | | **(mg/L)** |
| 27 Jun 19 | 18.50 | 185.10 | 2.25 | 3.49 | 28.63 | 6.49 | 1418.75 |
| 22 Jul 19 | 42.04 | 154.10 | 3.44 | 8.56 | 34.90 | 7.85 | 2352.00 |
| 4 Sep 19 | 29.33 | 44.27 | 1.60 | 5.17 | 30.00 | 7.42 | 1137.01 |
| 13 Sep 19 | 16.07 | 88.19 | 2.42 | 5.20 | 26.60 | 6.89 | 919.60 |
| 12 Dec 19 | 14.82 | 408.78 | 5.81 | 12.27 | 11.50 | ND | 4221.69 |

Table S2: Surface water FTHg and FMeHg concentrations of open water, saltmarsh, partially degraded wetland, freshwater wetland, T-North, T-Middle, and T-South.

| Water THg (ng/L) | | | | | | |
|---|---|---|---|---|---|---|
| Site | Size | Mean | Std Dev | Max | Min | Median |
| Open water | 26 | 1.90 | 1.52 | 7.45 | 0.25 | 1.84 |
| Saltmarsh | 29 | 4.41 | 2.69 | 11.53 | 1.02 | 3.71 |
| Partially degraded wetland | 29 | 5.27 | 4.03 | 13.04 | 0.33 | 3.71 |
| Freshwater wetland | 28 | 8.20 | 3.44 | 14.94 | 1.62 | 7.36 |
| T-North | 29 | 2.37 | 0.52 | 3.40 | 1.28 | 2.40 |
| T-Middle | 27 | 2.10 | 0.66 | 3.46 | 0.82 | 2.15 |
| T-South | 27 | 1.96 | 0.42 | 2.80 | 0.83 | 1.92 |
| Water MeHg (ng/L) | | | | | | |
| Open water | 26 | 0.095 | 0.10 | 0.33 | 0.00 | 0.07 |
| Saltmarsh | 29 | 1.58 | 1.51 | 5.16 | 0.03 | 1.16 |
| Partially degraded wetland | 29 | 1.74 | 2.34 | 10.59 | 0.02 | 0.73 |
| Freshwater wetland | 28 | 1.20 | 1.07 | 3.86 | 0.06 | 0.80 |
| T-North | 28 | 0.22 | 0.17 | 0.81 | 0.04 | 0.15 |
| T-Middle | 28 | 0.12 | 0.09 | 0.35 | 0.00 | 0.12 |
| T-South | 27 | 0.13 | 0.36 | 1.96 | 0.00 | 0.05 |

# APPENDIX D. MERCURY AND ISOTOPE LEVELS IN MACROINVERTEBRATE AND FISH SAMPLES

Table S1: THg, MeHg, δ $^{13}$C, δ $^{15}$N, δ $^{34}$S and C/N levels in the freshwater wetland (FW), partially degraded wetland (PDW), and saltmarsh (SM) at Georgetown, South Carolina

| Dates (m/y) | Freshwater wetland | Dry wt. (g) | Ind. | Length (~cm) | Ave. THg (ng/g) | Ave. MeHg (ng/g) | δ $^{13}$C (‰) | δ $^{15}$N (‰) | δ $^{34}$S (‰) | C/N |
|---|---|---|---|---|---|---|---|---|---|---|
| Mar 18 | Mosq.fish | 0.46 | 7 | ND | 187.30 | 206.17 | -33.55 | 7.00 | 11.30 | 4.22 |
| Mar 18 | Mosq.fish | 0.64 | 7 | ND | 332.20 | 257.65 | -32.73 | 7.21 | 12.42 | 4.42 |
| Aug 18 | Mosq.fish | 0.35 | 4 | ND | ND | 184.06 | -32.22 | 6.71 | 12.09 | 5.87 |
| Aug 18 | Mosq.fish | 0.13 | 1 | ND | 213.09 | 184.78 | -29.57 | 6.02 | 11.00 | 4.35 |
| Nov 18 | Mosq.fish | 0.35 | 11 | 1.3 | 267.71 | 198.07 | -30.24 | 6.82 | 11.38 | 5.02 |
| Mar 19 | Mosq.fish | 0.20 | 3 | 3 | 322.01 | 312.82 | -31.11 | 7.42 | 11.20 | 5.32 |
| Mar 19 | Mosq.fish | 0.34 | 1 | ND | 225.42 | 225.05 | ND | ND | ND | ND |
| Mar 19 | Mosq.fish | 0.20 | 3 | 2 | 270.34 | 219.37 | -31.09 | 7.31 | 11.33 | 5.52 |
| Sep 19 | Mosq.fish | 0.17 | 2 | 2 | 336.12 | 277.35 | -29.34 | 6.46 | 10.93 | 4.18 |
| Sep 19 | Mosq.fish | 0.19 | 4 | 1.5 | 367.74 | 347.51 | -28.55 | 5.88 | 10.58 | 5.11 |
| Mar 18 | Crayfish | 1.06 | 1 | ND | 81.89 | 66.91 | -33.66 | 6.76 | 12.90 | 5.22 |
| Mar 18 | Crayfish | 0.23 | 1 | ND | 101.67 | 88.53 | -32.32 | 4.34 | 13.30 | 3.29 |
| Mar 18 | Crayfish | 1.87 | 1 | ND | 107.80 | 86.06 | -29.78 | 3.76 | 12.00 | 4.14 |
| Aug 18 | Crayfish | 0.96 | 1 | ND | 97.32 | 86.39 | -27.77 | 3.60 | 12.40 | 4.46 |
| Aug 18 | Crayfish | 0.69 | 16 | ND | 101.83 | 52.54 | -28.50 | 3.38 | 11.10 | 3.99 |
| Nov 18 | Crayfish | 0.74 | 1 | ND | 73.44 | 51.66 | ND | ND | ND | ND |
| Nov 18 | Crayfish | 0.49 | 9 | 2 | 79.46 | 46.67 | -28.90 | 3.99 | 11.38 | 5.04 |
| Nov 18 | Crayfish | 0.76 | 11 | 2.3 | 85.72 | 41.41 | -30.32 | 4.17 | 11.51 | 4.17 |
| Mar 19 | Crayfish | 1.92 | 3 | 4 | 78.11 | 69.59 | -27.83 | 3.56 | 11.02 | 4.19 |
| Mar 19 | Crayfish | 1.46 | 1 | ND | 148.87 | 82.00 | -26.88 | 2.40 | 10.91 | 5.31 |
| Mar 19 | Crayfish | 1.36 | 5 | 4 | 80.62 | 64.72 | -27.39 | 3.48 | 11.54 | 4.60 |
| Sep 19 | Crayfish | 1.33 | 1 | 5 | 89.39 | 52.58 | -27.79 | 3.38 | 9.49 | 4.82 |
| Sep 19 | Crayfish | 0.84 | 5 | 3 | 114.15 | 62.08 | ND | ND | ND | ND |
| Mar 18 | Amphipod | 0.37 | <50 | 0.7 | 164.71 | 55.31 | -31.60 | 3.12 | 12.90 | 5.39 |
| Aug 18 | WaterTupelo | NA | bulk | fresh | ND | ND | -33.15 | 2.20 | 8.49 | 33.28 |
| Aug 18 | Cypress | NA | bulk | fresh | ND | ND | -31.16 | 3.19 | 8.78 | 35.21 |
| Sep 19 | WaterTupelo | NA | bulk | fresh | ND | ND | -32.42 | -2.05 | 6.98 | 46.31 |
| Sep 19 | Cypress | NA | bulk | fresh | ND | ND | -30.65 | 3.55 | 7.37 | 42.40 |

| Dates (m/y) | Partially degraded wetland | Dry wt. (g) | Ind. | Length (~cm) | Ave. THg (ng/g) | Ave. MeHg (ng/g) | δ $^{13}$C (‰) | δ $^{15}$N (‰) | δ $^{34}$S (‰) | C/N |
|---|---|---|---|---|---|---|---|---|---|---|
| Mar 18 | Mosq.fish | 0.41 | 2 | ND | 41.76 | 37.63 | -30.52 | 7.38 | 7.80 | 3.94 |

| | | | | | | | | | | |
|---|---|---|---|---|---|---|---|---|---|---|
| Aug 18 | Mosq.fish | 0.12 | 3 | 1.5 | 176.78 | 126.83 | -29.51 | 6.99 | ND | 3.80 |
| Aug 18 | Mosq.fish | 0.30 | 3 | 2 | 180.95 | 153.77 | -28.02 | 5.47 | 12.50 | 4.39 |
| Aug 18 | Mosq.fish | 0.13 | 3 | 1.5 | ND | 150.25 | ND | ND | ND | ND |
| Nov 18 | Mosq.fish | 0.25 | 2 | 3.5 | 157.67 | 141.13 | -28.65 | 6.54 | 11.35 | 6.26 |
| Nov 18 | Mosq.fish | 0.39 | 11 | 2 | ND | 249.72 | -29.58 | 6.93 | 11.61 | 4.93 |
| Nov 18 | Mosq.fish | 0.33 | 4 | 2.5 | ND | 142.09 | ND | ND | ND | ND |
| Mar 19 | Mosq.fish | 0.27 | 5 | ND | 448.10 | 360.90 | -29.65 | 6.98 | 12.78 | 4.78 |
| Mar 19 | Mosq.fish | 0.22 | 7 | ND | 299.24 | 216.48 | ND | ND | ND | ND |
| Mar 19 | Mosq.fish | 0.26 | 10 | 2.2 | 430.63 | 303.48 | -29.77 | 7.34 | 12.39 | 4.47 |
| Sep 19 | Mosq.fish | 0.20 | 2 | 2.4 | 184.20 | 15.84 | -30.04 | 5.20 | 12.63 | 6.83 |
| Sep 19 | Mosq.fish | 0.22 | 2 | 2 | 224.82 | 186.57 | -28.88 | 6.74 | 7.20 | 4.10 |
| Mar 18 | Crayfish | 0.81 | 1 | ND | 80.87 | 65.20 | -25.56 | 1.54 | 13.50 | 5.06 |
| Aug 18 | Crayfish | 0.39 | 9 | 1 | 136.28 | 102.38 | -26.96 | 2.90 | 12.50 | 3.77 |
| Aug 18 | Crayfish | 0.70 | 1 | ND | 11.61 | 74.15 | -26.57 | 1.89 | 11.65 | 4.40 |
| Nov 18 | Crayfish | 0.70 | 1 | ND | ND | 46.32 | -25.46 | 0.80 | 12.29 | 5.79 |
| Nov 18 | Crayfish | 0.53 | 1 | ND | ND | 62.36 | -26.50 | 1.45 | 12.75 | 5.75 |
| Mar 19 | Crayfish | 1.32 | 4 | 4 | 99.37 | 58.68 | -29.56 | 2.94 | 14.22 | 4.11 |
| Mar 19 | Crayfish | 1.54 | 1 | ND | 99.61 | 59.00 | -26.92 | 2.20 | 12.08 | 4.78 |
| Mar 19 | Crayfish | 0.61 | 2 | 4.5 | 81.47 | 66.58 | ND | ND | ND | ND |
| Sep 19 | Crayfish | 0.48 | 1 | 3.3 | 155.35 | 68.27 | -25.93 | 2.18 | 14.04 | 4.97 |
| Sep 19 | Crayfish | 0.39 | 1 | 3 | 110.45 | 98.65 | -26.27 | 1.58 | 14.17 | 4.70 |
| Mar 18 | Dragonfly larvae | 0.21 | 6 | ND | 135.78 | 104.30 | -31.30 | 3.16 | 13.80 | 3.95 |
| Mar 18 | Dragonfly larvae | 0.26 | 7 | ND | 137.60 | 90.55 | -30.13 | 2.88 | 14.20 | 4.20 |
| Nov 18 | Soil litter | NA | bulk | dry | ND | ND | -28.94 | -3.89 | 12.30 | 89.93 |
| Nov 18 | Cypress | NA | bulk | dry | ND | ND | -28.58 | 0.29 | 11.97 | 69.65 |
| Mar 19 | WaterTupelo | NA | bulk | fresh | ND | ND | -30.72 | 3.63 | 16.41 | 43.45 |
| Sep 19 | WaterTupelo | NA | bulk | fresh | ND | ND | -32.40 | -1.40 | 16.73 | 33.09 |
| Sep 19 | Cypress | NA | bulk | dry | ND | ND | -28.23 | 0.44 | 11.79 | 70.82 |

| **Dates (m/y)** | **Saltmarsh** | **Dry wt. (g)** | **Ind.** | **Length (~cm)** | **Ave. THg (ng/g)** | **Ave. MeHg (ng/g)** | **δ $^{13}$C (‰)** | **δ $^{15}$N (‰)** | **δ $^{34}$S (‰)** | **C/N** |
|---|---|---|---|---|---|---|---|---|---|---|
| Mar 18 | Mosq.fish | 0.13 | | ND | 20.14 | 10.71 | -26.50 | 9.08 | 11.40 | 4.00 |
| Nov 18 | Mosq.fish | 0.51 | 7 | 2.5 | 64.13 | 43.36 | -26.28 | 10.61 | 6.13 | 4.38 |
| Mar 19 | Mosq.fish | 0.27 | 5 | 2.5 | 61.96 | 54.28 | -25.82 | 10.96 | 9.06 | 4.51 |
| Mar 19 | Mosq.fish | 0.25 | 5 | 2.1 | 72.09 | 45.63 | ND | ND | ND | ND |
| Mar 19 | Mosq.fish | 0.23 | 6 | 2 | 44.45 | 42.98 | -26.78 | 10.12 | 9.23 | 4.66 |
| Sep 19 | Mosq.fish | 0.07 | 1 | 2.5 | 47.73 | 24.23 | -26.38 | 9.16 | 10.01 | 4.76 |
| Sep 19 | Mosq.fish | 0.11 | 3 | 1.5 | 26.06 | 21.58 | -28.17 | 8.57 | 9.32 | 4.68 |
| Mar 19 | Mummichog | 1.01 | 1 | 7 | 80.20 | 70.10 | -23.70 | 11.55 | 10.06 | 3.35 |
| Mar 19 | Mummichog | 0.17 | 1 | 3.6 | 12.93 | 10.83 | -26.68 | 9.42 | 7.48 | 4.51 |
| Mar 18 | Mud crab | 0.18 | | ND | 27.73 | 10.85 | -25.25 | 8.11 | 9.90 | 4.44 |
| Nov 18 | Mud crab | 0.49 | 3 | 1.4 | 24.75 | 15.19 | -23.05 | 6.09 | 11.48 | 4.21 |

| | | | | | | | | | | |
|---|---|---|---|---|---|---|---|---|---|---|
| Nov 18 | Mud crab | 0.40 | 2 | 1.3 | 34.65 | 17.83 | -22.45 | 6.94 | 14.27 | 4.70 |
| Sep 19 | Mud crab | 0.43 | 1 | 1.5 | 25.96 | 7.37 | -26.23 | 6.41 | 9.68 | 3.71 |
| Sep 19 | Mud crab | 0.67 | 1 | 2 | 19.40 | 6.13 | -25.24 | 6.72 | 11.89 | 4.90 |
| Aug 18 | Fiddler crab | 1.34 | 1 | ND | 13.80 | 6.33 | -25.07 | 5.39 | 8.70 | 4.72 |
| Aug 18 | Fiddler crab | 1.26 | 1 | ND | 21.27 | 6.56 | -24.72 | 5.17 | 9.70 | 5.20 |
| Nov 18 | Shrimp | 0.42 | 16 | 1.5 | 42.96 | 105.06 | -24.26 | 9.46 | 10.44 | 3.91 |
| Aug 18 | Spartina | NA | bulk | fresh | ND | ND | -27.41 | 3.67 | 8.32 | 49.83 |
| Aug 18 | Spartina | NA | bulk | fresh | ND | ND | -27.30 | 4.14 | 11.49 | 38.70 |
| Nov 18 | Spartina | NA | bulk | dry | ND | ND | -26.55 | 4.29 | 10.15 | 45.01 |
| Nov 18 | Spartina | NA | bulk | fresh | ND | ND | -27.51 | 5.88 | 11.73 | 49.52 |